ERDC/GSL TR-09-22

Geotechnical and Structures Laboratory

US Army Corps
of Engineers®
Engineer Research and
Development Center

Laboratory Characterization of Cor-Tuf Concrete With and Without Steel Fibers

Erin M. Williams, Steven S. Graham,
Paul A. Reed, and Todd S. Rushing

July 2009

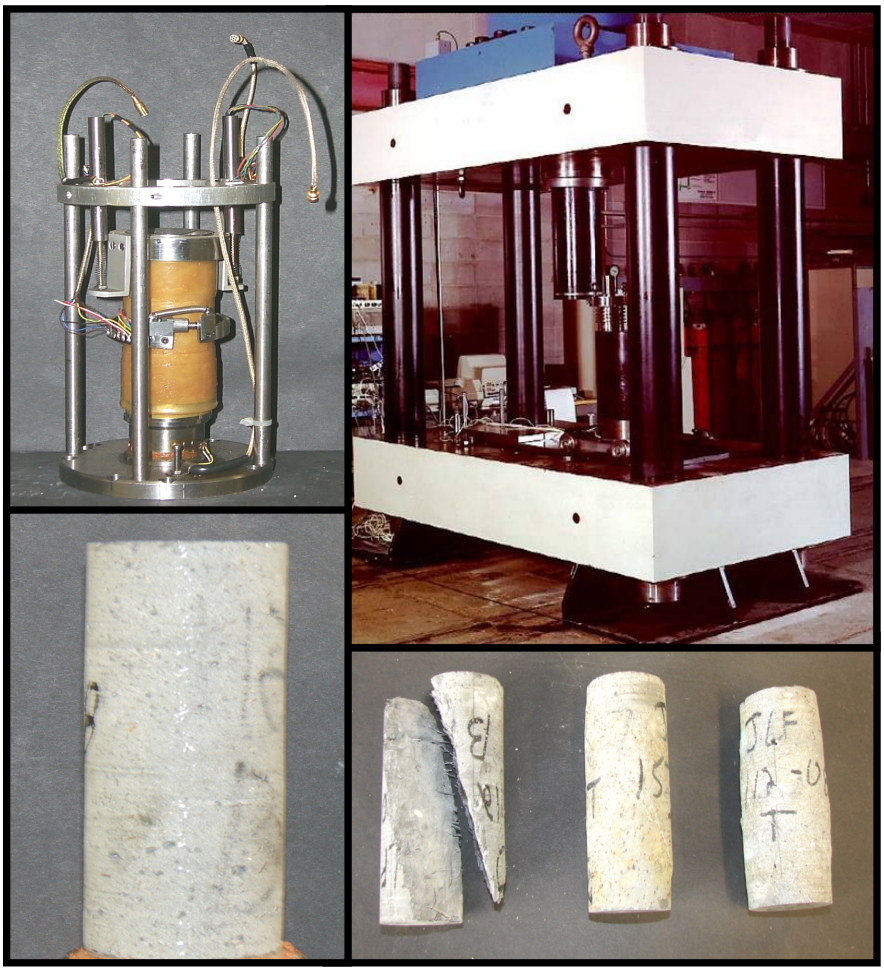

ERDC/GSL TR-09-22
July 2009

Laboratory Characterization of Cor-Tuf Concrete With and Without Steel Fibers

Erin M. Williams, Steven S. Graham,
Paul A. Reed, and Todd S. Rushing

Geotechnical and Structures Laboratory
U.S. Army Engineer Research and Development Center
3909 Halls Ferry Road
Vicksburg, MS 39180-6199

Final report

Prepared for Headquarters, U.S. Army Corps of Engineers
Washington, DC 20314-1000

Under Scalable Technology for Adaptive Response Work Package
Dynamic Behavior of Advanced Urban Materials Work Unit

and Defeat of Emerging Adaptive Threats Work Package
Multi-scale Material Property Characterization Work Unit

Abstract: Personnel of the Geotechnical and Structures Laboratory, U.S. Army Engineer Research and Development Center, conducted a series of laboratory experiments to investigate the strength and constitutive property behavior of baseline ultra-high-performance composite (Cor-Tuf) concrete with and without steel fibers. A total of 23 mechanical property tests were successfully completed for Cor-Tuf1 and Cor-Tuf2 concrete. The mechanical property tests included hydrostatic compression, unconfined compression (UC), triaxial compression (TXC), unconfined direct pull (DP), uniaxial strain, and uniaxial strain load/constant volume strain loading tests. In addition to the mechanical property tests, nondestructive pulse-velocity measurements and mass properties were obtained on each specimen. The TXC tests exhibited a continuous increase in maximum principal stress difference with increasing confining stress. A compression failure surface was developed from the TXC test results at six levels of confining pressure and from the results of the UC tests. The results for the DP tests were used to determine the unconfined tensile strength of the concretes, which were less than 10% of the unconfined compressive strength. The Cor-Tuf with the steel fibers exhibits slightly greater strength with increasing confining pressure than the Cor-Tuf without steel fibers. Overall, the results from all of the compression tests for both Cor-Tuf concretes were very similar.

Contents

Figures and Tables

Figures

Tables

Preface

This laboratory mechanical property investigation of Cor-Tuf concrete with and without steel fibers was conducted by personnel of the U.S. Army Engineer Research and Development Center (ERDC). The study was conducted with funds provided by Directorate of Military Programs, Headquarters, U.S. Army Corps of Engineers, as part of the Research, Development, Test, and Evaluation (RDT&E) Program, under the Scalable Technology for Adaptive Response and Defeat of Emerging Adaptive Threats Work Packages.

This study was conducted in 2008 by ERDC staff members of the Impact and Explosion Effects Branch (IEEB) and the Concrete and Materials Branch (CMB), Engineering Systems and Materials Division (ESMD), Geotechnical and Structures Laboratory (GSL), under the general direction of Henry S. McDevitt, Jr., Chief, IEEB; Toney K. Cummins, Chief, CMB; Dr. Larry N. Lynch, Chief, ESMD; Dr. William P. Grogan, Deputy Director, GSL; and Dr. David W. Pittman, Director, GSL.

The Principal Investigator for this project was Erin M. Williams, IEEB. Steven S. Graham, IEEB, served as co-investigator for this project and processed the material property data. Paul A. Reed, IEEB, performed laboratory characterization tests under the technical direction of Williams. Dr. Todd S. Rushing, CMB, developed the baseline Cor-Tuf mix design and assisted in preparing the report. Instrumentation support was provided by Johnny L. Morrow, Engineering and Informatic Systems Division, ERDC Information Technology Laboratory.

COL Gary E. Johnston was Commander and Executive Director of ERDC. Dr. James R. Houston was Director.

1 Introduction

Background

Personnel of the Geotechnical and Structures Laboratory (GSL), U.S. Army Engineer Research and Development Center (ERDC), conducted a series of laboratory experiments to investigate the strength and constitutive property behavior of baseline ultra-high-performance composite (Cor-Tuf) concrete with and without steel fibers. A total of 23 successful mechanical property tests were conducted for Cor-Tuf1 and Cor-Tuf2 concrete. The mechanical property tests consisted of hydrostatic compression, unconfined compression, triaxial compression, unconfined direct pull, uniaxial strain, and uniaxial strain load/constant volume strain tests. In addition to the mechanical property tests, nondestructive pulse-velocity measurements and mass properties were obtained on each specimen. This report discusses the mechanical property tests for each material and compares the results.

Purpose and scope

The purpose of this report is to document the results from the laboratory mechanical property tests conducted on the concrete specimens. In addition, results from the nondestructive pulse-velocity measurements and mass properties are documented. The physical and composition properties, test procedures, and test results are documented in Chapter 2. Comparative plots and analyses of results from the Cor-Tuf concrete with fibers and the Cor-Tuf concrete without fibers experiments are presented in Chapters 3 and 4, respectively. In Chapter 5, results from both series of tests are compared. A summary is provided in Chapter 6.

2 Laboratory Tests

Material description

Cor-Tuf is the nomenclature given to a family of ultra-high-performance concretes (UHPCs) developed at GSL, ERDC. UHPCs are distinguished by their high compressive strengths (ranging from 190 to 244 MPa in the case of the Cor-Tuf cylinders). Since the fresh and hardened properties of UHPCs can be very sensitive to slight changes in constitutive materials, the exact mixture proportion is often adjusted to achieve desired properties. For the in-depth comparative study described here, an exact mixture proportion was determined based on fixed constitutive material lots and was designated "Cor-Tuf" as a reference material.

The Cor-Tuf material composition was designed to develop ultra high compressive strength while maintaining workability and production economy. Cor-Tuf can be broadly characterized as a reactive powder concrete (RPC). RPCs are composed of fine aggregates and pozzolanic powders but do not include coarse aggregates like those found in conventional concrete. The maximum particle size in Cor-Tuf is limited to that of the silica sand, which is a foundry grade Ottawa sand that has a maximum size of approximately 0.6 mm.

The mixture proportion for Cor-Tuf is reported in Table 1. Included in Cor-Tuf are processed fine silica sand, finely ground quartz flour, Portland cement, and amorphous micro-silica (also known as silica fume). Additionally, a polycarboxylate type superplasticizer was included to decrease water demand, aid mixing, and improve workability. The water-to-cement ratio was restricted to about 0.21 for Cor-Tuf, which is far lower than values typical of conventional concrete.[1]

For comparative purposes, two preparations of Cor-Tuf were produced for this study, i.e., Cor-Tuf1 with steel fibers and Cor-Tuf2 without steel fibers. The weight of steel fibers in Cor-Tuf1 is given in Table 1 as a mass fraction relative to the mass of cement. This loading corresponds to a volumetric content of about 3.6%, which is somewhat greater than is normally recommended for typical fiber-reinforced concrete applications.

[1] Conventional concretes have a water-to-cement ratio near 0.40.

Table 1. Cor-Tuf mixture composition.

Material	Product	Proportion by Weight
Cement	Lafarge, Class H, Joppa, MO	1.00
Sand	US Silica, F55, Ottawa, IL	0.967
Silica flour	US Silica, Sil-co-Sil 75, Berkeley Springs, WV	0.277
Silica fume	Elkem, ES 900 W	0.389
Superplasticizer	W.R. Grace, ADVA 170	0.0171
Water (tap)	Vicksburg, MS municipal water	0.208
Steel fibers[1]	Bekaert, Dramix® ZP305	0.310
[1] Steel fibers used in Cor-Tuf1 material only		

The steel fiber incorporated into Cor-Tuf was the Dramix® ZP305 product from Bekaert Corporation (Figure 1). The ZP305 fibers were adhered together in bundles with a water-soluble adhesive when purchased. During the mixing process, the fibers dispersed as the adhesive dissolved in the fresh concrete. The steel fibers were introduced into the fresh concrete mixture after reaching a flowable paste-like consistency. Ideally, mixing results in random orientation of the fibers within the cementitous matrix. The manufacturer's product data sheet stated that the ZP305 fibers were approximately 30 mm long, had a diameter of approximately 0.55 mm, and were hooked at each end. The tensile strength for the steel fibers was reported by the manufacturer to be 1,100 MPa.

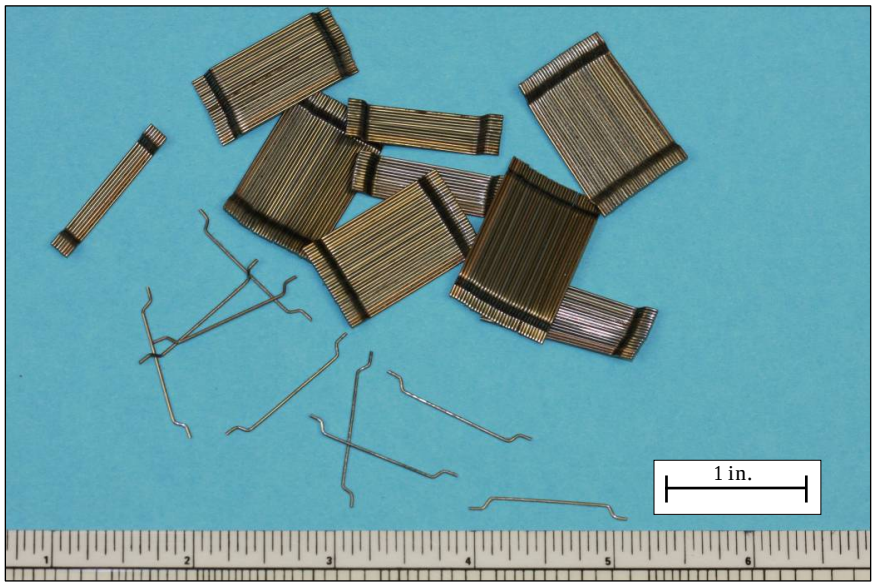

Figure 1. Bekaert Dramix® ZP305 fibers.

The test specimens used in this investigation were prepared from samples cored from 56-cm-diameter solid cylinders of Cor-Tuf1 and 2. The concretes in the solid drums were placed by personnel of the ERDC Concrete and Materials Branch (CMB).

Processing, curing, specimen preparation, and quality testing

The Cor-Tuf concretes prepared for the characterization presented herein required specific processing conditions. Batch mixing was accomplished using a high-shear batch plant with a capacity of 1 m^3. For optimal mixing, the batches were sized to yield about 0.6 m^3, or about 60% capacity. This size assured that enough material was present to completely engage the mixing paddles while not exceeding the torque limit of the mixer motors.

The four dry constituent materials were pre-weighed, loaded into the mixer by hand, and dry-blended for five minutes. The water and super-plastizer were pre-weighed and combined before being gradually added to the dry mixture while actively mixing. Mixing time was approximately 15 min to achieve a wetted, flowable paste. In the case of Cor-Tuf1, a pre-weighed amount of steel fibers were added by hand to the mixer under shear, and the concrete was then allowed to mix for about 10 more minutes. In the case of Cor-Tuf2, which did not receive steel fibers, the concrete was mixed for about 10 min beyond the paste condition so that the two preparations received equivalent total mixing times.

A variety of specimens were cast by CMB to determine the unconfined compressive strength of Cor-Tuf. From Cor-Tuf2, six 75-mm-diam by 150-mm-high cylinders were cast for strength testing, and one galvanized steel washtub was filled to form a bulk cylinder for subsequent coring. Six 75-mm by 150-mm cylinders, six 100-mm by 200-mm cylinders, and one washtub were cast from Cor-Tuf1. Additionally, Cor-Tuf1 was sampled prior to adding steel fibers, and three 75-mm by 150-mm cylinders were cast for comparison with Cor-Tuf2.

The Cor-Tuf underwent a prescribed curing regimen. The fresh specimens were placed in an environmentally controlled facility at 22°C and 100% humidity. They were removed from their molds, returned to the facility after 24 hr, and remained there until 7-days' age. The specimens were then submerged in a water bath that was maintained at 85°C for 4 days. Finally, they were dried in an oven for 2 days at 85°C for a cumulative age of 13 days.

The cured cylinders were tested to determine their unconfined compressive strengths according to American Society for Testing and Materials (ASTM) C 39 (ASTM 2005a); these results are listed in Table 2. The large bulk cylinders of each material were cored at CMB, and test specimens were prepared for additional mechanical property tests.

Table 2. Unconfined compressive strengths for Cor-Tuf sample cylinders.

Cor-Tuf1 UC Strength, MPa			Cor-Tuf2 UC Strength, MPa
75-by 150-mm Cylinder	100-by 200-mm Cylinder	75-by 150-mm Cylinder Without Steel Fibers	75-by 100-mm Cylinder
237	216	216	228
231	219	208	225
243	226	206	209
233	228		190
238	229		225
244			209

Composition property tests

Prior to performing the mechanical property tests, the height, diameter, and weight of each test specimen were determined. These measurements were used to compute the specimen's wet, bulk, or "as-tested" density. Results from these determinations are provided in Table 3 for the Cor-Tuf1 concrete and Table 4 for the Cor-Tuf2 concrete. Measurements of posttest water content[1] were conducted in accordance with procedures given in ASTM D 2216 (ASTM 2005d). Based on the appropriate values of posttest water content, wet density, and an assumed specific gravity (2.93 for Cor-Tuf1 concrete and 2.77 for Cor-Tuf2 concrete), values of dry density, porosity, degree of saturation, and volumes of air, water, and solids were calculated (Tables 3 and 4). These tables also list the maximum, minimum, and mean values and the standard deviation about the mean for each quantity. The Cor-Tuf1 specimens had a mean wet density of 2.557 Mg/m^3, a mean water content of 2.73%, and a mean dry density of

[1] Water content is defined as the weight of water removed during drying in a standard oven divided by the weight of dry solids.

Table 3. Physical and composition properties of Cor-Tuf1 concrete.

Test Number	Type of Test	Wet Density Mg/m³	Posttest Water Content %	Dry Density Mg/m³	Porosity %	Degree of Saturation %	Volume of Air %	Volume of Water %	Volume of Solids %	Axial P-wave Velocity km/s	Radial P-wave Velocity km/s	Axial S-wave Velocity km/s	Radial S-wave Velocity km/s
01	UC	2.584	2.79	2.514	14.20	49.40	7.18	7.01	85.80	5.12	4.97	3.15	3.19
02	UC	2.552	2.68	2.485	15.18	43.89	8.52	6.66	84.82	5.04	4.97	3.11	3.15
03	HC	2.552	1.64	2.510	14.32	28.75	10.20	4.12	85.68	5.04	4.95	3.14	3.13
04	HC	2.563	1.60	2.523	13.89	29.07	9.85	4.04	86.11	4.99	4.93	3.12	3.11
05	UX	2.551	3.51	2.464	15.89	54.42	7.24	8.65	84.11	5.01	4.93	3.13	3.16
06	UX	2.555	3.53	2.468	15.77	55.26	7.05	8.71	84.23	5.02	4.93	3.11	3.11
07	TXC/50	2.533	2.67	2.467	15.81	41.65	9.23	6.59	84.19	5.06	4.98	3.12	3.15
08	TXC/50	2.559	2.34	2.501	14.66	39.92	8.80	5.85	85.34	5.04	4.94	3.13	3.10
09	TXC/100	2.524	3.78	2.432	17.00	54.07	7.81	9.19	83.00	5.18	5.00	3.17	3.17
10	TXC/100	2.593	3.01	2.517	14.09	53.76	6.52	7.58	85.91	5.07	5.01	3.14	3.16
11	TXC/200	2.553	3.73	2.462	15.99	57.43	6.81	9.18	84.01	5.07	4.95	3.12	3.13
13	TXC/200	2.565	4.03	2.466	15.85	62.68	5.92	9.94	84.15	5.01	4.99	3.10	3.11
15	TXC/300	2.557	4.04	2.457	16.14	61.53	6.21	9.93	83.86	5.02	4.93	3.13	3.09
16	TXC/300	2.612	3.84	2.515	14.16	68.23	4.50	9.66	85.84	5.07	4.96	3.16	3.15
17	TXC/10	2.565	2.69	2.498	14.74	45.60	8.02	6.72	85.26	5.07	4.99	3.13	3.13
18	TXC/10	2.539	2.46	2.478	15.44	39.47	9.35	6.09	84.56	5.05	4.95	3.13	3.14
19	TXC/20	2.562	2.41	2.501	14.63	41.19	8.61	6.03	85.37	5.05	4.99	3.14	3.21
20	TXC/20	2.555	2.72	2.488	15.10	44.81	8.33	6.77	84.90	5.01	4.89	3.13	3.18
21	UX/CV	2.548	2.43	2.487	15.11	39.99	9.07	6.04	84.89	5.02	4.85	3.08	3.12
22	UX/CV	2.555	3.70	2.464	15.91	57.29	6.80	9.12	84.09	5.05	4.96	3.14	3.17
23	DP	2.557	1.11	2.529	13.70	20.48	10.90	2.81	86.30	5.00	4.91	3.11	3.14
24	DP	2.535	1.14	2.506	14.46	19.75	11.61	2.86	85.54	5.02	4.93	3.13	3.12
25	DP	2.553	0.88	2.531	13.62	16.35	11.40	2.23	86.38	5.03	4.92	3.14	3.11
N		23	23	23	23	23	23	23	23	23	23	23	23
Mean		2.557	2.73	2.490	15.03	44.57	8.26	6.77	84.97	5.04	4.95	3.13	3.14
Stdv		0.019	0.965	0.027	0.909	14.278	1.817	2.356	0.909	0.040	0.039	0.020	0.029
Max		2.612	4.04	2.531	17.00	68.23	11.61	9.94	86.38	5.18	5.01	3.17	3.21
Min		2.524	0.88	2.432	13.62	16.35	4.50	2.23	83.00	4.99	4.85	3.08	3.09

Table 4. Physical and composition properties of Cor-Tuf2 concrete.

Test Number	Type of Test	Wet Density Mg/m3	Posttest Water Content %	Dry Density Mg/m3	Porosity %	Degree of Saturation %	Volume of Air %	Volume of Water %	Volume of Solids %	Axial P-wave Velocity km/s	Radial P-wave Velocity km/s	Axial S-wave Velocity km/s	Radial S-wave Velocity km/s
01	HC	2.343	1.36	2.312	16.55	19.00	13.40	3.14	83.45	5.05	4.97	3.14	3.25
02	UX	2.347	3.99	2.257	18.51	48.66	9.50	9.01	81.49	5.11	4.96	3.21	3.26
03	HC	2.320	1.46	2.286	17.46	19.12	14.12	3.34	82.54	5.03	4.95	3.16	3.25
04	UX	2.324	3.97	2.235	19.30	45.97	10.43	8.87	80.70	5.05	4.96	3.18	3.24
05	TXC/10	2.322	2.39	2.267	18.14	29.87	12.72	5.42	81.86	5.07	4.97	3.17	3.22
06	TXC/10	2.310	3.01	2.243	19.04	35.46	12.29	6.75	80.96	5.05	4.94	3.20	3.25
07	TXC/20	2.319	2.78	2.257	18.54	33.84	12.26	6.27	81.46	5.03	4.97	3.13	3.23
08	TXC/20	2.337	2.16	2.287	17.42	28.35	12.48	4.94	82.58	5.10	4.98	3.18	3.29
09	TXC/50	2.314	2.93	2.248	18.83	34.99	12.24	6.59	81.17	5.08	4.99	3.17	3.26
10	TXC/50	2.341	3.56	2.261	18.38	43.80	10.33	8.05	81.62	5.09	4.99	3.19	3.26
11	TXC/100	2.334	3.53	2.255	18.60	42.79	10.64	7.96	81.40	5.02	4.99	3.16	3.24
13	UX/CV	2.335	3.96	2.246	18.90	47.06	10.01	8.90	81.10	5.04	4.98	3.17	3.22
14	UX/CV	2.335	3.96	2.246	18.90	47.06	10.01	8.90	81.10	5.04	4.98	3.17	3.22
15	UX	2.320								5.03	4.96	3.15	3.24
16	UX/CV	2.317								5.07	4.95	3.18	3.26
17	TXC/100	2.321	3.27	2.248	18.85	39.00	11.50	7.35	81.15	5.04	4.97	3.17	3.26
18	TXC/200	2.335	4.28	2.239	19.17	49.98	9.59	9.58	80.83	5.07	4.97	3.17	3.23
19	TXC/200	2.332	4.34	2.235	19.31	50.25	9.61	9.70	80.69	5.00	4.98	3.16	3.23
20	TXC/300	2.329	4.17	2.236	19.28	48.36	9.96	9.32	80.72	5.07	4.98	3.16	3.24
21	TXC/300	2.327	4.52	2.227	19.61	51.32	9.55	10.07	80.39	5.02	4.97	3.17	3.23
23	UC	2.336	3.58	2.256	18.57	43.48	10.50	8.08	81.43	5.08	4.99	3.17	3.23
24	UC	2.318	3.66	2.236	19.26	42.50	11.08	8.19	80.74	5.00	4.98	3.16	3.24
26	DP	2.330	1.10	2.304	16.81	15.08	14.27	2.53	83.19	5.04	4.99	3.16	3.26
N		23	21	21	21	21	21	21	21	23	23	23	23
Mean		2.328	3.24	2.256	18.54	38.85	11.26	7.28	81.46	5.05	4.97	3.17	3.24
Stdv		0.010	1.023	0.023	0.838	11.061	1.541	2.261	0.838	0.030	0.014	0.017	0.018
Max		2.347	4.52	2.312	19.61	51.32	14.27	10.07	83.45	5.11	4.99	3.21	3.29
Min		2.310	1.10	2.227	16.55	15.08	9.50	2.53	80.39	5.00	4.94	3.13	3.22

2.490 Mg/m^3. The Cor-Tuf2 specimens had a mean wet density of 2.328 Mg/m^3, a mean water content of 3.24%, and a mean dry density of 2.256 Mg/m^3.

Ultrasonic pulse-velocity determinations

Prior to performing the mechanical property tests, ultrasonic pulse-velocity measurements were collected on each test specimen. This involved measuring the transit distance and time for each P-wave (compressional) or S-wave (shear) pulse to propagate through a given specimen. The velocity was then computed by dividing the transit distance by the transit time. A matching pair of 1-MHz piezoelectric transducers were used to transmit and receive the ultrasonic P-waves. A pair of 2.25-MHz piezoelectric transducers were used to transmit and receive the ultrasonic S-waves. The transit time was measured with a 100-MHz digital oscilloscope and the transit distance with a digital micrometer. All of these velocity determinations were made under atmospheric conditions, i.e., no prestress of any kind was applied to the specimens. The tests were conducted in accordance with procedures given in ASTM C 597 (ASTM 2005c).

One compressional-wave (P-wave) and one shear-wave (S-wave) velocity were determined axially through each specimen. Six radial P-wave velocities were determined, i.e., two transverse to each other at elevations of 1/4, 1/2, and 3/4 of the specimen height. Two radial S-wave velocities were measured; both of these determinations were made at the mid-height of the specimen transverse to each other. The various P- and S-wave velocities determined for the test specimens are provided in Tables 3 and 4. The radial-wave velocities listed in Tables 3 and 4 are the average values.

Mechanical property tests

All of the mechanical property tests were conducted quasi-statically with axial strain rates on the order of 10^{-4} to 10^{-5} per second and times to peak load on the order of 5 to 30 min. Mechanical property data were obtained under several stress and strain paths. Undrained compressibility data were obtained during the hydrostatic loading phases of the triaxial compression (TXC) tests and from two hydrostatic compression (HC) tests. Shear and failure data were obtained from unconfined compression (UC) tests, unconsolidated-undrained TXC tests, and direct pull (DP) tests. One-dimensional compressibility data were obtained from undrained uniaxial strain (UX) tests with lateral stress measurements. Undrained strain-path

tests were also conducted during the test program. All of the strain-path tests were initially loaded under uniaxial strain boundary conditions to a prescribed level of stress or strain. At the end of the UX loading, a constant axial-to-radial-strain ratio (ARSR) of -2.0 was applied. The ARSR = -2.0 path is a constant volumetric strain loading path, and these paths will be referred to as UX/CV tests. The terms undrained and unconsolidated signify that no pore fluid (liquid or gas) was allowed to escape or drain from the membrane-enclosed specimens. The completed test matrix for Cor-Tuf1 concrete is presented in Table 5, and Table 6 presents the test matrix for Cor-Tuf2 concrete. Tables 5 and 6 list the types of tests conducted, the number of tests, the test numbers for each group, and the nominal peak radial stress applied to specimens prior to shear loading or during the HC, UX, or strain-path loading.

Table 5. Completed Cor-Tuf1 concrete test matrix.

Type of Test	No. of Tests	Test Nos.	Nominal Peak Radial Stress, MPa
Hydrostatic compression	2	3, 4	510
Triaxial compression	2	1, 2	0
	2	17, 18	10
	2	19, 20	20
	2	7, 8	50
	2	9, 10	100
	2	11, 13	200
	2	15, 16	300
UX strain	2	5, 6	510
UX/CV	1	21	50
	1	22	100
Direct Pull	3	23, 24, 25	0
Total # tests:	23		

Specimen preparation

The mechanical property test specimens were cut from sections of the Cor-Tuf1 and Cor-Tuf2 concrete using a diamond-bit core barrel by following the procedures provided in ASTM C 42 (ASTM 2005b). The test specimens were cut to the correct length, and the ends were ground flat and parallel to each other and perpendicular to the sides of the core in accordance with procedures in ASTM D 4543 (ASTM 2005e). The prepared test specimens had a nominal height of 110 mm and diameter of 50 mm.

Table 6. Completed Cor-Tuf2 concrete test matrix.

Type of Test	No. of Tests	Test Nos.	Nominal Peak Radial Stress, MPa
Hydrostatic compression	2	1, 3	510
Triaxial compression	2	23, 24	0
	2	5, 6	10
	2	7, 8	20
	2	9, 10	50
	2	11, 17	100
	2	18, 19	200
	2	20, 21	300
UX strain	3	2, 4, 15	510
UX/CV	1	13	50
	1	14	100
	1	16	200
DP	1	26	0
Total # tests:	23		

Prior to testing, each specimen was placed between hardened steel top and base caps. With the exception of the UC and the DP test specimens, two 0.6-mm-thick membranes and an Aqua seal® membrane were placed around the specimen. The exterior of the outside membrane was coated with a liquid synthetic rubber to inhibit deterioration caused by the confining-pressure fluid (Figure 2). The fluid was a mixture of kerosene and hydraulic oil. Finally, the specimen, along with its top cap and base cap assembly, was placed on the instrumentation stand of the test apparatus, and the instrumentation setup was initiated.

Test devices

Three sets of test devices were used in this test program. The axial load for all of the UC tests was provided by a 3.3-MN (750,000-lb) loader. The application of load was manually controlled with this test device. No pressure vessel was required for the UC tests; only a base, load cell, and vertical and radial deformeters were necessary.

Direct pull tests were performed by using the direct pull apparatus, in which end caps were attached to unconfined specimens with Sikadur® Crack Fix structural epoxy. A manual hydraulic pump was used to pressurize the direct pull chamber. When the direct pull chamber is pressurized, a piston retracts, producing tensile loading in the test specimen. Measurements for the loading of the specimen were recorded by the load cell.

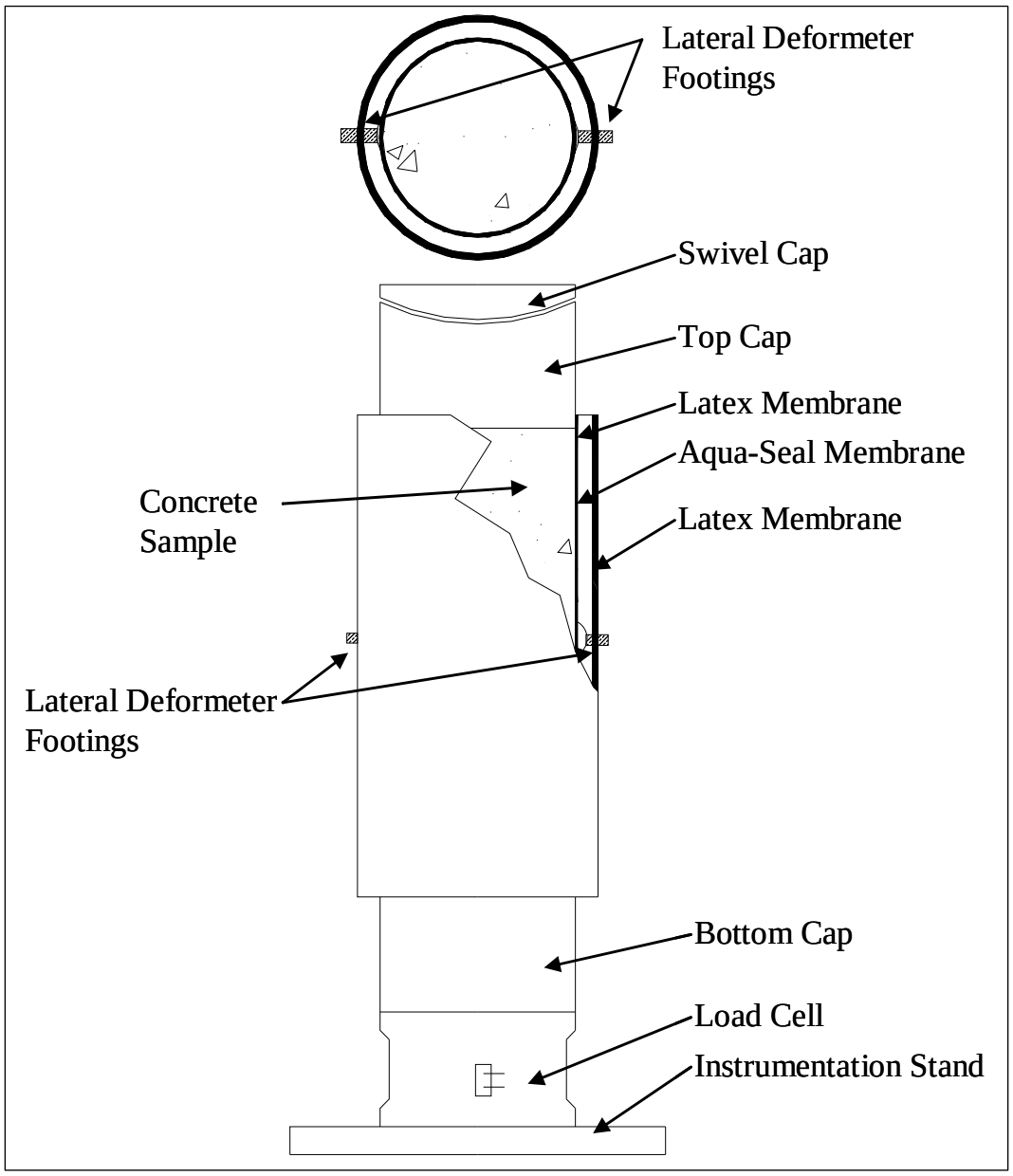

Figure 2. Typical test specimen setup.

All of the remaining tests were conducted in a 600-MPa capacity pressure vessel (Figure 3), and the axial load was provided by an 8.9-MN loader. With this loader, the application of load, pressure, and axial displacement were regulated by a servo-controlled data acquisition system. This servo-controlled system allowed the user to program rates of load, pressure, and axial displacement to achieve the desired stress or strain path. Confining pressure was measured external to the pressure vessel by a pressure transducer mounted in the confining fluid line. A load cell mounted in the base

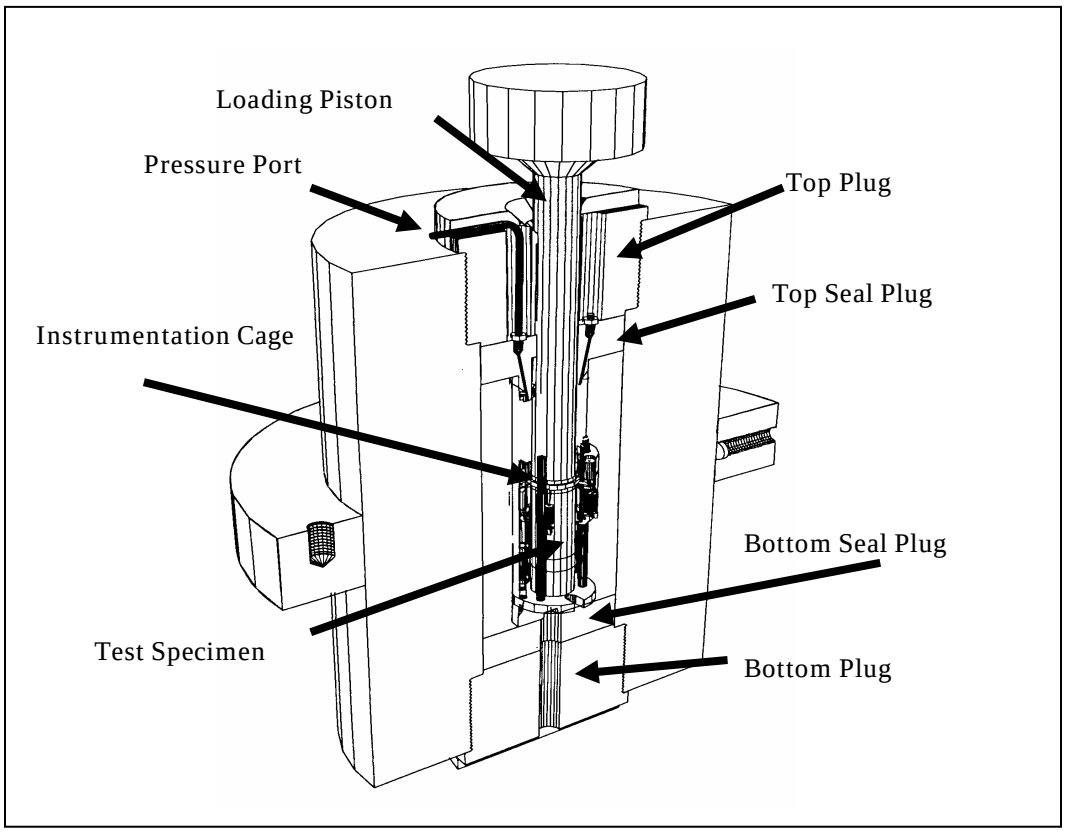

Figure 3. 600-MPa pressure vessel details.

of the specimen pedestal was used to measure the applied axial loads inside the pressure vessel (Figure 2).

Outputs from the various instrumentation sensors were electronically amplified and filtered, and the conditioned signals recorded by computer-controlled 16-bit analog-to-digital converters. The data acquisition systems were programmed to sample the data channels every 1 to 5 sec, convert the measured voltages to engineering units, and store the data for further posttest processing.

Test instrumentation

The vertical deflection measurement system in all the test areas except the DP test area consisted of two linear variable differential transformers (LVDTs) mounted vertically on the instrumentation stands and positioned 180-deg apart. They were oriented to measure the displacement between the top and base caps, thus providing a measure of the axial deformations of the specimen. For the confined tests, a linear potentiometer was mounted external to the pressure vessel to measure the displacement

of the piston through which axial loads were applied. This provided a backup to the vertical LVDTs, in case they exceeded their calibrated range.

Two types of radial deflection measurement systems (lateral deformeters) were used in this test program. The output of each deformeter was calibrated to the radial displacement of the two footings that were glued to the sides of the test specimen (Figure 2). These two small steel footings were mounted 180-deg apart at the specimen's mid-height. The footing faces were machined to match the curvature of the test specimen. A threaded post extended from the outside of each footing and protruded through the membrane. The footings were mounted to the specimen prior to placement of the membrane. Once the membranes were in place, steel caps were screwed onto the threaded posts to seal the membrane to the footing. The lateral deformeter ring was attached to these steel caps with setscrews. The completed specimen lateral deformeter setup is shown in Figure 4.

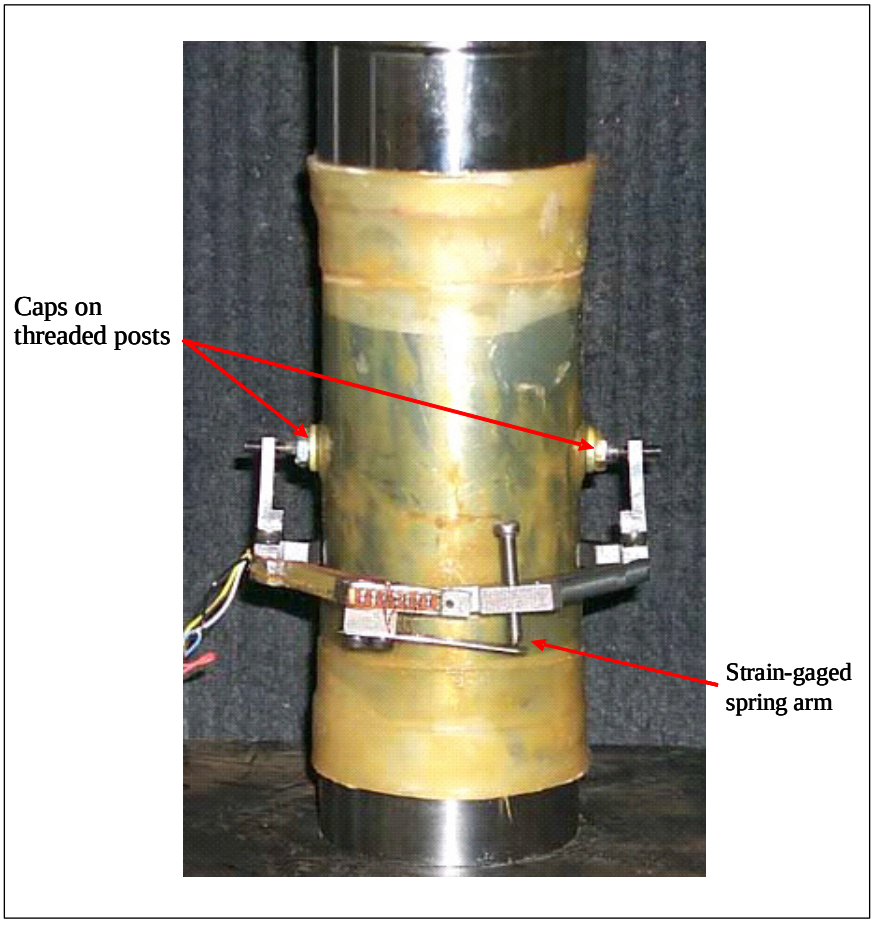

Figure 4. Spring-arm lateral deformeter mounted on test specimen.

One type of lateral deformeter consisted of an LVDT mounted on a hinged ring; the LVDT measured the expansion or contraction of the ring. This lateral deformeter was used over smaller ranges of radial deformation when the greatest measurement accuracy was required. This lateral deformeter was used for all of the HC, UC, UX, and strain-path tests. This design is similar to the radial-deformeter design provided by Bishop and Henkel (1962). When the specimen expanded (or contracted), the hinged-deformeter ring opened (or closed), causing a change in the electrical output of the horizontally mounted LVDT.

The second type of lateral deformeter, which was used for all of the TXC tests, consisted of two strain-gaged, steel springarms mounted on a double-hinged ring; the strain-gaged arms deflected as the ring expanded or contracted. This lateral deformeter was used when the greatest radial deformation range was required and therefore, was less accurate than the LVDT deformeter. With this deformeter, when the specimen expanded or contracted, the rigid deformeter ring flexed about its hinge, causing a change in the electrical output of the strain-gaged spring-arm. The output of the spring-arms was calibrated to the specimen's deformation. Radial measurements were not performed during the DP tests.

Test descriptions

The TXC tests were conducted in two phases. During the first phase, the hydrostatic compression phase, the cylindrical test specimen was subjected to an increase in hydrostatic pressure while measurements of the specimen's height and diameter changes were made. The data are typically plotted as pressure versus volumetric strain, the slope of which, assuming elastic theory, is the bulk modulus, K. The second phase of the TXC test, the shear phase, was conducted after the desired confining pressure was applied during the HC phase. While holding the desired confining pressure constant, axial load was increased, and measurements of the changes in the specimen's height and diameter were made. The axial (compressive) load was increased until the specimen failed. The shear data are generally plotted as principal stress difference versus axial strain, the slope of which represents Young's modulus, E. The maximum principal stress difference that a given specimen can support or the principal stress difference at 15% axial strain during the shear loading, whichever occurs first, is defined as the peak strength.

The UC tests were performed in accordance with ASTM C 39 (ASTM 2005a). The UC test is a TXC test in which no confining pressure is applied. The maximum principal stress difference observed during a UC test is defined as the unconfined compressive strength of the material.

Tension shear data were obtained for Cor-Tuf1 and Cor-Tuf2 concrete by performing direct pull (DP) tests. The DP tests have no confining pressure during the tests. To conduct the DP tests, end caps were attached with epoxy to the specimen. The end caps were screwed into the direct pull apparatus, and the specimen was pulled apart vertically when pressure was applied to the piston.

A uniaxial strain (UX) test was conducted by applying axial load and confining pressure simultaneously so that, as the cylindrical specimen shortened, its diameter remained unchanged, i.e., zero radial strain boundary conditions were maintained. The data are generally plotted as axial stress versus axial strain, the slope of which is the constrained modulus, M. The data are also plotted as principal stress difference versus mean normal stress, the slope of which is twice the shear modulus, G, divided by the bulk modulus, K, i.e., 2G/K, or, in terms of Poisson's ratio ν, $3(1-2\nu)/(1+\nu)$.

The strain-path tests in this test program were conducted in two phases. Initially, the specimen was subjected to a uniaxial-strain loading up to a desired level of mean normal, radial, or axial stress. At the end of the UX loading, a constant axial-to-radial-strain ratio of -2.0 was applied; these tests were identified earlier as UX/CV tests. In order to conduct these tests, the software controlling the servo-controls had to correct the measured inputs for system compressibility and for the nonlinear calibrations of specific transducers.

Definition of stresses and strains

During the mechanical property tests, measurements were typically made of the axial and radial deformations of the specimen as confining pressure and/or axial load was applied or removed. These measurements along with the pretest measurements of the initial height and diameter of the

specimen were used to convert the measured test data to true stresses and engineering strains.[1]

Axial strain, ε_a, was computed by dividing the measured axial deformation, Δh (change in height), by the original height, h_o, i.e., $\varepsilon_a = \Delta h / h_o$. Similarly, radial strain, ε_r, was computed by dividing the measured radial deformation, Δd (change in diameter), by the original diameter, d_o, i.e., $\varepsilon_r = \Delta d / d_o$. For this report, volumetric strain was assumed to be the sum of the axial strain and twice the radial strain, $\varepsilon_v = \varepsilon_a + 2\varepsilon_r$.

The principal stress difference, q, was calculated by dividing the axial load by the current cross-sectional area of the specimen, A, which is equal to the original cross-sectional area, A_o, multiplied by $(1 - \varepsilon_r)^2$. In equation form,

$$q = (\sigma_a - \sigma_r) = \frac{Axial\ Load}{A_o(1-\varepsilon_r)^2} \quad (1)$$

where σ_a is the axial stress and σ_r is the radial stress. The axial stress is related to the confining pressure and the principal stress difference by

$$\sigma_a = q + \sigma_r \quad (2)$$

The mean normal stress, p, is the average of the applied principal stresses. In cylindrical geometry,

$$p = \frac{(\sigma_a + 2\sigma_r)}{3} \quad (3)$$

[1] Compressive stresses and strains are positive in this report.

3 Analyses of Test Results for Cor-Tuf Concrete with Steel Fibers

Hydrostatic compression tests

Undrained compressibility data were obtained from two HC tests and during the hydrostatic loading phases of the 12 TXC tests. The pressure-volume data from the two HC tests are plotted in Figure 5. The initial dry densities of the specimens for HC tests 3 and 4 were 2.510 and 2.523 Mg/m^3, respectively. Figure 6 presents the pressure time-histories for the HC tests. During the HC tests, the pressure was intentionally held constant for a period of time prior to the unloading cycles. During each hold in pressure, the volumetric strains continued to increase, indicating that Cor-Tuf1 concrete was susceptible to creep (Figures 5 and 6). The Cor-Tuf1 concrete began to exhibit inelastic strains at a pressure level of approximately 300 MPa and at a volumetric strain of approximately 1%. This was the pressure and strain level at which the pressure-volume response and the initial bulk modulus began to soften appreciably. Based on the data from HC tests and the HC portion of the TXC tests, the initial elastic bulk modulus, K, for Cor-Tuf1 concrete is approximately 25.2 GPa.

Triaxial compression tests

Shear and failure data were successfully obtained from 2 unconfined compression tests and 12 unconsolidated-undrained TXC tests. Recall from Chapter 2 that the second phase of the TXC test, the shear phase, was conducted after the desired confining pressure is applied during the HC phase. The UC tests are a special type of TXC test without the application of confining pressure. Results from the UC tests are plotted in Figures 7 and 8, and results from the TXC tests are plotted in Figures 9 through 20. In all the figures, the axial and volumetric strains at the beginning of the shear phase were set to zero, i.e., only the strains during shear are plotted.

Stress-strain data from the two UC tests in Figures 7 and 8 are plotted as principal stress difference versus axial strain during shear and as principal stress difference versus volumetric strain during shear. Deformeters, instead of strain gages, were used to measure the axial and radial strains of the UC test specimens. During the UC tests, no attempt was made to capture the post-peak (or softening) stress-strain behavior of this material.

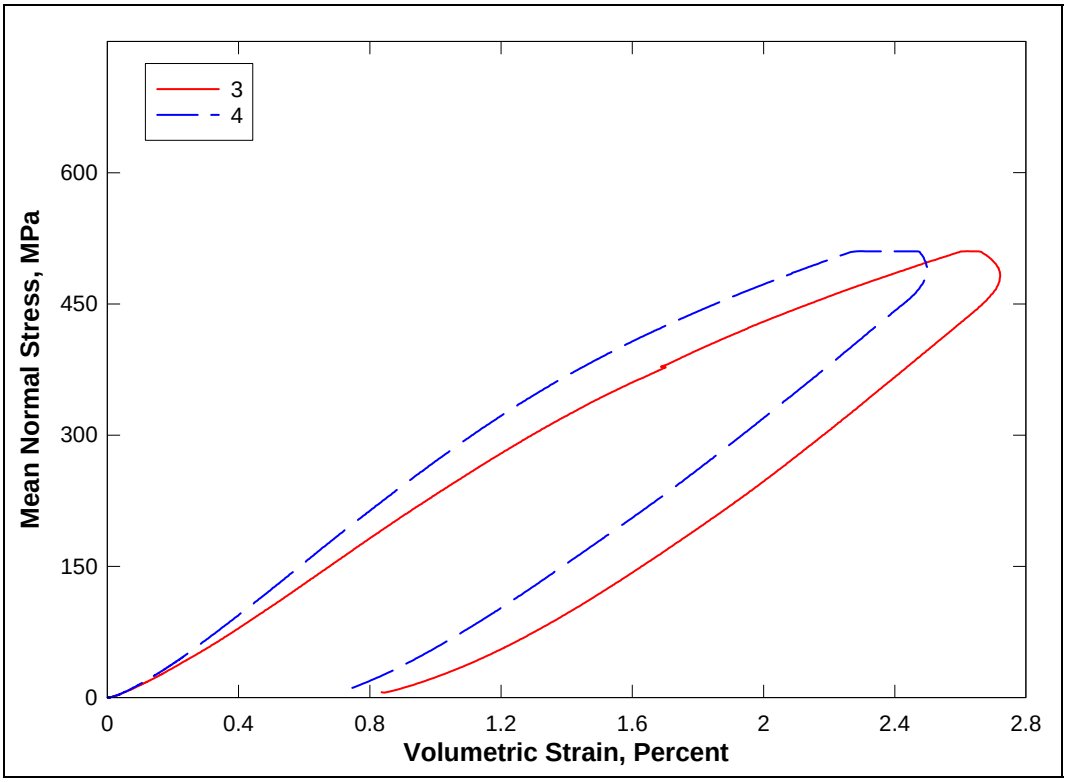

Figure 5. Pressure-volume responses from the HC tests on Cor-Tuf1 concrete.

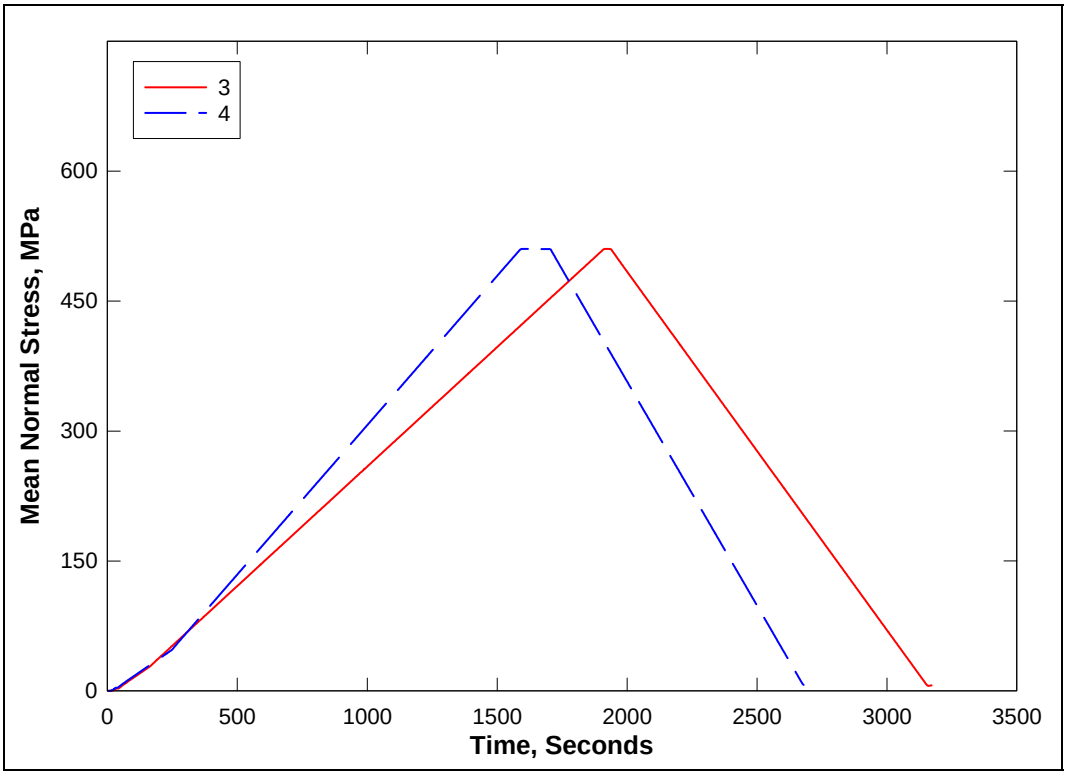

Figure 6. Pressure time-histories from the HC tests on Cor-Tuf1 concrete.

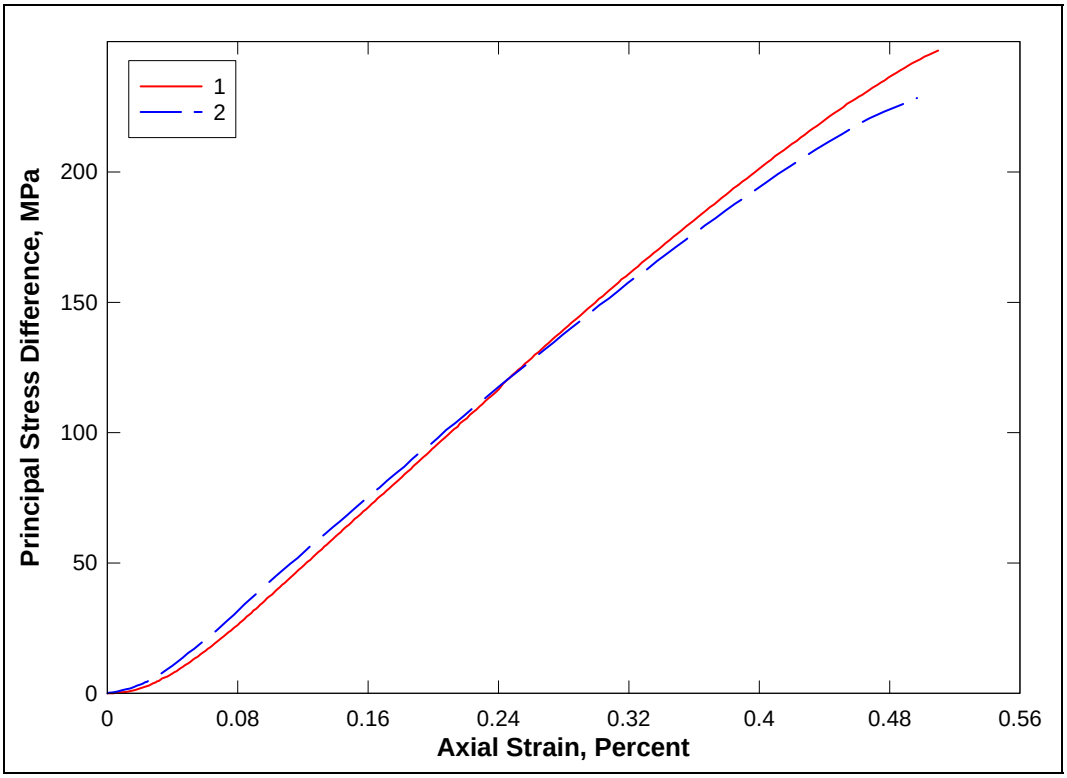

Figure 7. Stress-strain responses from UC tests on Cor-Tuf1 concrete.

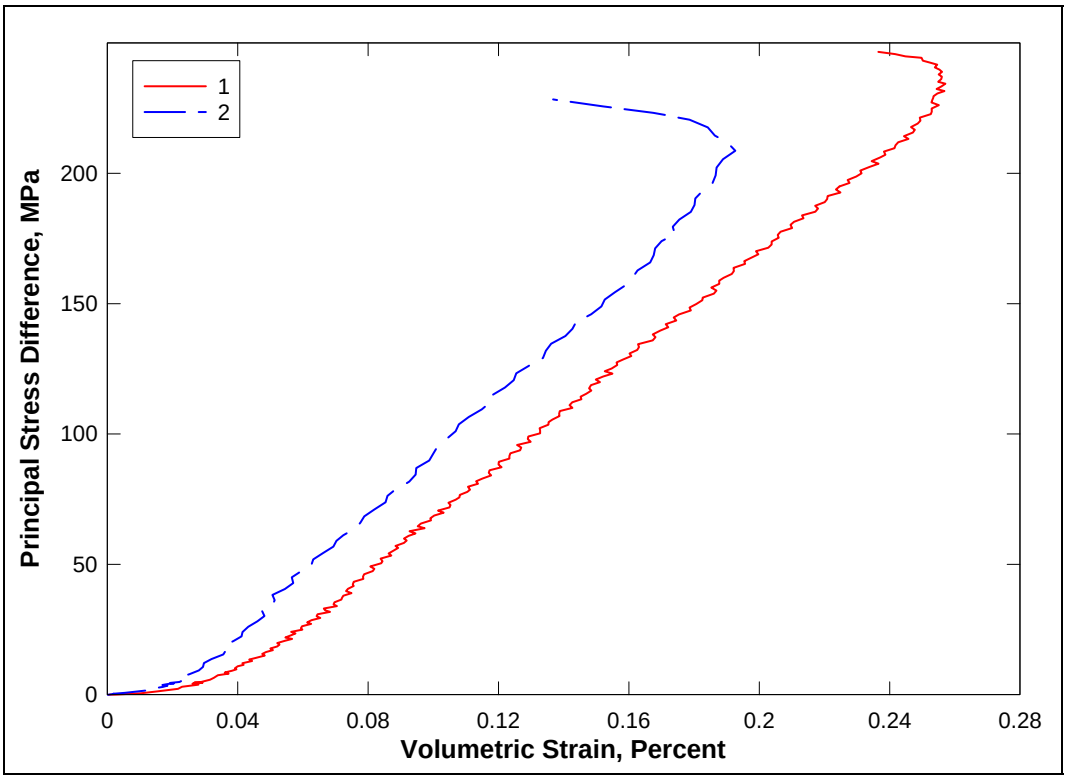

Figure 8. Stress difference-volumetric strain during shear from UC tests on Cor-Tuf1 concrete.

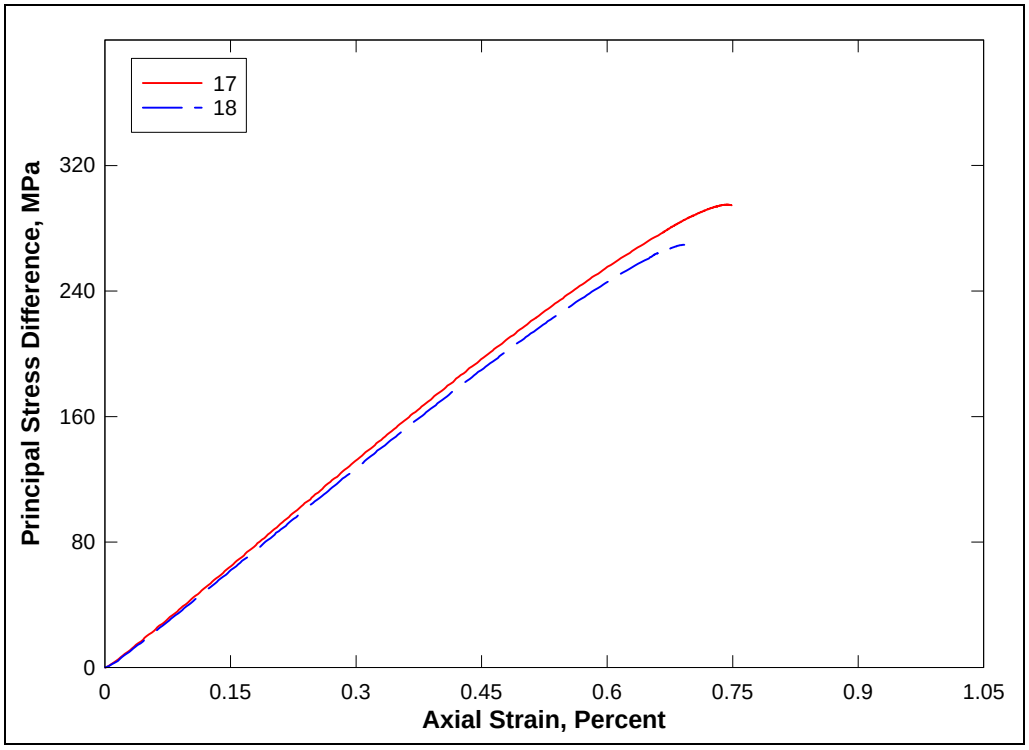

Figure 9. Stress-strain responses from TXC tests on Cor-Tuf1 concrete at a confining pressure of 10 MPa.

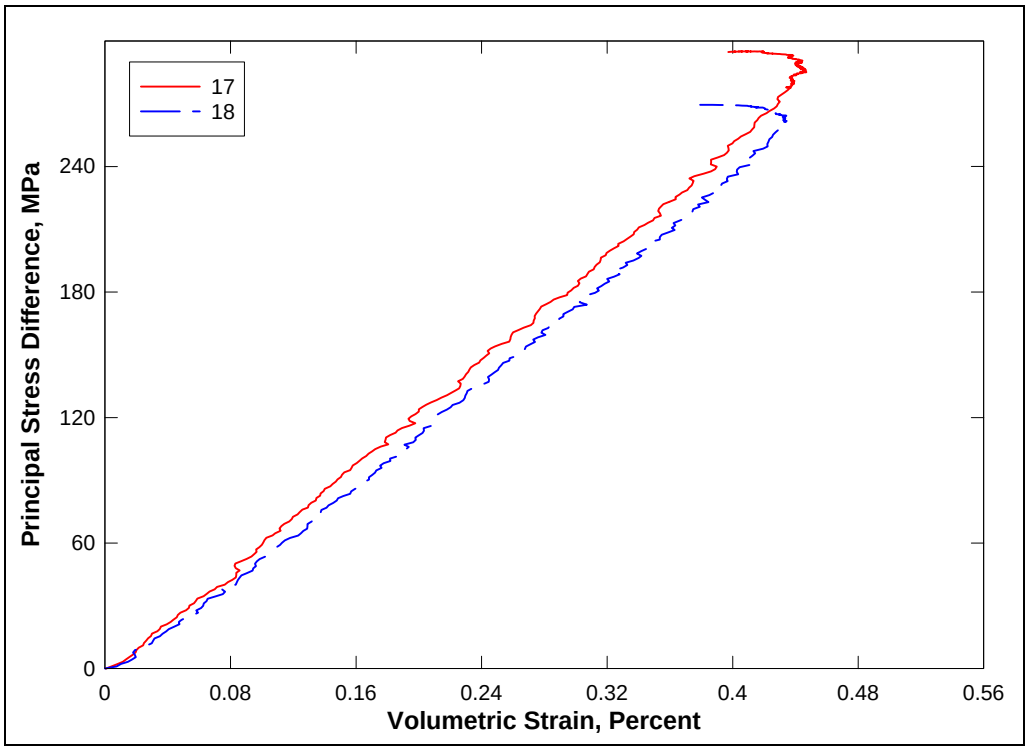

Figure 10. Stress difference-volumetric strain during shear from TXC tests on Cor-Tuf1 concrete at a confining pressure of 10 MPa.

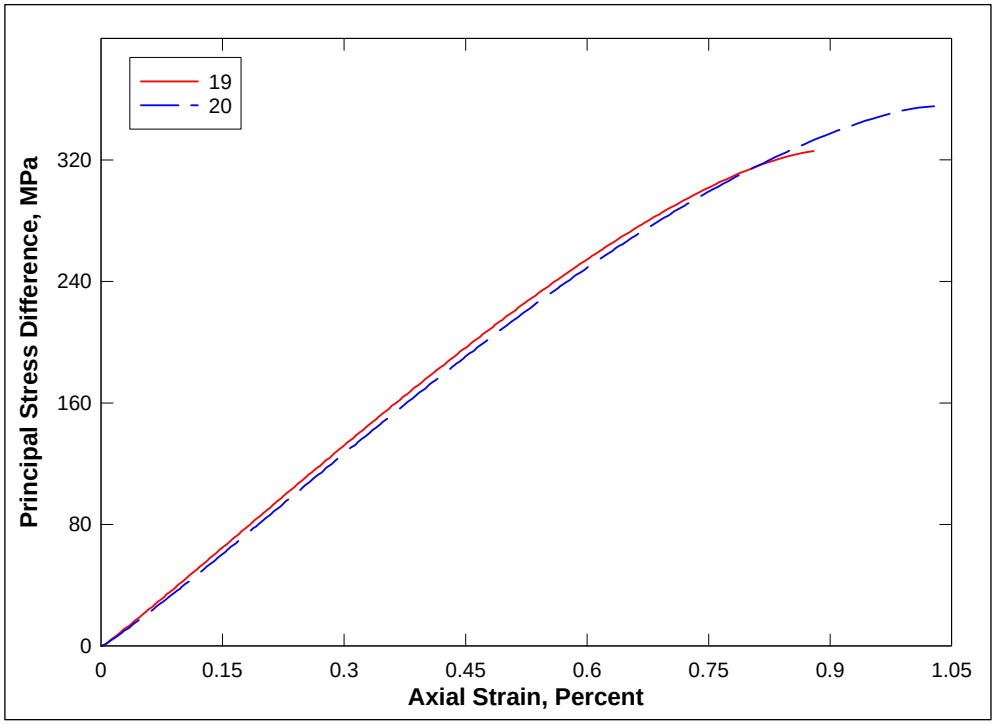

Figure 11. Stress-strain responses from TXC tests on Cor-Tuf1 concrete at a confining pressure of 20 MPa.

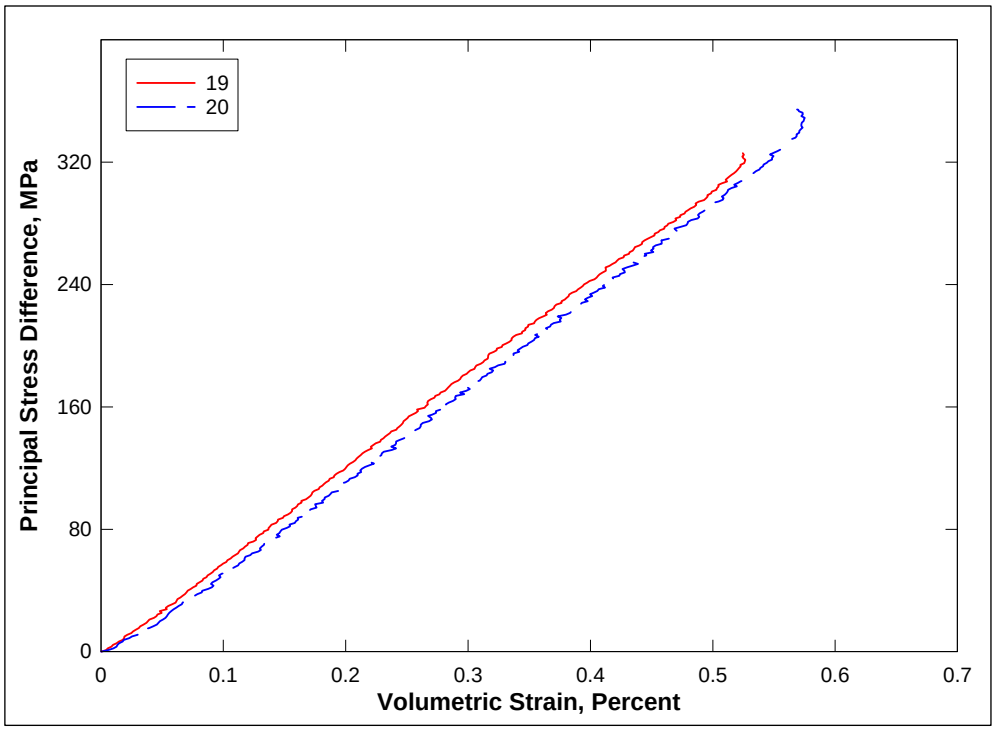

Figure 12. Stress difference-volumetric strain during shear from TXC tests on Cor-Tuf1 concrete at a confining pressure of 20 MPa.

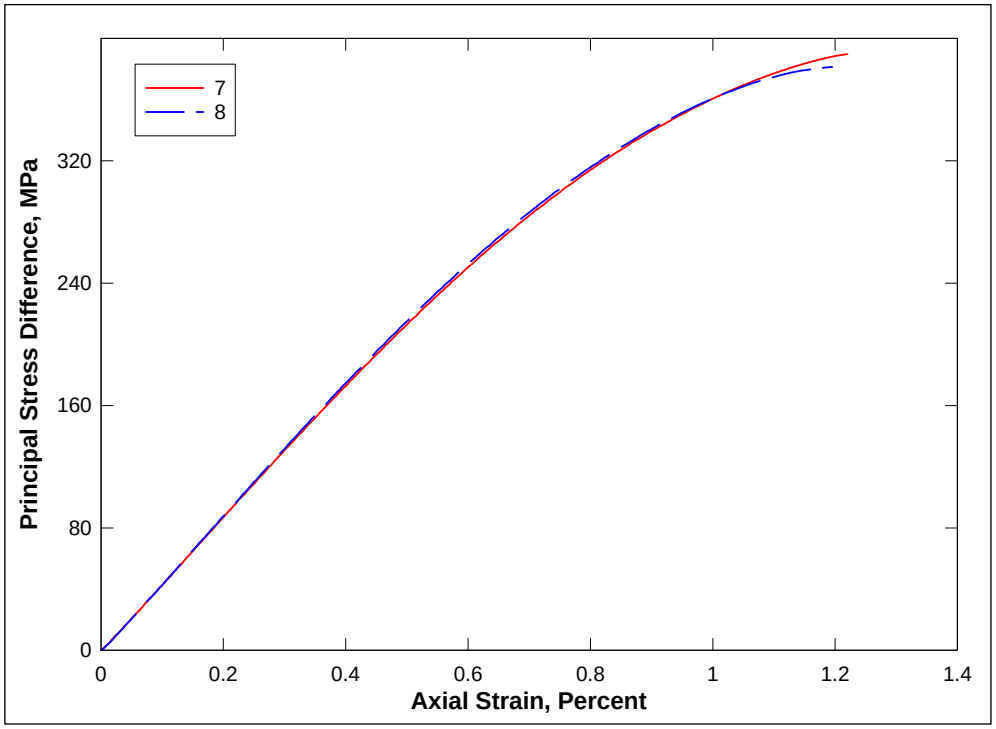

Figure 13. Stress-strain responses from TXC tests on Cor-Tuf1 concrete at a confining pressure of 50 MPa.

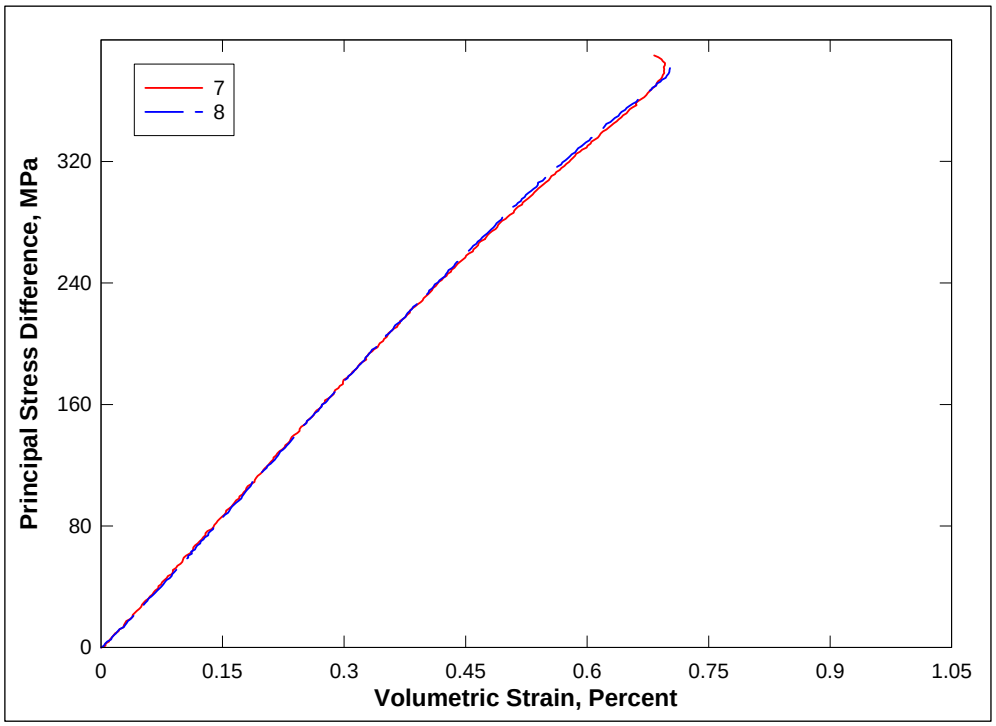

Figure 14. Stress difference-volumetric strain during shear from TXC tests on Cor-Tuf1 concrete at a confining pressure of 50 MPa.

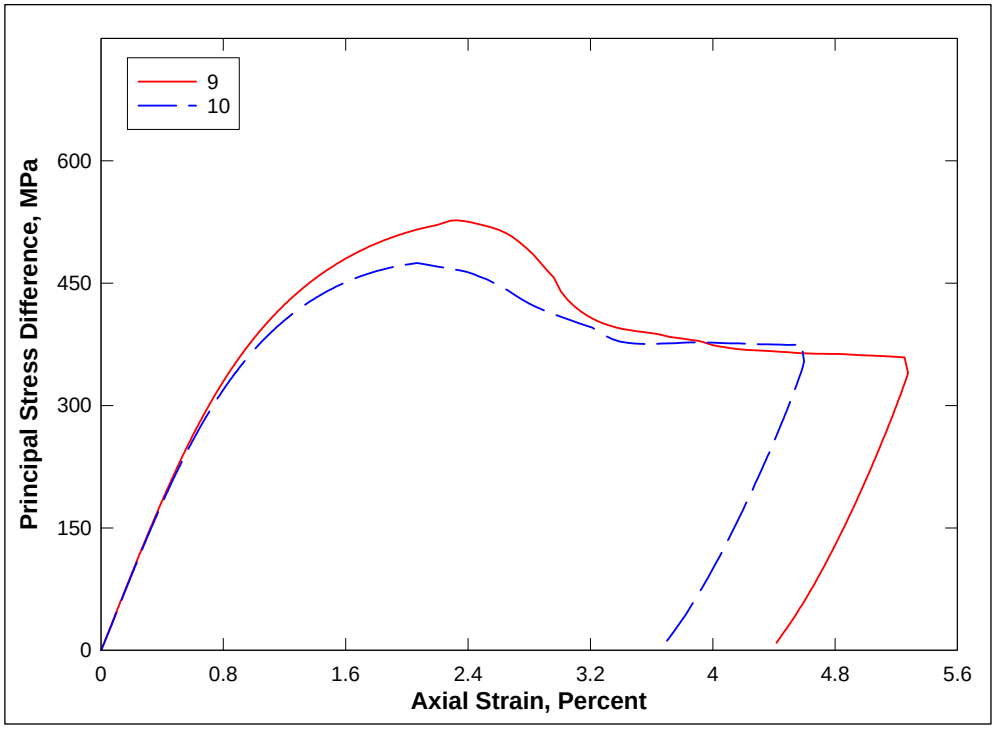

Figure 15. Stress-strain responses from TXC tests on Cor-Tuf1 concrete at a confining pressure of 100 MPa.

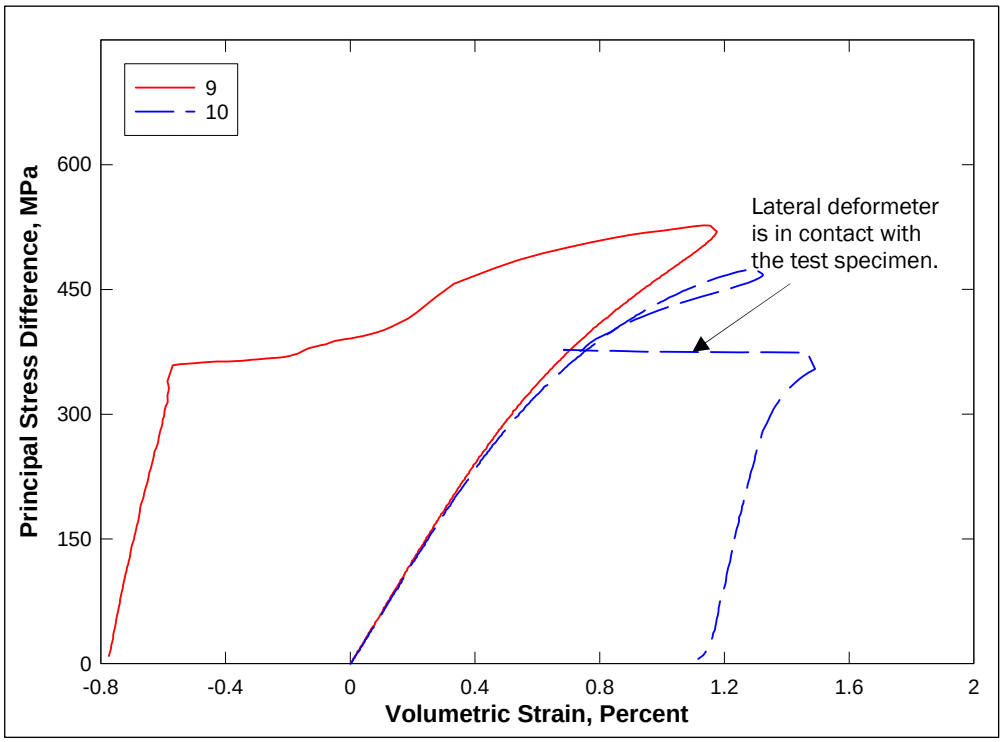

Figure 16. Stress difference-volumetric strain during shear from TXC tests on Cor-Tuf1 concrete at a confining pressure of 100 MPa.

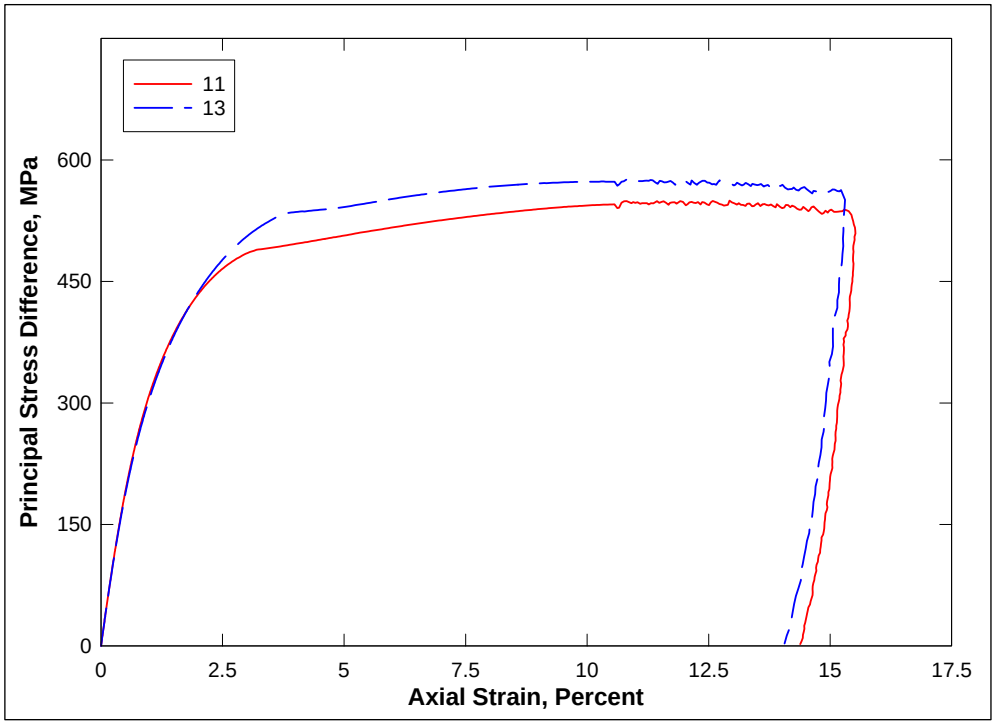

Figure 17. Stress-strain responses from TXC tests on Cor-Tuf1 concrete at a confining pressure of 200 MPa.

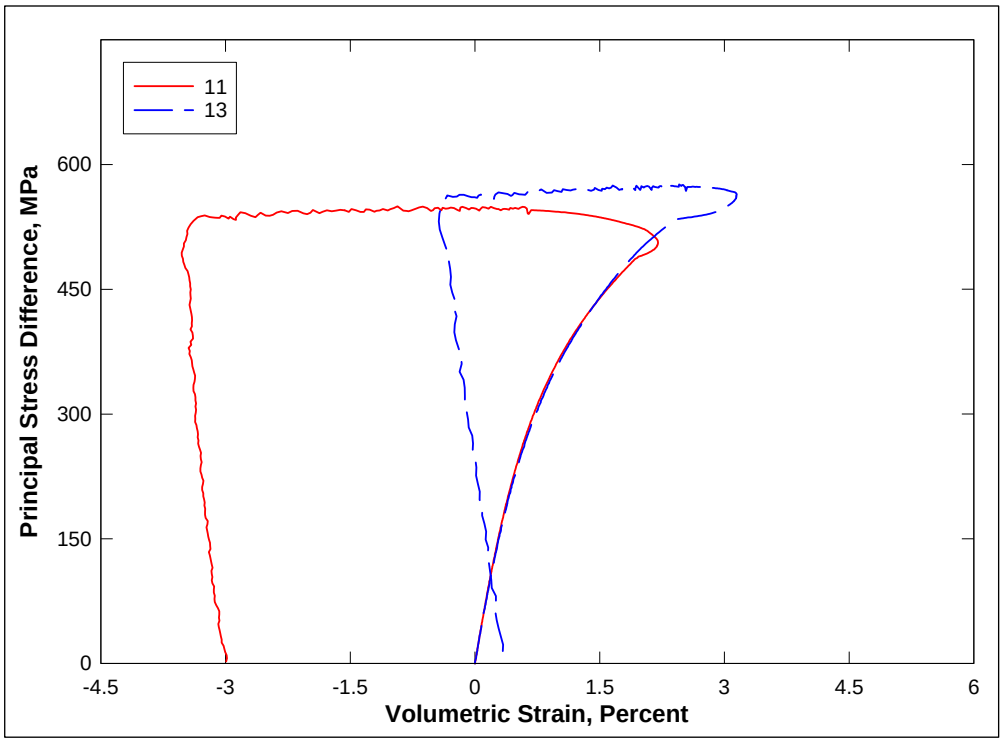

Figure 18. Stress difference-volumetric strain during shear from TXC tests on Cor-Tuf1 concrete at a confining pressure of 200 MPa.

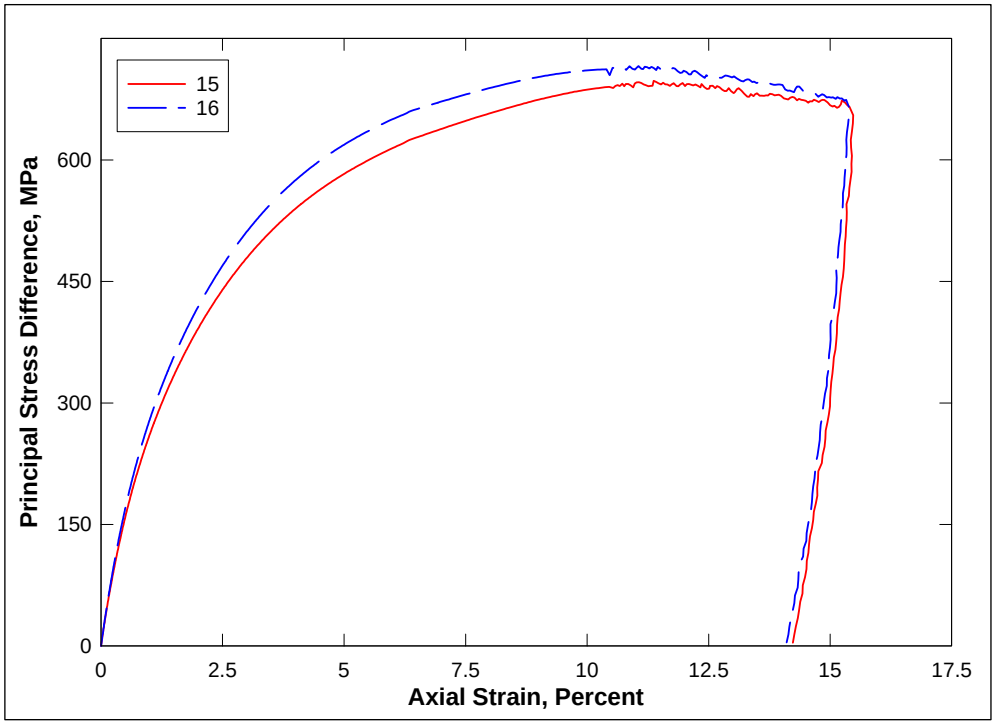

Figure 19. Stress-strain responses from TXC tests on Cor-Tuf1 concrete at a confining pressure of 300 MPa.

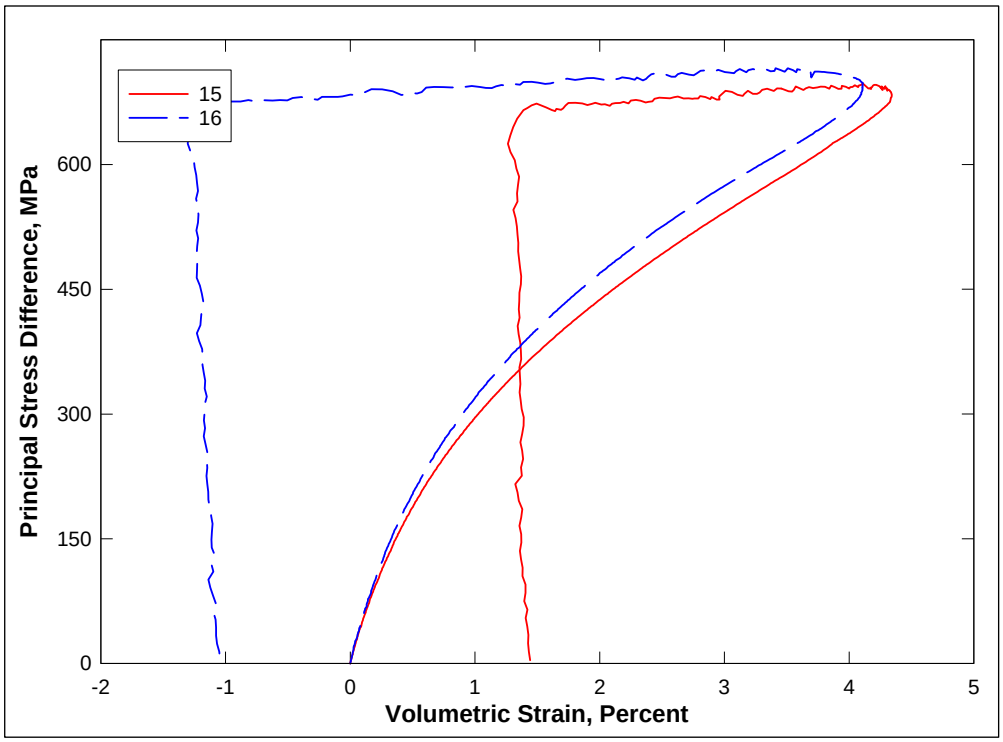

Figure 20. Stress difference-volumetric strain during shear from TXC tests on Cor-Tuf1 concrete at a confining pressure of 300 MPa.

The mean unconfined strength of Cor-Tuf1 concrete determined from both the UC specimens was 237 MPa. The initial dry densities for specimens 1 and 2 were 2.514 and 2.485 Mg/m^3, respectively.

Figures 9 through 20 present the results from the TXC tests conducted at nominal confining pressures of 10, 20, 50, 100, 200, and 300 MPa. The TXC test results are plotted as principal stress difference versus axial strain during shear and as principal stress difference versus volumetric strain during shear. The results were very good considering the inherent variability of the initial wet and dry densities and the water contents of the specimens. The wet densities of the TXC specimens ranged from 2.524 to 2.612 Mg/m^3, the dry densities ranged from 2.432 to 2.517 Mg/m^3, and the water contents ranged from 2.34 to 4.04%.

A few comments should also be made concerning the unloading results in general. The final unloading stress-strain responses at axial strains approaching 15% are less reliable than the unloadings at axial strains of less than 11%. The vertical deformeters went out of range at axial strains of approximately 11%. After that, an external deformeter with less resolution was used to measure axial displacement.

The reader should note the decrease in variations in the stress-strain data as pressure increased. The UC tests are very sensitive to small changes in the dry density and the specimen structure (Figures 7 and 8). This sensitivity resulted in variations of the initial loadings and peak strengths. The variations are less noticeable as confining pressures increase. This was a result of the confining pressure reducing the effects of differences in the initial inherent properties of the test specimens.

For comparison purposes, stress-strain data from the TXC tests are plotted in Figure 21. Figure 22 display the corresponding principal stress difference versus volumetric strain responses during shear. The initial loading of the TXC stress-strain responses are a function of the material's volume changes during shear and thus are dependent on the magnitude of the applied confining pressure and the position on the material's pressure-volume response relation. In Figure 21, the principal stress difference peaks and then drops off for specimens tested at confining pressures of 100 MPa and below. The specimens tested above 100 MPa confining pressure increased in strength during most of the test. The volumetric strain responses during shear loading shown in Figure 22 indicated that the test

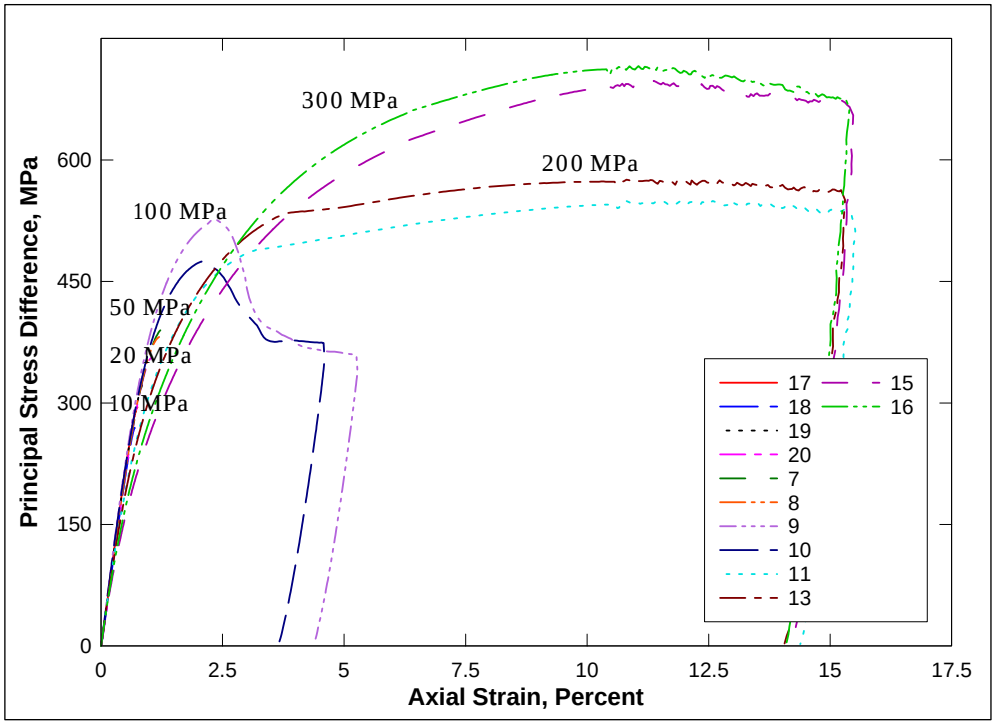

Figure 21. Stress-strain responses from TXC tests on Cor-Tuf1 concrete at confining pressures between 10 and 300 MPa.

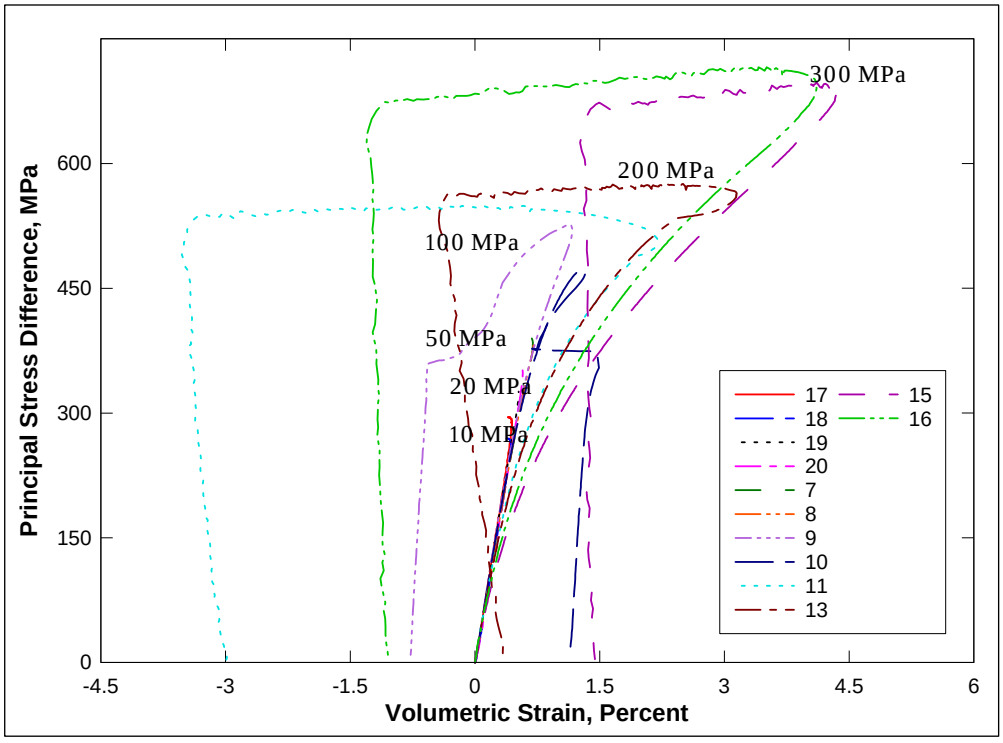

Figure 22. Stress difference-volumetric strain during shear from TXC tests on Cor-Tuf1 concrete at confining pressures between 10 and 300 MPa.

specimens began to dilate just prior to achieving peak strength at all confining pressure levels.

The TXC stress-strain results in Figure 21 illustrate both the brittle and ductile nature of this material. At confining pressures of 100 MPa and below, the material behaved in a brittle manner, i.e., the material strain softened after the peak stress occurs. At confining pressures of 200 MPa and above, the material behaved in a ductile manner, i.e., the stress-strain data exhibited strain hardening. At confining pressures between 100 and 200 MPa, the brittle-to-ductile transition occurs where the material flows at a constant value of principal stress difference.

Results from TXC tests at confining pressures from 10 to 300 MPa are also plotted in Figure 23 as radial strain during shear versus axial strain during shear. A contour of zero volumetric strain during shear is also shown in this figure. When the instantaneous slope of a curve is shallower than the contour of zero volumetric strain, the specimen is in a state of volumetric compression; when steeper, the specimen is in a state of dilation or volumetric expansion. Data points plotted below the contour signify that a test specimen has dilated, and the specimen's volume at that point is greater than its volume at the start of shear.

The failure data from all of the UC and TXC tests are plotted in Figure 24 as principal stress difference versus mean normal stress; one stress path at each confining stress is also plotted. In Figure 25, a recommended failure surface is plotted with the failure points. It is important to note that the failure points exhibit a continuous increase in principal stress difference with increasing values of mean normal stress. The failure surface for Cor-Tuf1 concrete plots below the failure data for the TXC test specimens at 100 MPa confining pressure and above the failure data for the TXC test specimens at 200 MPa confining pressure. At 100 MPa confining pressure, the initial dry density for test specimen 9 was above average (Table 3) while the initial dry density for test specimen 10 was below average. Both test specimens displayed strengths slightly greater than the failure surface. Test specimens 9 and 10 likely had intrinsic properties that resulted in both specimens being slightly stronger than expected for that confining pressure. Conversely, the test specimens at 200 MPa had slightly lower initial dry densities, which resulted in strengths that were slightly lower than if the test specimens had the average initial dry density. The response data from the 300 MPa TXC tests indicated that at a mean normal stress

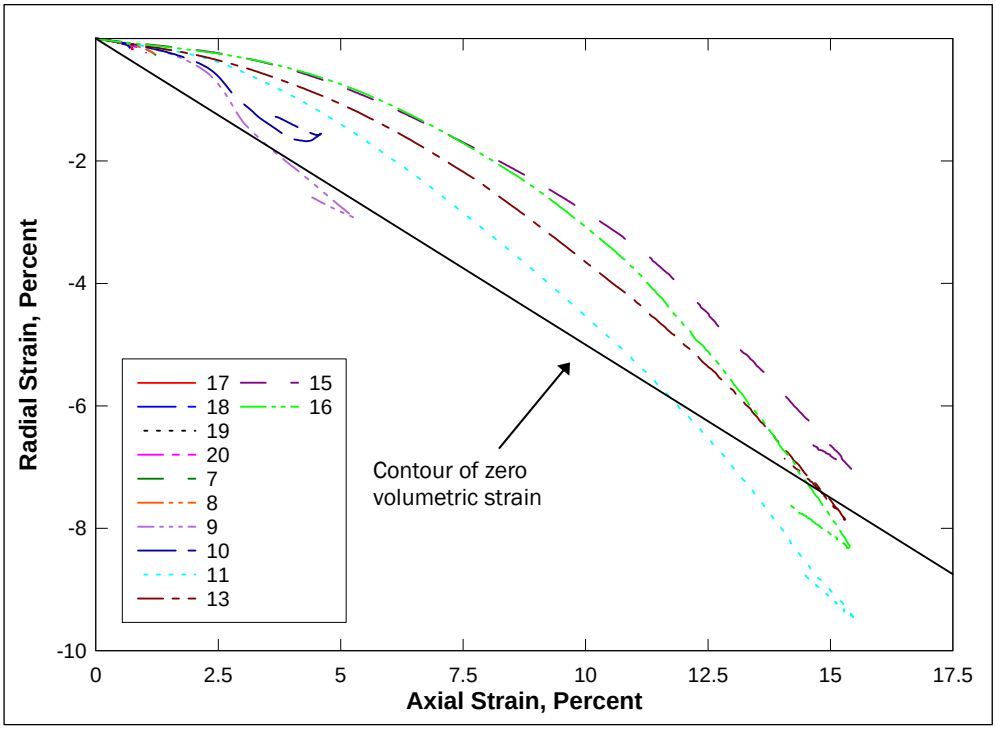

Figure 23. Radial strain-axial strain data during shear from TXC tests on Cor-Tuf1 concrete at confining pressures between 10 and 300 MPa.

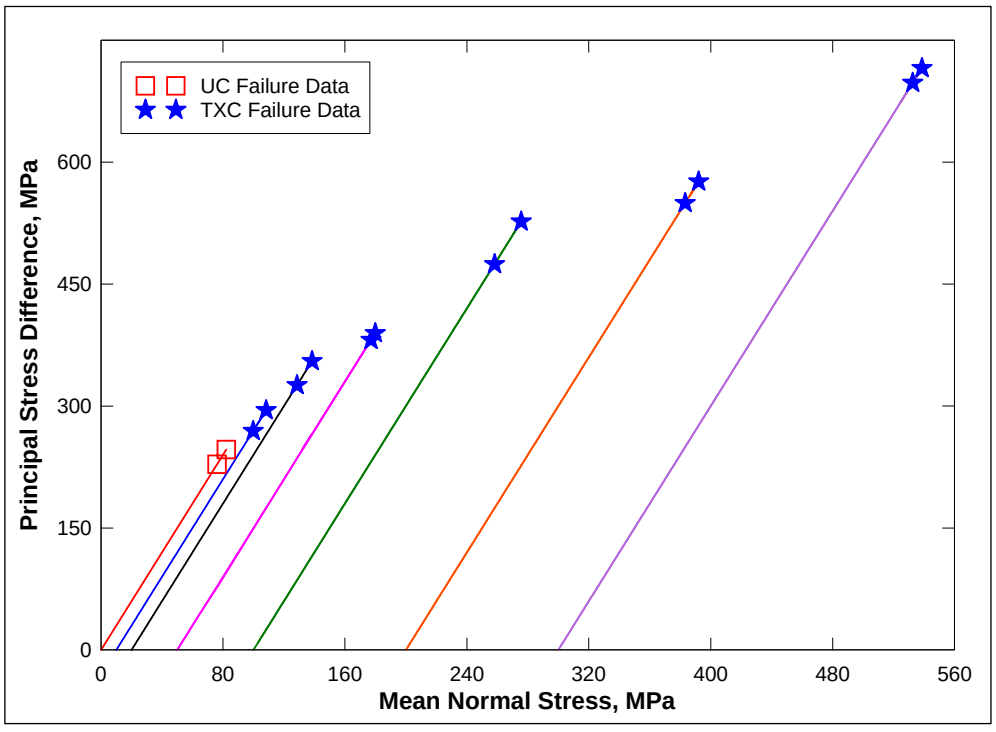

Figure 24. Shear failure data from UC and TXC tests on Cor-Tuf1 concrete.

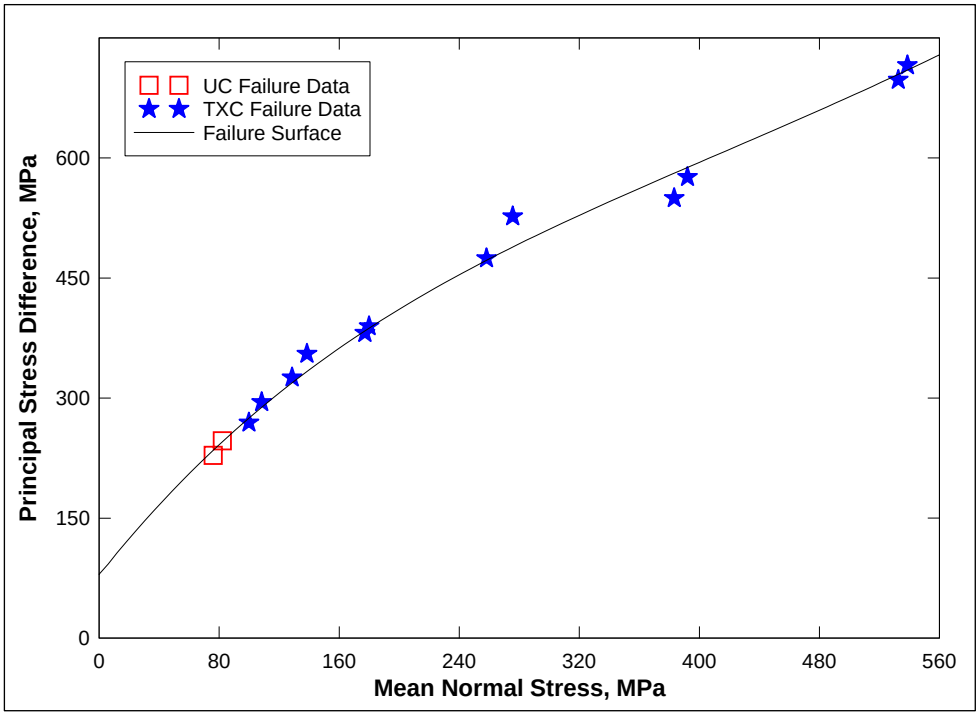

Figure 25. Failure data from UC and TXC tests on Cor-Tuf1 concrete and recommended failure surface.

of approximately 536 MPa, Cor-Tuf1 still had not reached void closure and was far from saturation. Materials such as concrete can continue to gain strength with increasing pressure until all of the air porosity in the specimen is crushed out.

Direct pull tests

Tension shear and failure data were successfully obtained from three direct pull tests. The DP tests were performed without the application of confining pressure. Results from the DP tests are plotted in Figure 26. All of the test specimens fractured. Failure from the DP tests occurred at an average mean normal stress of approximately -1.86 MPa at approximately -5.58 MPa principal stress difference. The absolute value of the tensile strength of Cor-Tuf1 concrete is 2.4% of the unconfined compressive strength (237 MPa). According to ACI 318-02 (2002), tensile strength of concrete is normally about 10 to 15% of the compressive strength. In this case, the tensile strength for Cor-Tuf1 is far less than the tensile strength generally predicted by ACI 318-02.

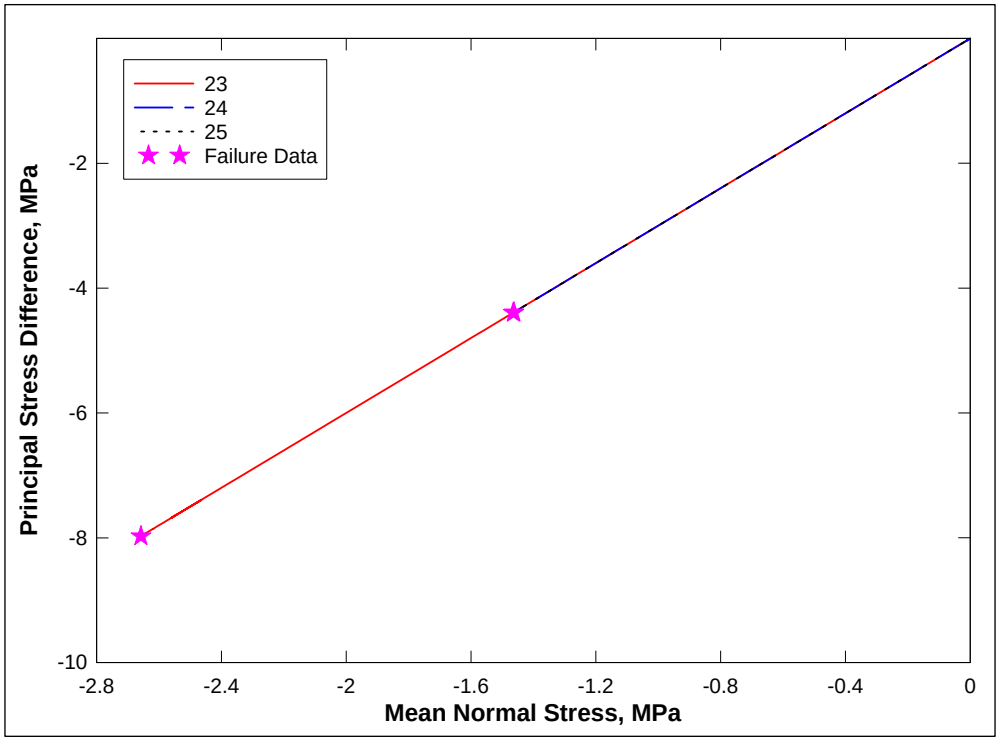

Figure 26. Stress paths and failure data from DP tests on Cor-Tuf1 concrete.

Uniaxial strain tests

One-dimensional compressibility data were obtained from two undrained uniaxial strain (UX) tests with lateral stress measurements. Data from the tests are plotted in Figures 27 through 29. The stress-strain data from the UX tests are plotted in Figure 27, the pressure-volume data in Figure 28, and the stress paths with the failure surface data in Figure 29. The UX responses indicate that neither test specimen reached a fully saturated state, i.e., the volumetric strains achieved during the tests were much less than the air voids contents of the specimens.

From the UX stress-strain loading data (Figure 27), an initial constrained modulus, M, of 47.4 GPa was calculated. UX data may also be plotted as principal stress difference versus mean normal stress; the slope of an elastic material in this space is 2G/K. An initial shear modulus of 16.7 GPa was calculated from the constrained modulus and the initial elastic bulk modulus, K (25.2 GPa), that was determined from the HC and TXC tests. These two values may be used to calculate the other elastic constants, i.e., an initial Young's modulus of 40.9 GPa and Poisson's ratio of 0.23.

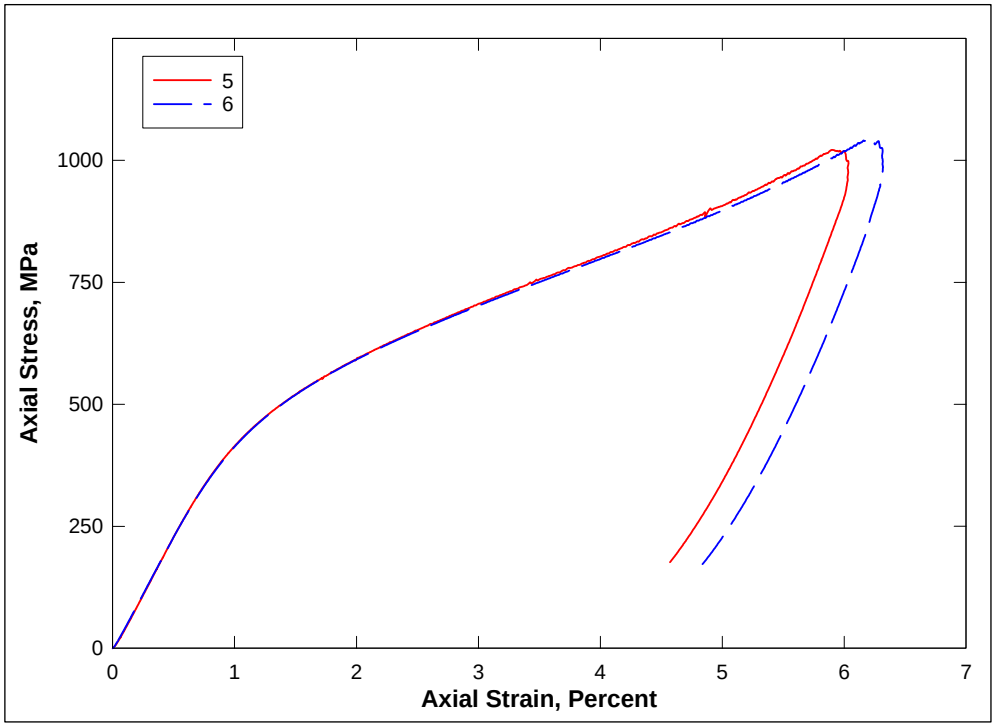

Figure 27. Stress-strain responses from UX tests on Cor-Tuf1 concrete.

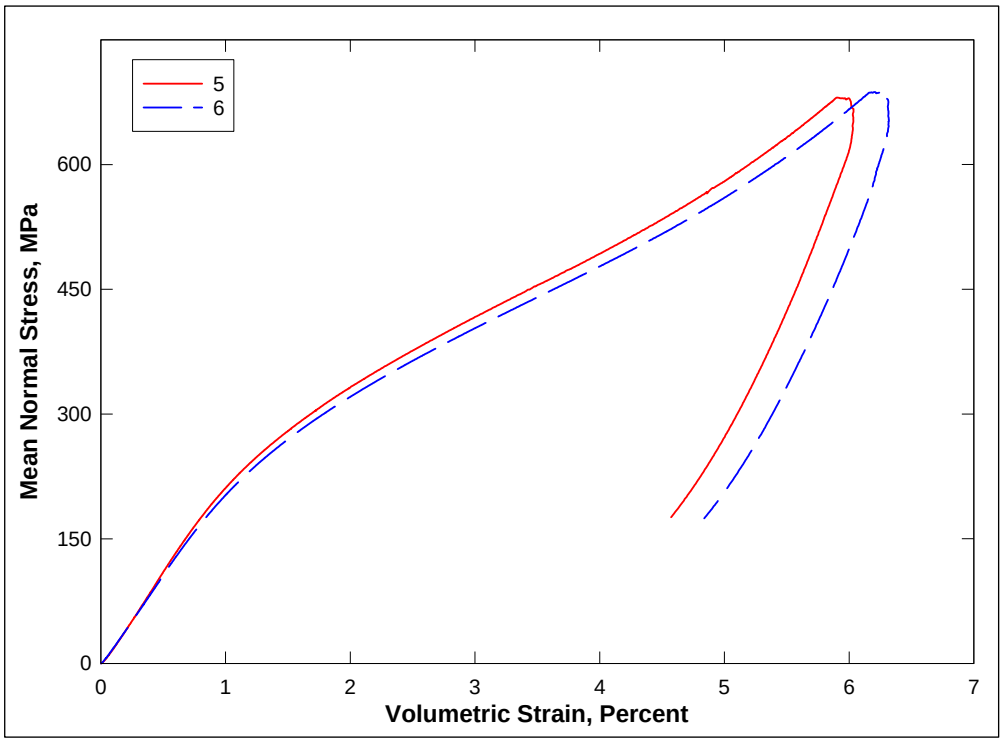

Figure 28. Pressure-volume responses from UX tests on Cor-Tuf1 concrete.

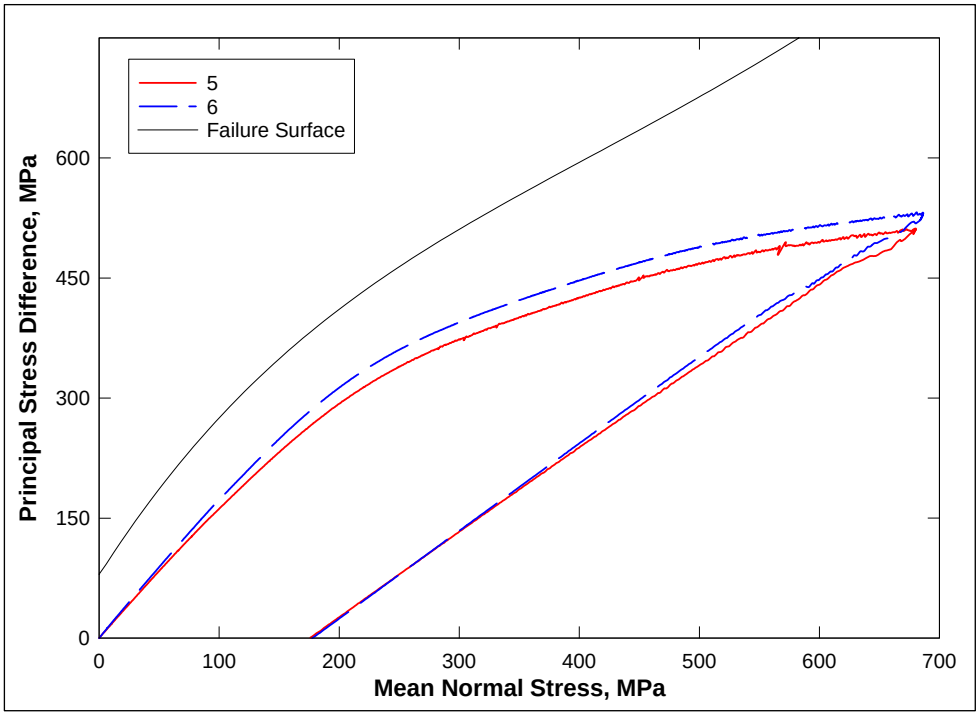

Figure 29. Stress paths from UX tests and failure surface from TXC tests on Cor-Tuf1 concrete.

The UX stress paths (Figure 29) trend below the TXC recommended failure surface even at very low stresses. As the principal stress difference increases, the paths soften slightly. The stress paths soften after the cement bonds start to crush, causing the data to plot below the failure surface. The stress paths for the two UX test specimens are very similar, which is likely a result of the test specimens' having very similar intrinsic properties. For example, the dry densities for these specimens were 2.464 Mg/m^3 for test specimen 5 and 2.468 Mg/m^3 for test specimen 6.

Figure 30 compares the pressure-volume responses from HC and UX tests. The initial dry densities of test specimens 3, 4, 5, and 6 were 2.510, 2.523, 2.464, and 2.468 Mg/m^3, respectively. The HC test specimens had higher initial dry densities than those for UX test specimens, which explain why the HC test specimens display a slightly steeper initial loading than the UX test specimens. The UX test specimens exhibited higher volumetric strains than the HC test specimens. This response comparison indicates additional shear-induced compaction due to UX loading that cannot occur during HC loading.

Strain path tests

This test program conducted one type of strain-path test. UX/CV refers to tests with uniaxial strain loading followed by constant volumetric strain loading. Results from two UX/CV tests conducted at two levels of peak axial stress during the initial UX phase are shown in Figures 31 through 34. The stress-strain data from the UX/CV tests are plotted in Figure 31, the pressure-volume data in Figure 32, the stress-paths with the failure surface data in Figure 33, and the strain paths in Figure 34. Shortly after starting the CV portion of the test, test specimen 21 failed. The stress path data in Figure 33 exhibit that during the CV loading, the specimen will contact the fail surface developed from the TXC tests. Test specimen 22 follows just below the failure surface during the majority of the CV loading.

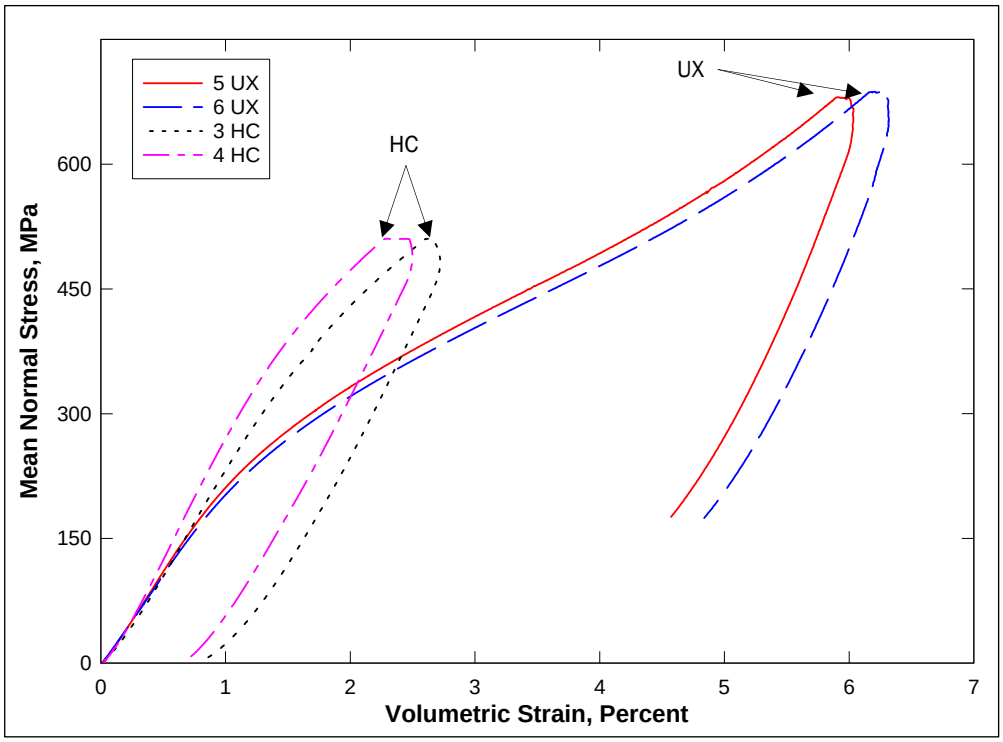

Figure 30. Comparison of pressure-volume responses from HC and UX tests on Cor-Tuf1 concrete.

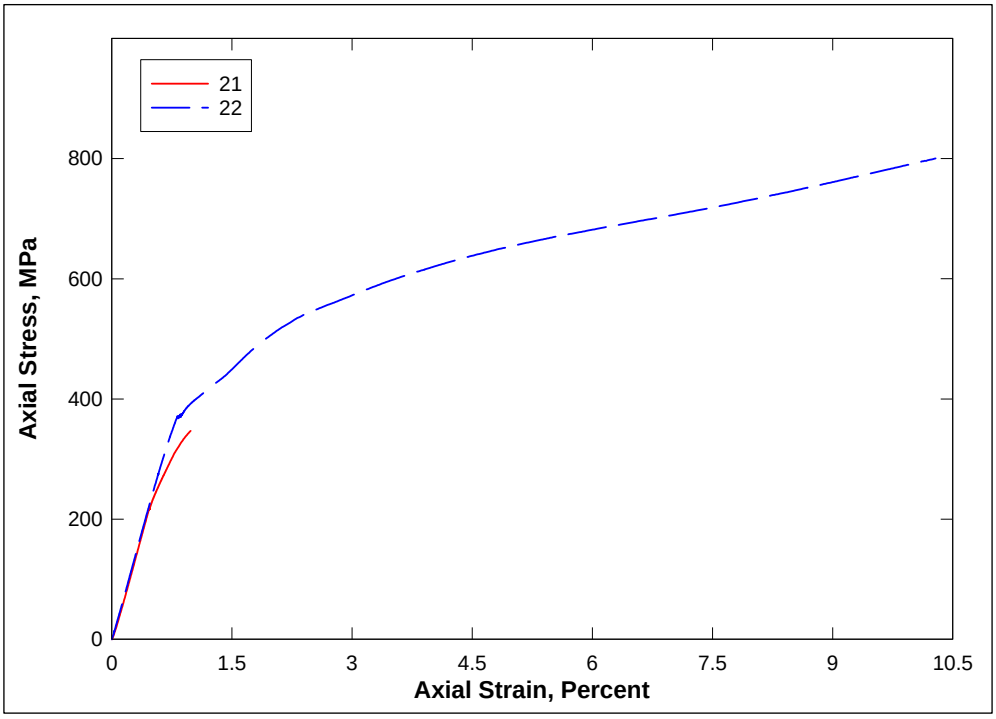

Figure 31. Stress-strain responses from UX/CV tests on Cor-Tuf1 concrete.

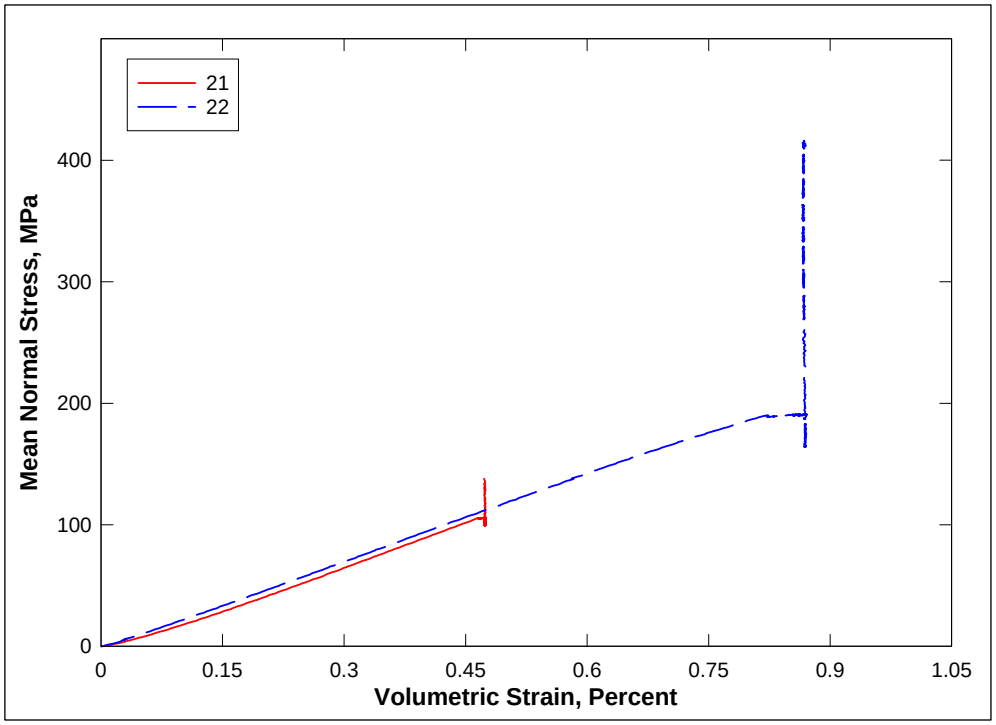

Figure 32. Pressure-volume responses from UX/CV tests on Cor-Tuf1 concrete.

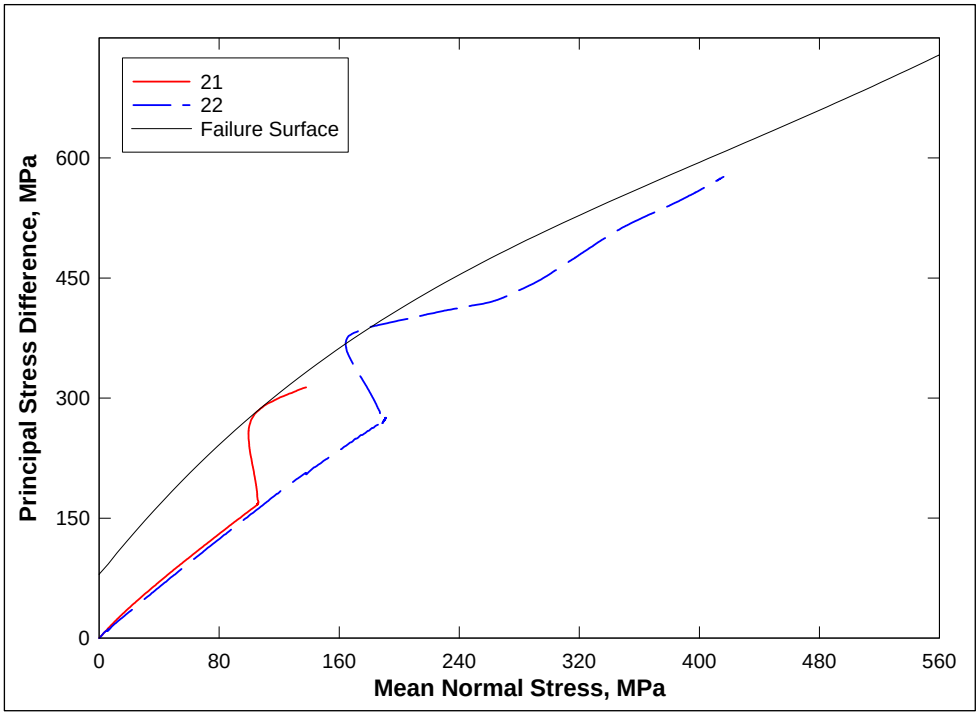

Figure 33. Stress paths from UX/CV tests and failure surface from TXC tests on Cor-Tuf1 concrete.

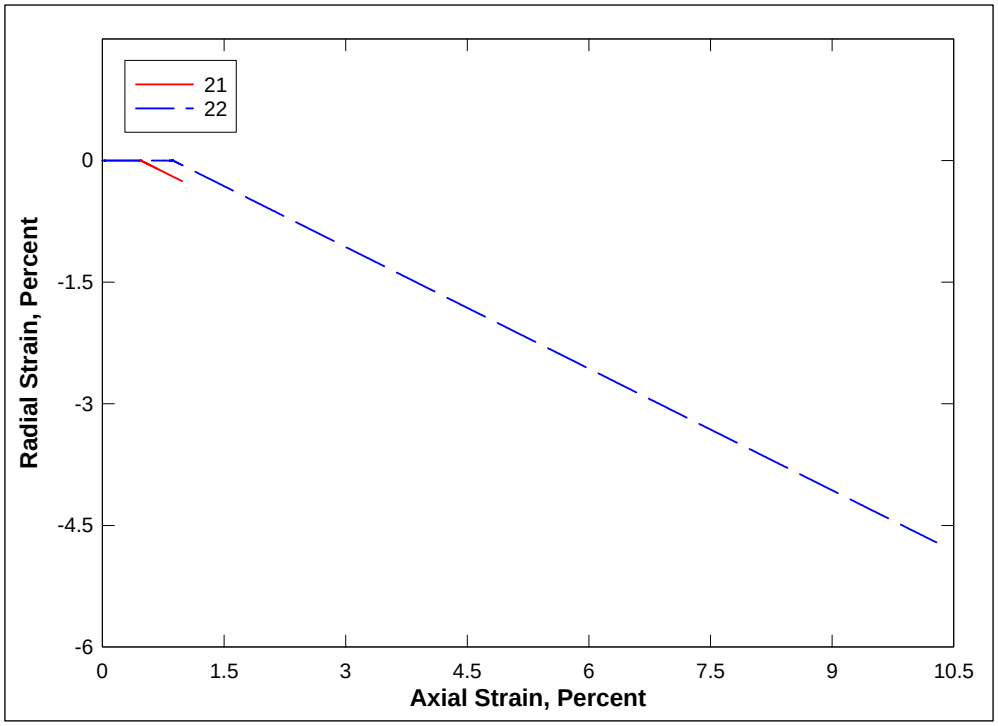

Figure 34. Strain paths from UX/CV tests on Cor-Tuf1 concrete.

4 Analyses of Test Results for Cor-Tuf Concrete without Steel Fibers

Hydrostatic compression tests

Undrained compressibility data were obtained from two HC tests and during the hydrostatic loading phases of the 12 TXC tests. The pressure-volume data from the HC tests are plotted in Figure 35. The initial dry densities of the specimens for HC tests 1 and 3 were 2.312 and 2.286 Mg/m^3, respectively. Figure 36 presents the pressure time-histories for the HC tests. During the HC tests, the pressure was intentionally held constant for a period of time prior to the unloading cycles. During each hold in pressure, the volume strains continued to increase, indicating that Cor-Tuf2 concrete was susceptible to creep (Figures 35 and 36). The Cor-Tuf2 concrete began to exhibit inelastic strains at a pressure level of approximately 280 MPa and at a volumetric strain of approximately 1.2%. This is the pressure and strain level at which the pressure-volume response and the initial bulk modulus began to soften appreciably. Based on the data from HC tests, the initial elastic bulk modulus, K, for Cor-Tuf2 concrete is approximately 22.7 GPa.

Triaxial compression tests

Shear and failure data were successfully obtained from two unconfined compression tests and 12 unconsolidated-undrained TXC tests. Recall from Chapter 2 that the second phase of the TXC test, the shear phase, was conducted after the desired confining pressure was applied during the HC phase. The UC tests are a special type of TXC test without the application of confining pressure. Results from the UC tests are plotted in Figures 37 and 38, and results from the TXC tests are plotted in Figures 39 through 50. In all the figures, the axial and volumetric strains at the beginning of the shear phase were set to zero, i.e., only the strains during shear are plotted.

Stress-strain data from the UC tests in Figures 37 and 38 are plotted as principal stress difference versus axial strain during shear and as principal stress difference versus volumetric strain during shear, respectively. Deformeters instead of strain gages were used to measure the axial and radial strains of the UC test specimens. During the UC tests, no attempt

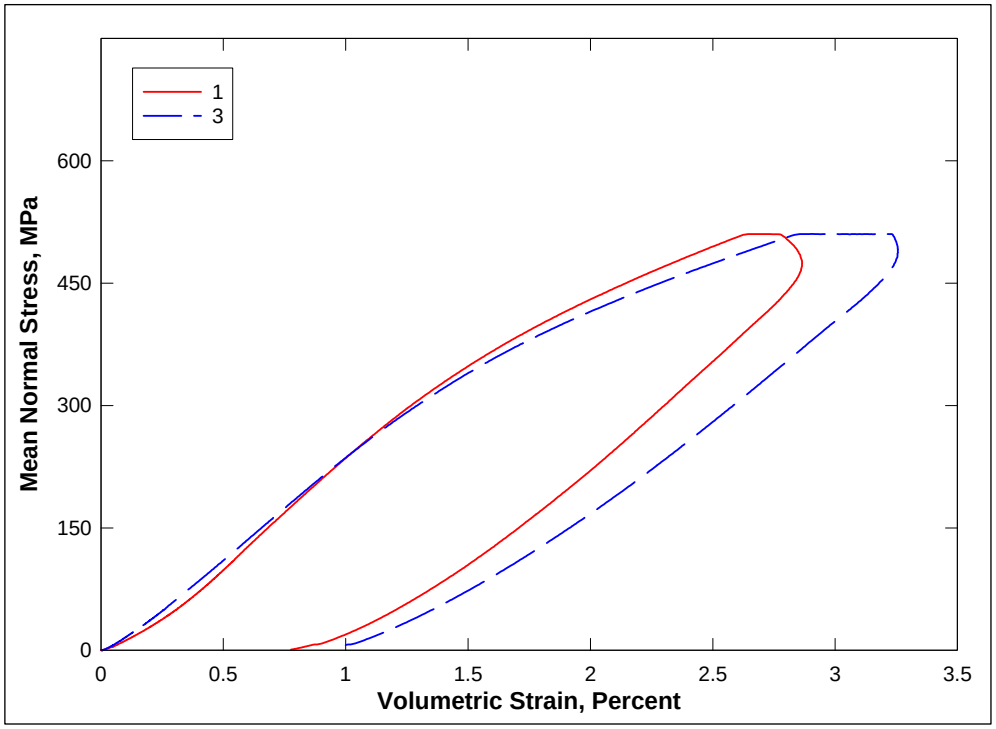

Figure 35. Pressure-volume responses from the HC tests on Cor-Tuf2 concrete.

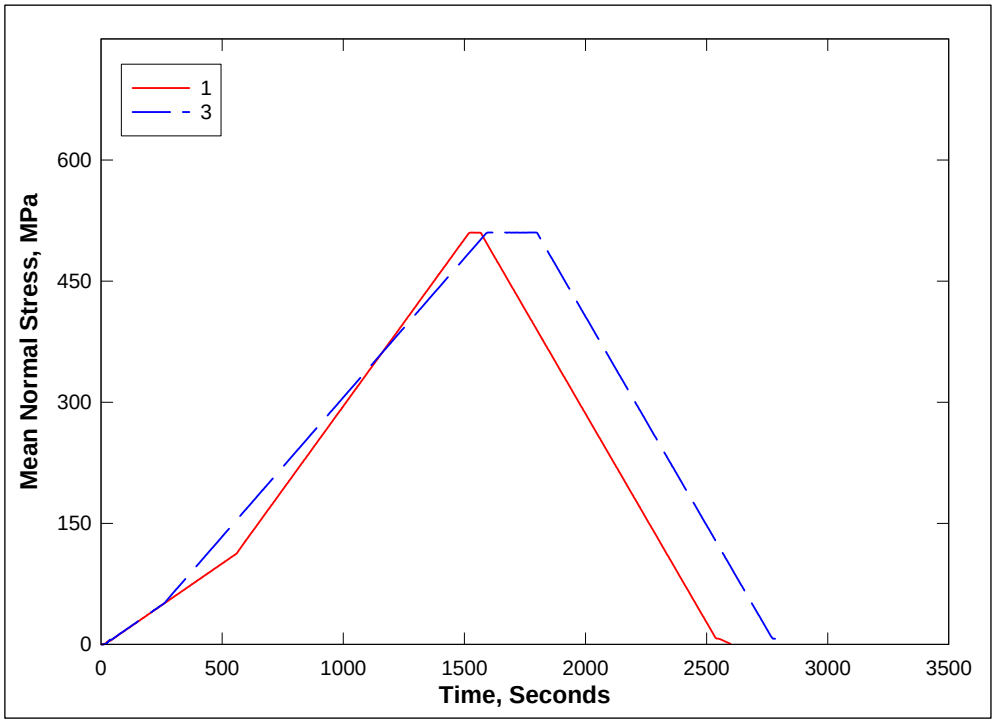

Figure 36. Pressure time-histories from the HC tests on Cor-Tuf2 concrete.

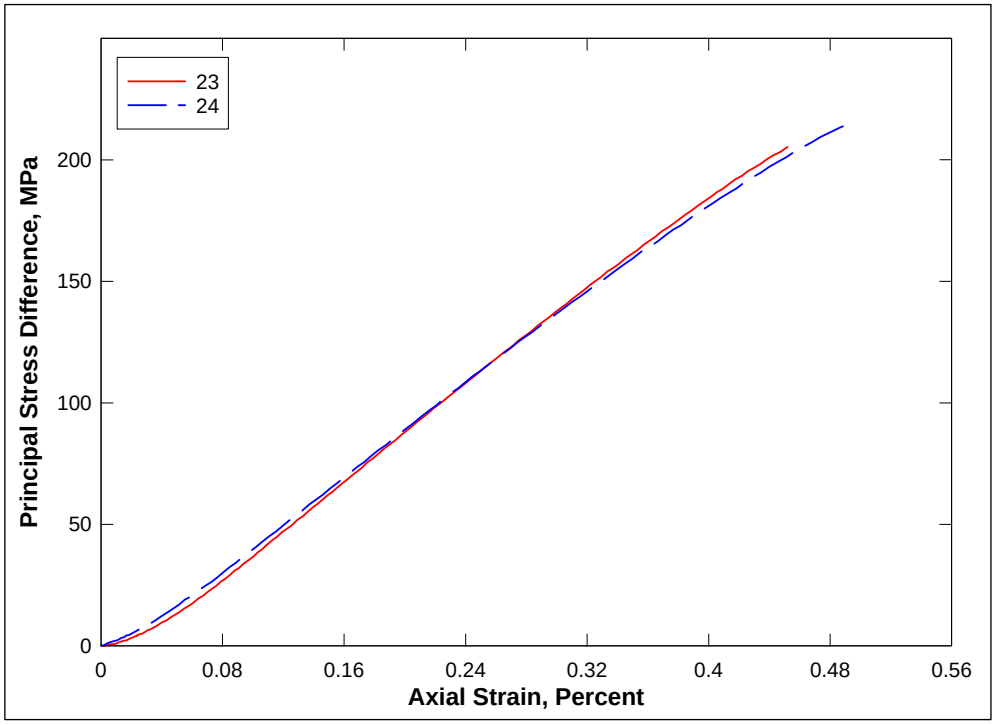

Figure 37. Stress-strain responses from UC tests on Cor-Tuf2 concrete.

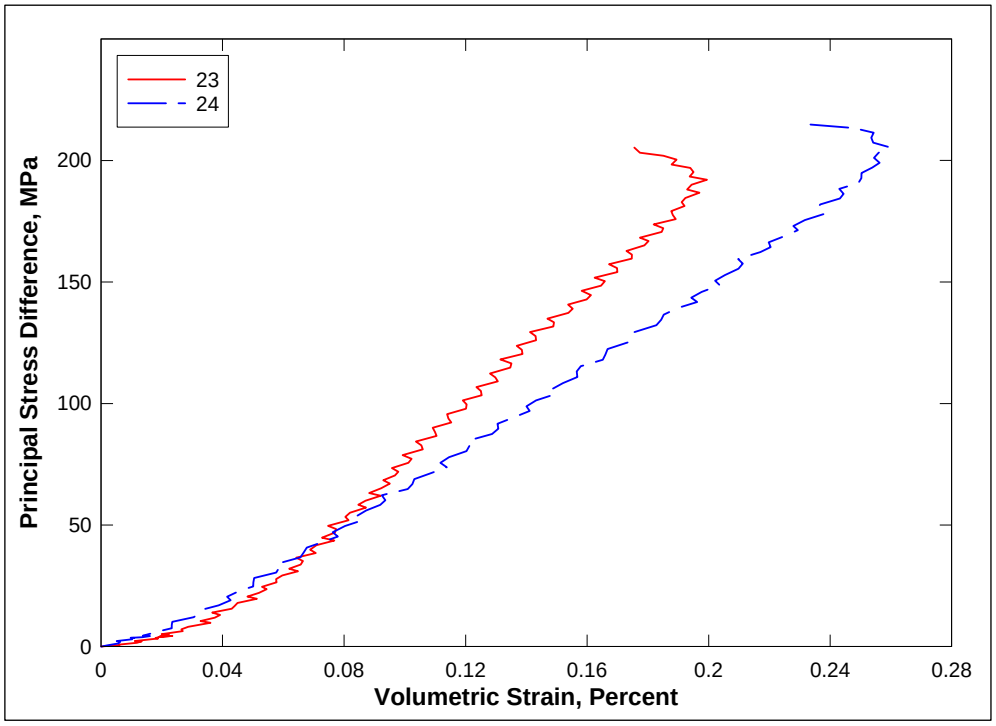

Figure 38. Stress difference-volumetric strain during shear from UC tests on Cor-Tuf2 concrete.

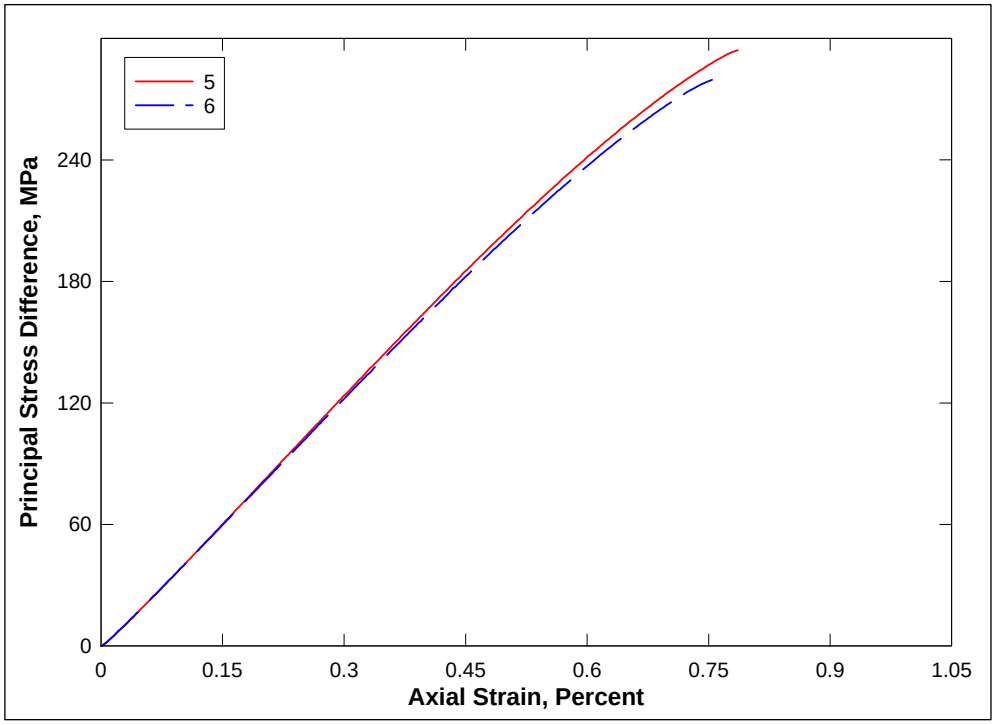

Figure 39. Stress-strain responses from TXC tests on Cor-Tuf2 concrete at a confining pressure of 10 MPa.

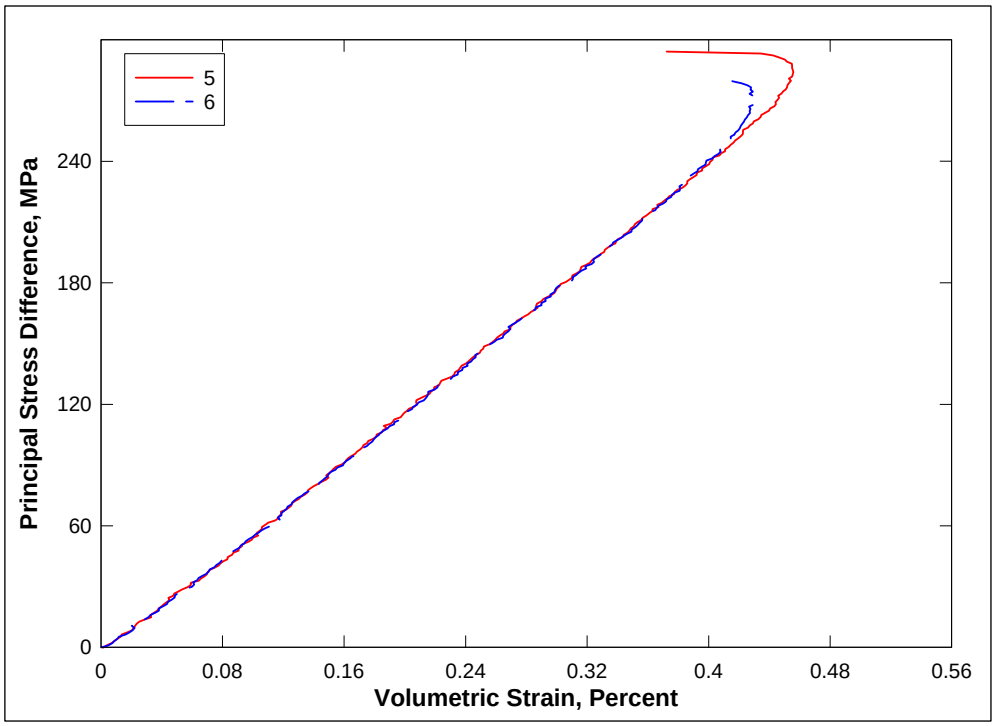

Figure 40. Stress difference-volumetric strain during shear from TXC tests on Cor-Tuf2 concrete at a confining pressure of 10 MPa.

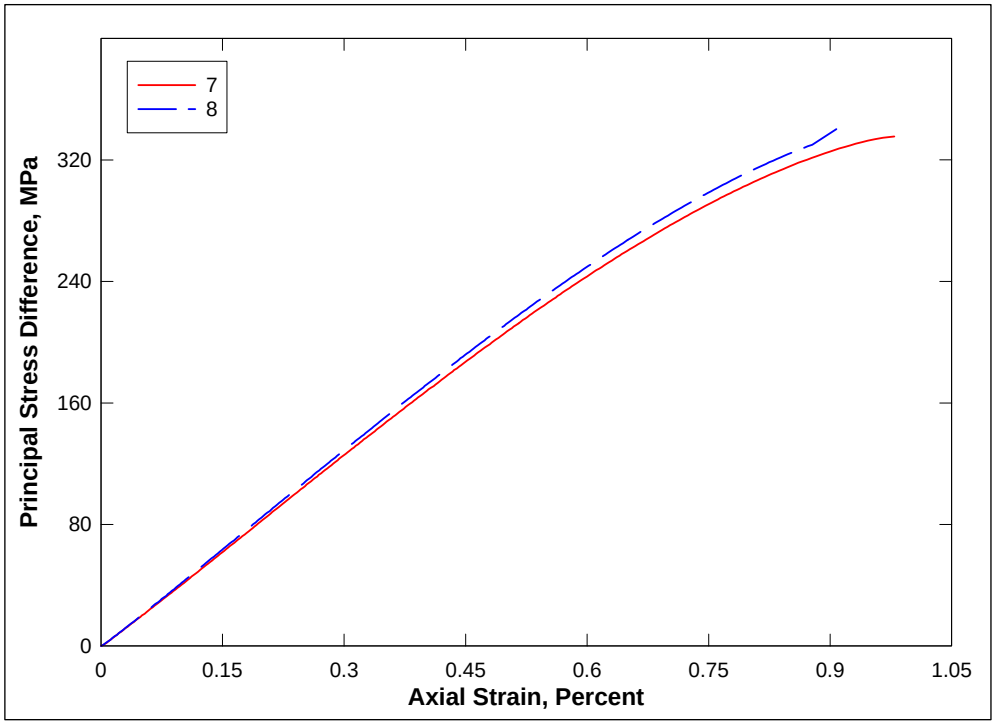

Figure 41. Stress-strain responses from TXC tests on Cor-Tuf2 concrete at a confining pressure of 20 MPa.

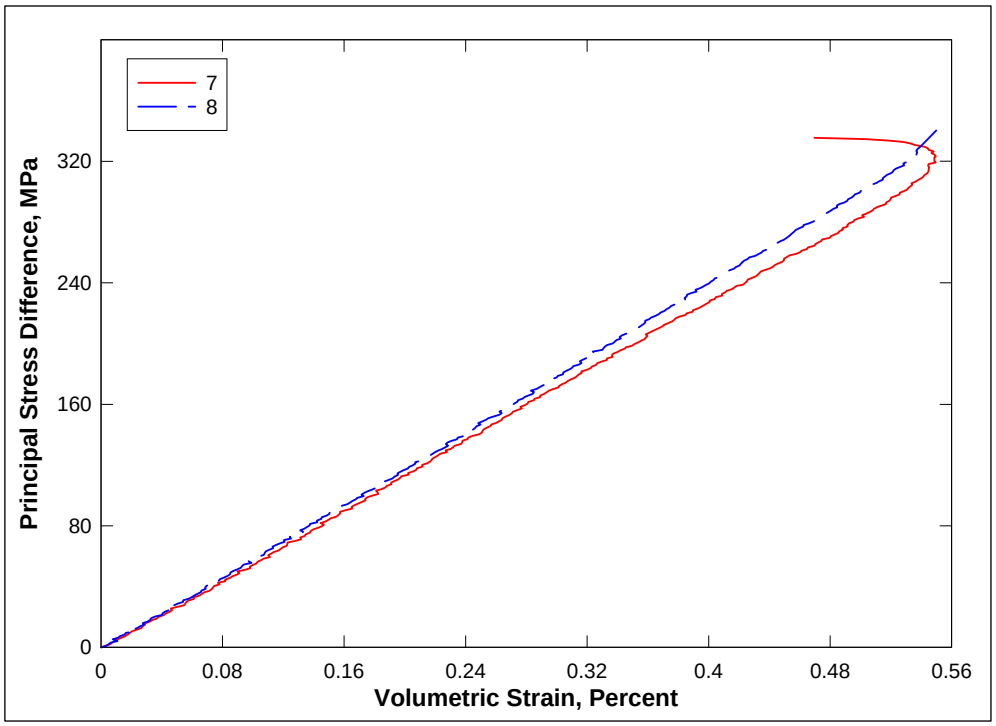

Figure 42. Stress difference-volumetric strain during shear from TXC tests on Cor-Tuf2 concrete at a confining pressure of 20 MPa.

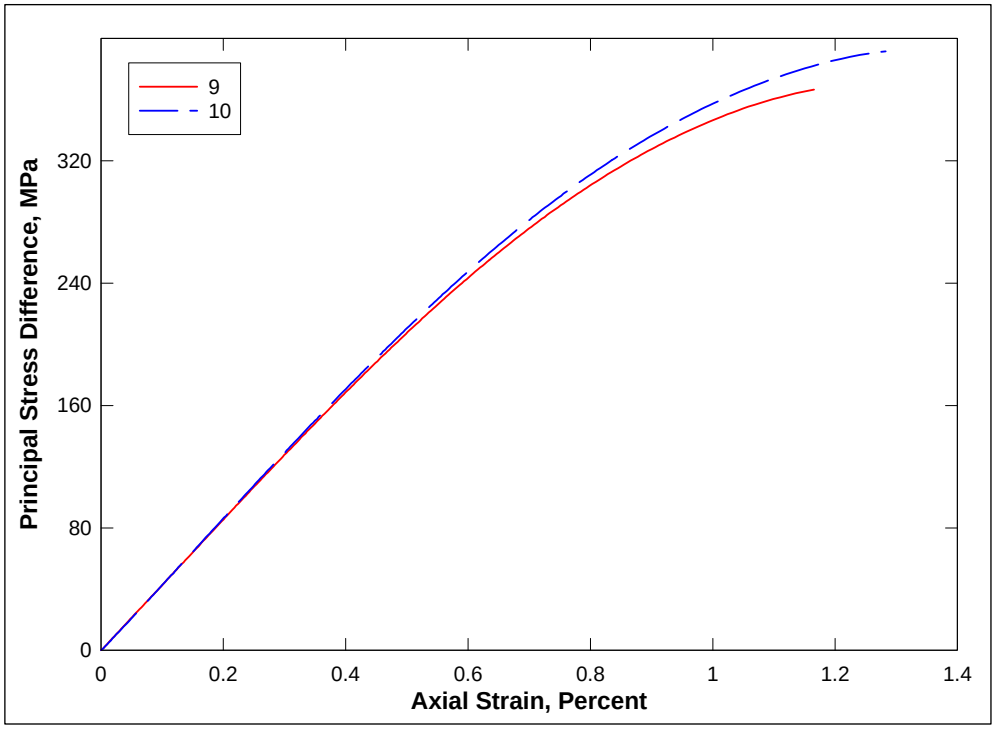

Figure 43. Stress-strain responses from TXC tests on Cor-Tuf2 concrete at a confining pressure of 50 MPa.

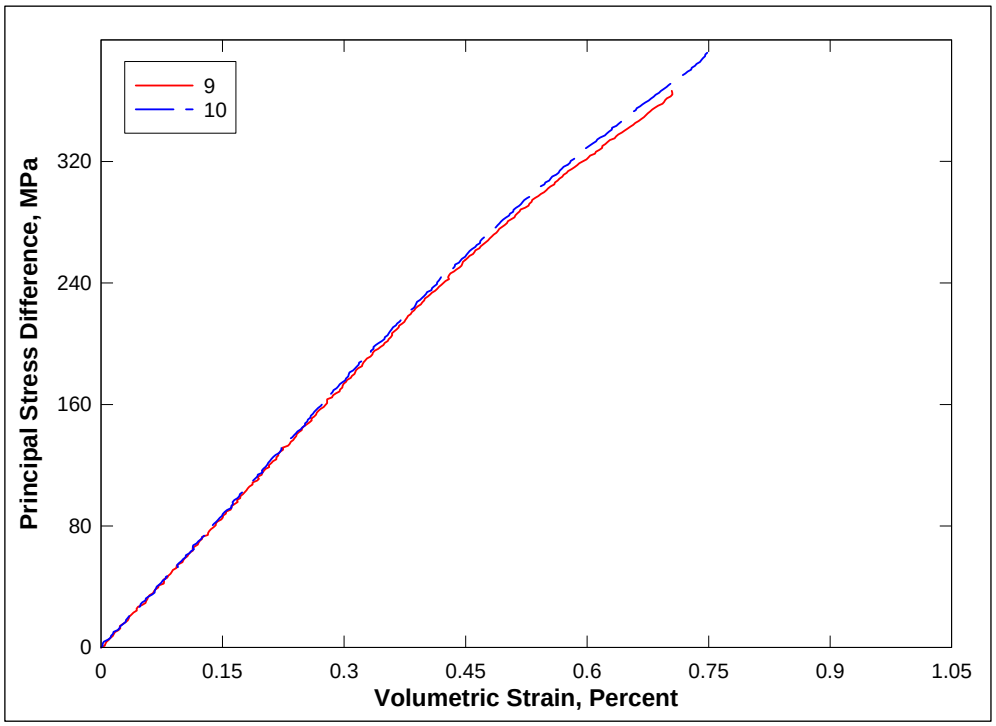

Figure 44. Stress difference-volumetric strain during shear from TXC tests on Cor-Tuf2 concrete at a confining pressure of 50 MPa.

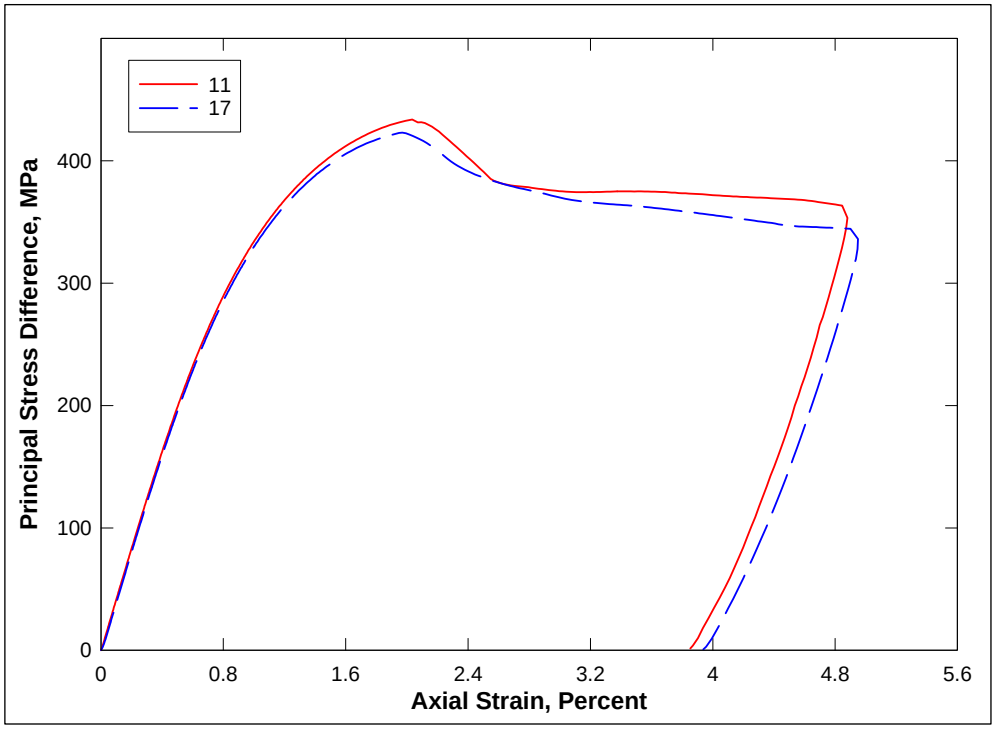

Figure 45. Stress-strain responses from TXC tests on Cor-Tuf2 concrete at a confining pressure of 100 MPa.

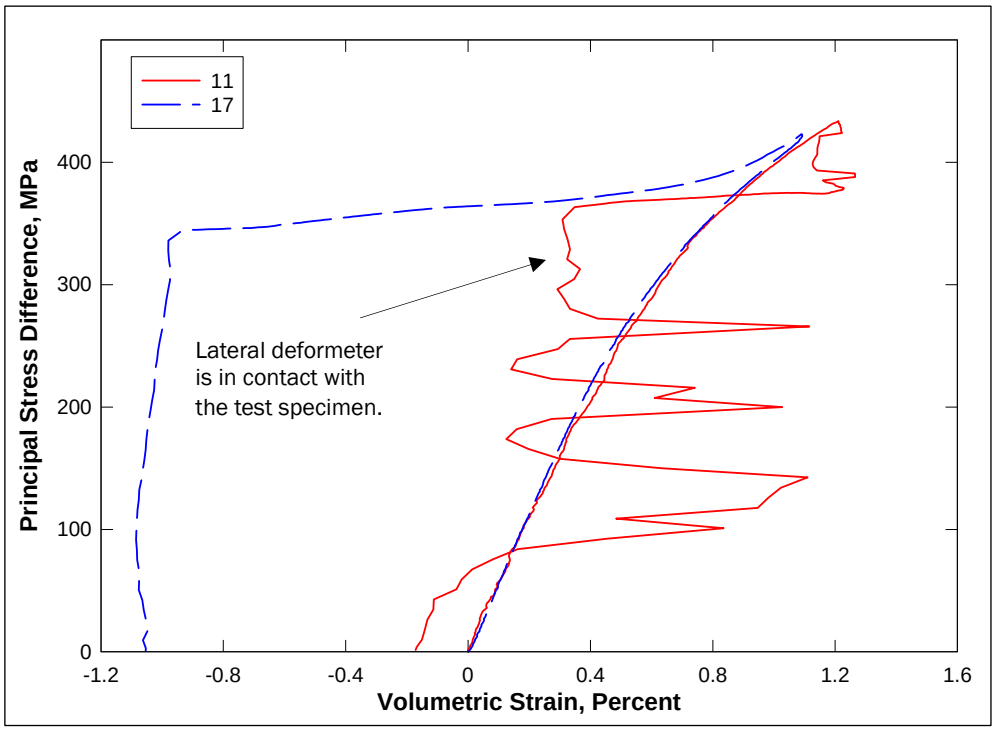

Figure 46. Stress difference-volumetric strain during shear from TXC tests on Cor-Tuf2 concrete at a confining pressure of 100 MPa.

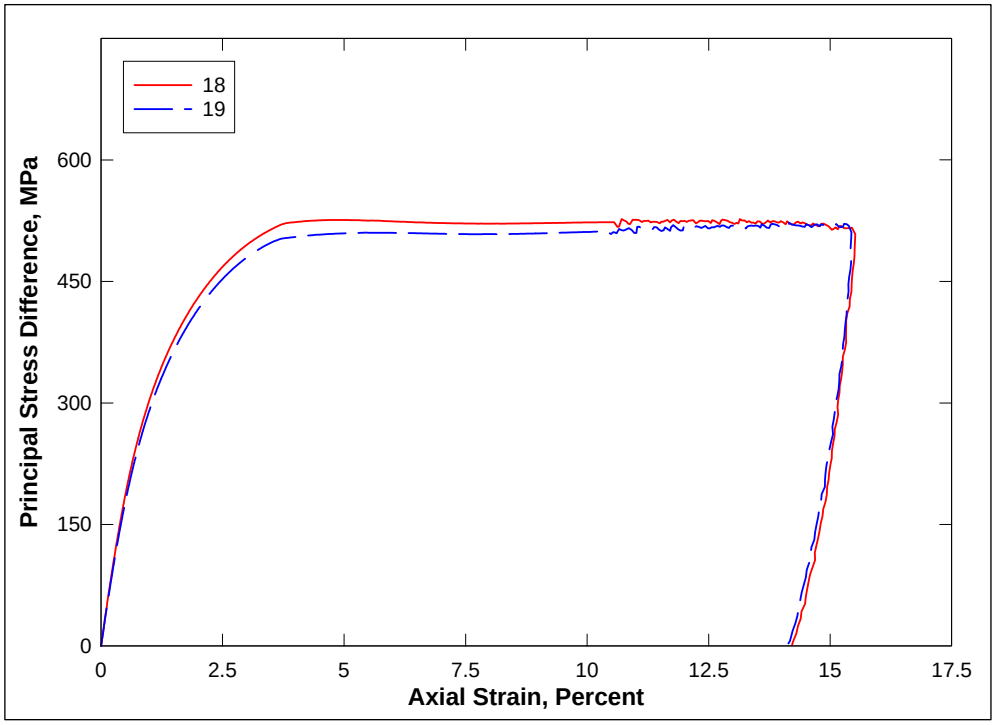

Figure 47. Stress-strain responses from TXC tests on Cor-Tuf2 concrete at a confining pressure of 200 MPa.

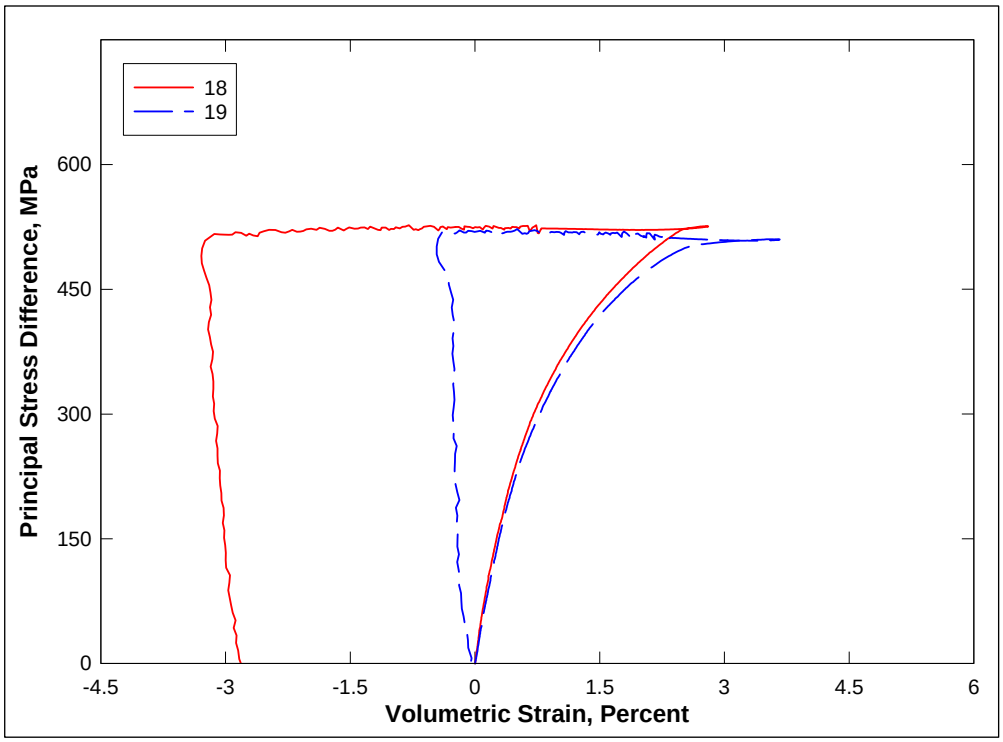

Figure 48. Stress difference-volumetric strain during shear from TXC tests on Cor-Tuf2 concrete at a confining pressure of 200 MPa.

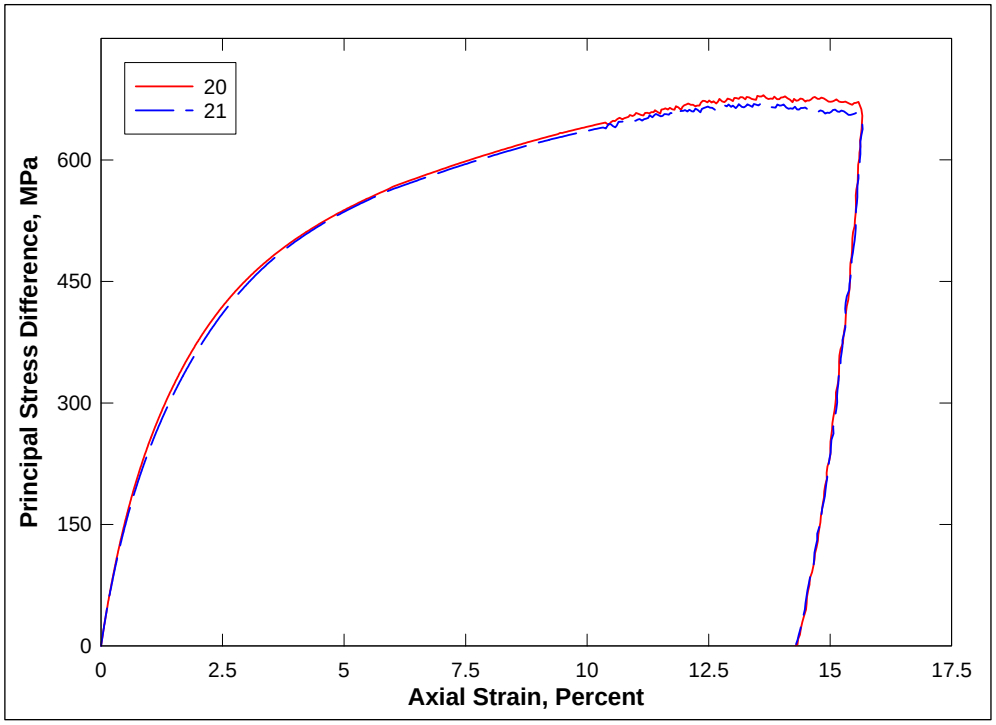

Figure 49. Stress-strain responses from TXC tests on Cor-Tuf2 concrete at a confining pressure of 300 MPa.

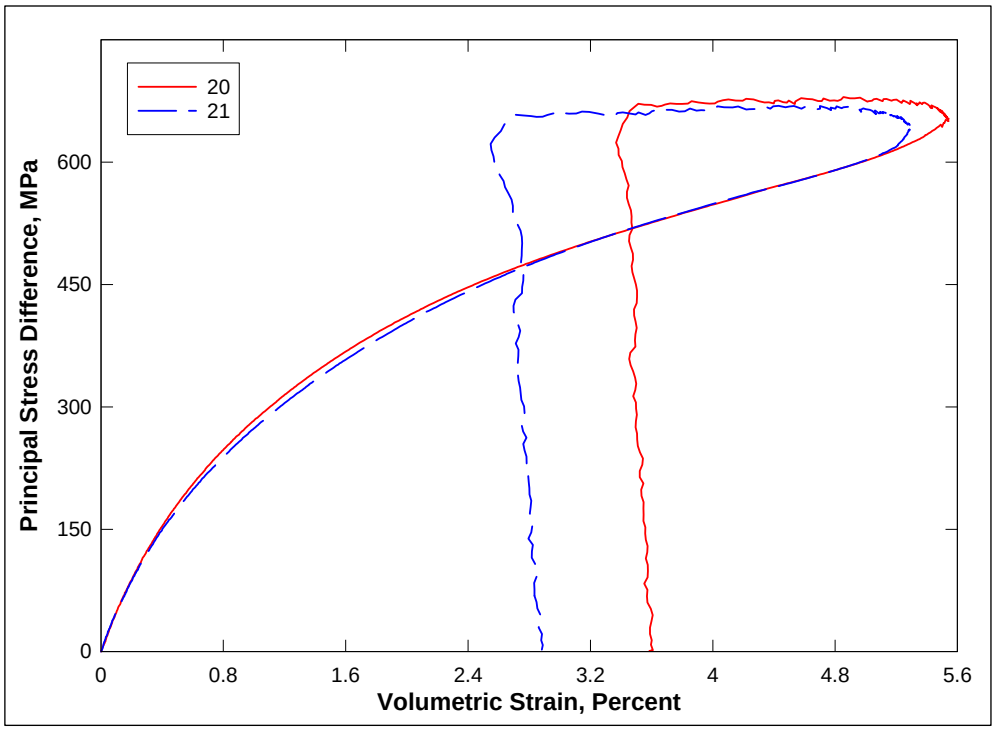

Figure 50. Stress difference-volumetric strain during shear from TXC tests on Cor-Tuf2 concrete at a confining pressure of 300 MPa.

was made to capture the post-peak (or softening) stress-strain behavior of this material. The mean unconfined strength of Cor-Tuf2 concrete determined from the two UC specimens was 210 MPa. The dry densities for specimens 23 and 24 were 2.256 and 2.236 Mg/m^3, respectively.

Figures 39 through 50 present the results from the TXC tests conducted at nominal confining pressures of 10, 20, 50, 100, 200, and 300 MPa. The TXC results are plotted as principal stress difference versus axial strain during shear and as principal stress difference versus volumetric strain during shear. In Figure 46, the lateral deformeter was erratic during test 11. The erratic behavior is a result of the lateral deformeter being in contact with the membrane surrounding the specimen. Therefore, the volumetric strain response for test 11 is not accurate, but overall the results for the TXC tests are very good and show little data scatter considering the inherent variability of the initial wet and dry densities and the water contents of the specimens. The wet densities of the TXC specimens ranged from 2.310 to 2.341 Mg/m^3, the dry densities ranged from 2.227 to 2.287 Mg/m^3, and the water contents ranged from 2.16 to 4.52%.

For comparison purposes, stress-strain data from these TXC tests are plotted in Figure 51. Principal stress difference versus volumetric strain during shear from these TXC tests is plotted in Figure 52. The initial loading of the TXC stress-strain responses are a function of the material's volume changes during shear and thus are dependent on the magnitude of the applied confining pressure and the position on the material's pressure-volume response relation. In Figure 51, the principal stress difference peaks and then drops off for specimens tested at confining pressures of 100 MPa and below. The specimens tested at confining pressure of 200 MPa and above exhibit increasing strength with increasing shear strain. The data in Figure 52 display specimen dilation only for the test specimens tested at confining pressures of 100 MPa and above. The specimens tested at confining pressures of 50 MPa and below display only compressive volumetric strains to the peak principal stress difference; therefore, minimal dilation occurred for these test specimens.

The TXC stress-strain results illustrate both the brittle and ductile nature of this material. At confining pressures of 100 MPa and below, the material behaved in a brittle manner, i.e., the material strain softened. At confining pressures of 200 MPa and above, the material behaved in a

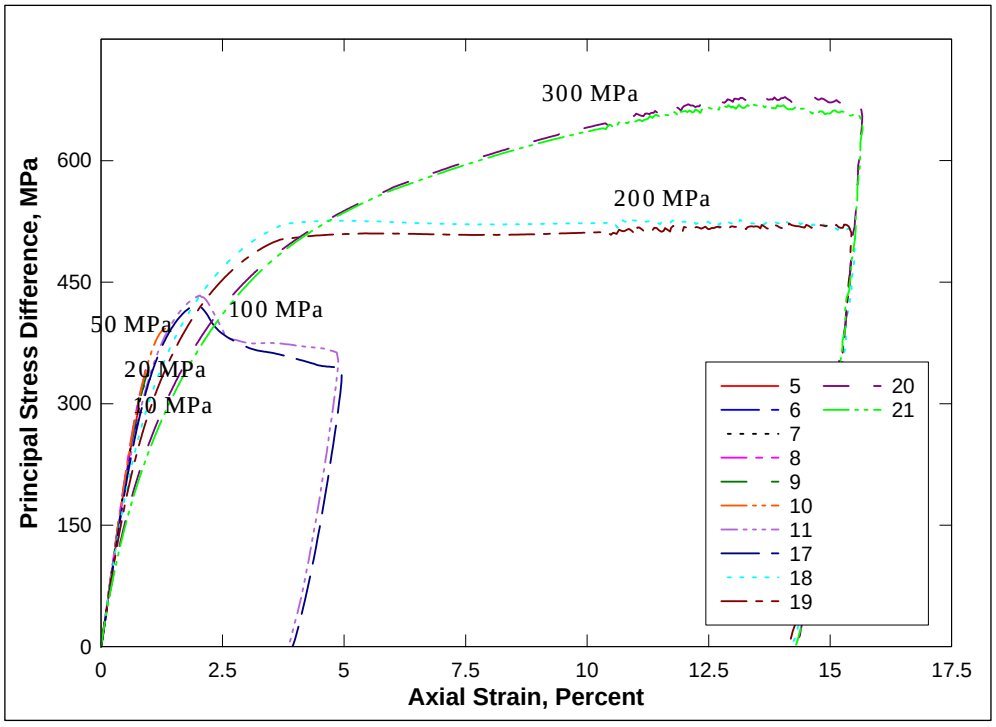

Figure 51. Stress-strain responses from TXC tests on Cor-Tuf2 concrete at confining pressures between 10 and 300 MPa.

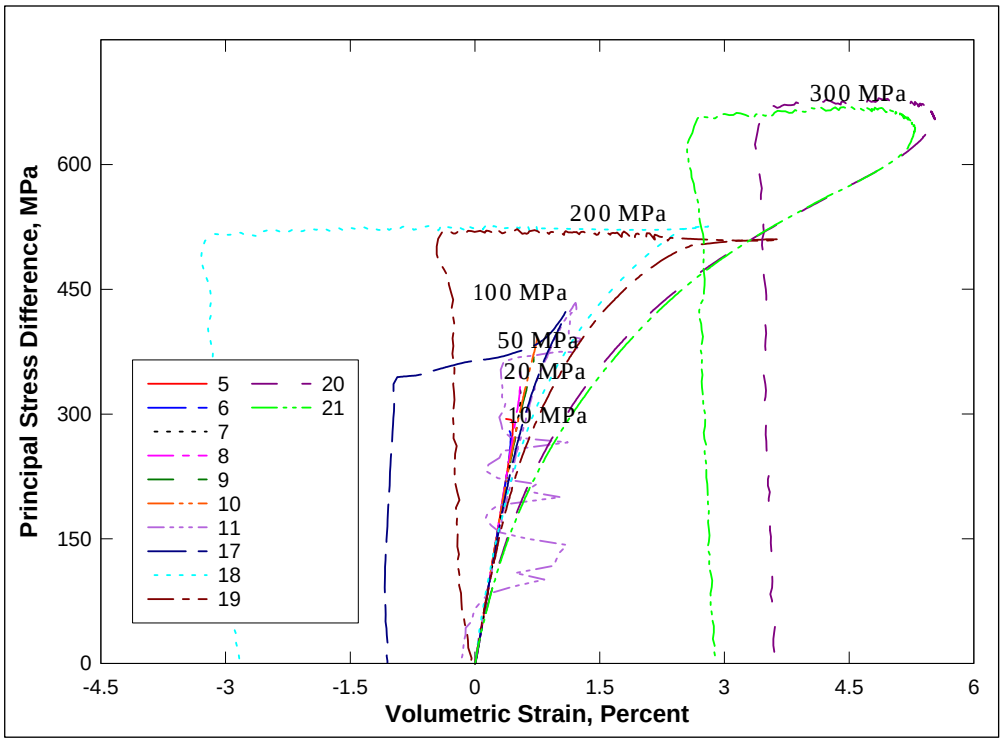

Figure 52. Stress difference-volumetric strain during shear from TXC tests on Cor-Tuf2 concrete at confining pressures between 10 and 300 MPa.

ductile manner, i.e., the stress-strain data exhibited strain hardening. Between confining pressures of 100 and 200 MPa, a brittle-to-ductile transition occurs where the material flows at a constant value of principal stress difference.

Results from TXC tests at confining pressures from 10 to 300 MPa are plotted in Figure 53 as radial strain during shear versus axial strain during shear. This figure also shows a contour of zero volumetric strain during shear. When the instantaneous slope of a curve is shallower than the contour of zero volumetric strain, the specimen is in a state of volume compression; when steeper, the specimen is in a state of dilation or volume expansion. Data points plotted below the contour signify that a test specimen has dilated and that the specimen's volume at that point is greater than its volume at the start of shear.

The failure data from all of the UC and TXC tests are plotted in Figure 54 as principal stress difference versus mean normal stress; one stress path at each confining stress is also plotted. In Figure 55, a recommended failure surface is plotted with the failure points. The quality of the failure data is good, and the scatter is minimal. It is important to note that the failure points exhibit a continuous increase in principal stress difference with increasing values of mean normal stress. The response data from the 300 MPa TXC tests indicated that at a mean normal stress of approximately 525 MPa, Cor-Tuf2 still had not reached void closure and is far from saturation. Materials such as concrete can continue to gain strength with increasing pressure until all of the air porosity in the specimen is crushed out, i.e., when void closure is reached. It is important to recognize that void closure can be attained during the shear loading phase of the TXC tests as well as under hydrostatic loading conditions. At levels of mean normal stress above void closure, the failure surface has a minimal slope.

Direct pull tests

Tension shear and failure data were successfully obtained from only one direct pull test. Two additional DP tests were attempted, but the tensile strength of the glue used to hold the specimens in place during the test was less than the tensile strength of the test specimens. All DP tests were performed without the application of confining pressure. Data from the one successful DP test is plotted in Figure 56. The test specimen fractured.

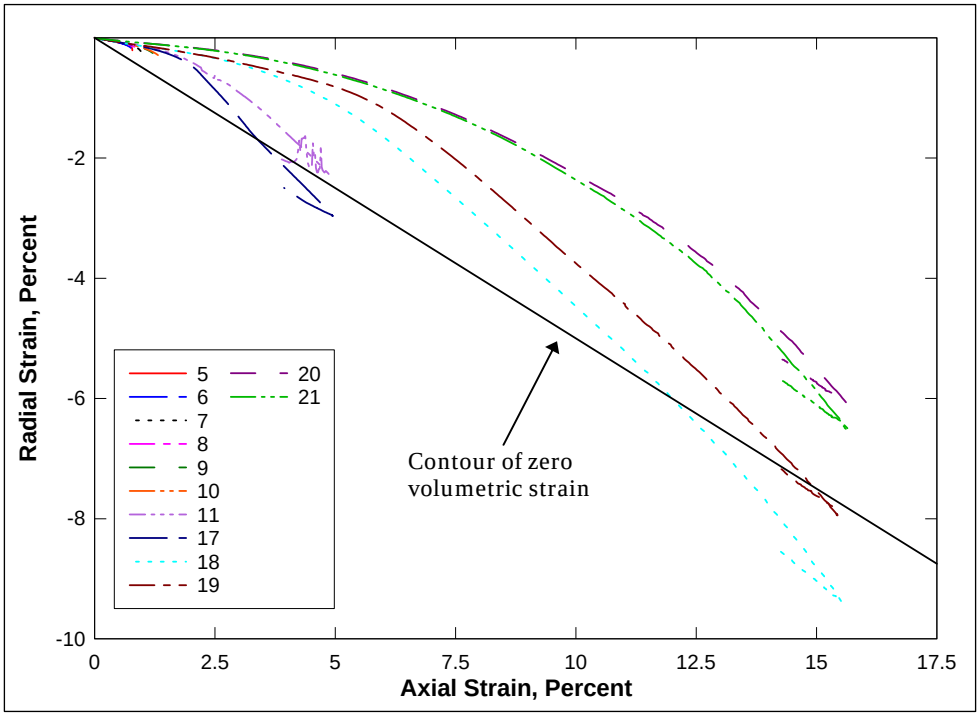

Figure 53. Radial strain-axial strain data during shear from TXC tests on Cor-Tuf2 concrete at confining pressures between 10 and 300 MPa.

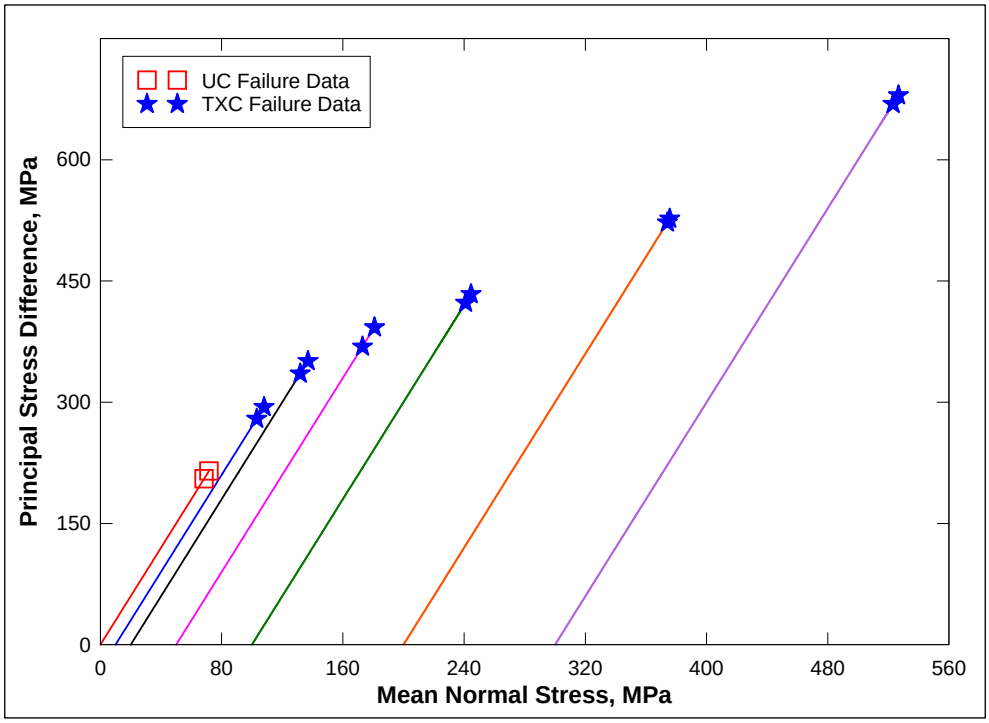

Figure 54. Failure data from UC and TXC tests on Cor-Tuf2 concrete at confining pressures between 10 and 300 MPa.

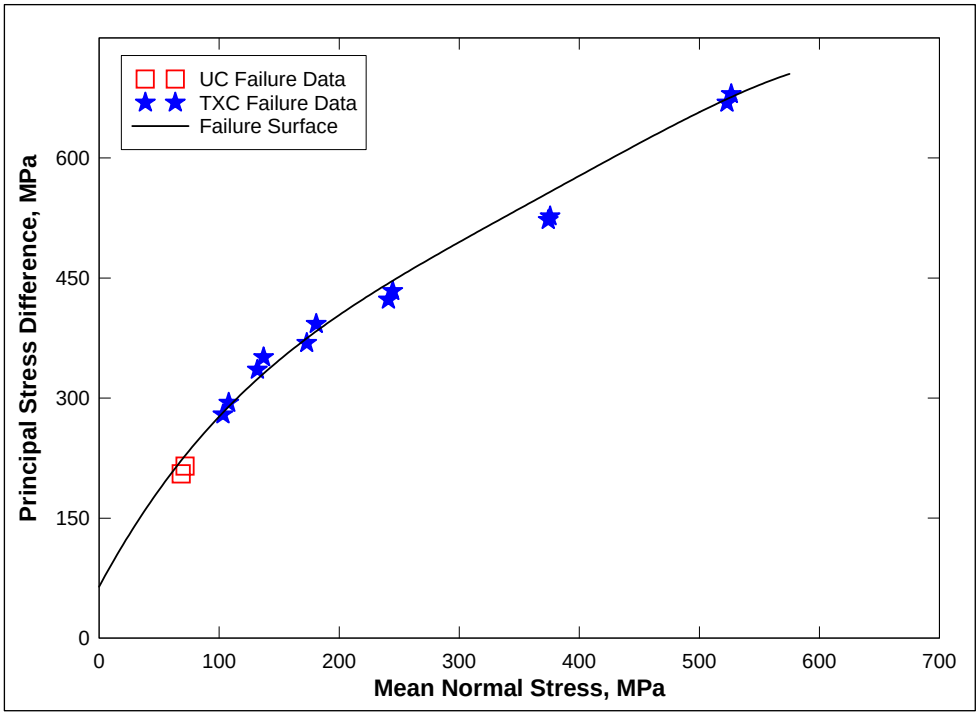

Figure 55. Failure data from UC and TXC tests on Cor-Tuf2 concrete and recommended failure surface.

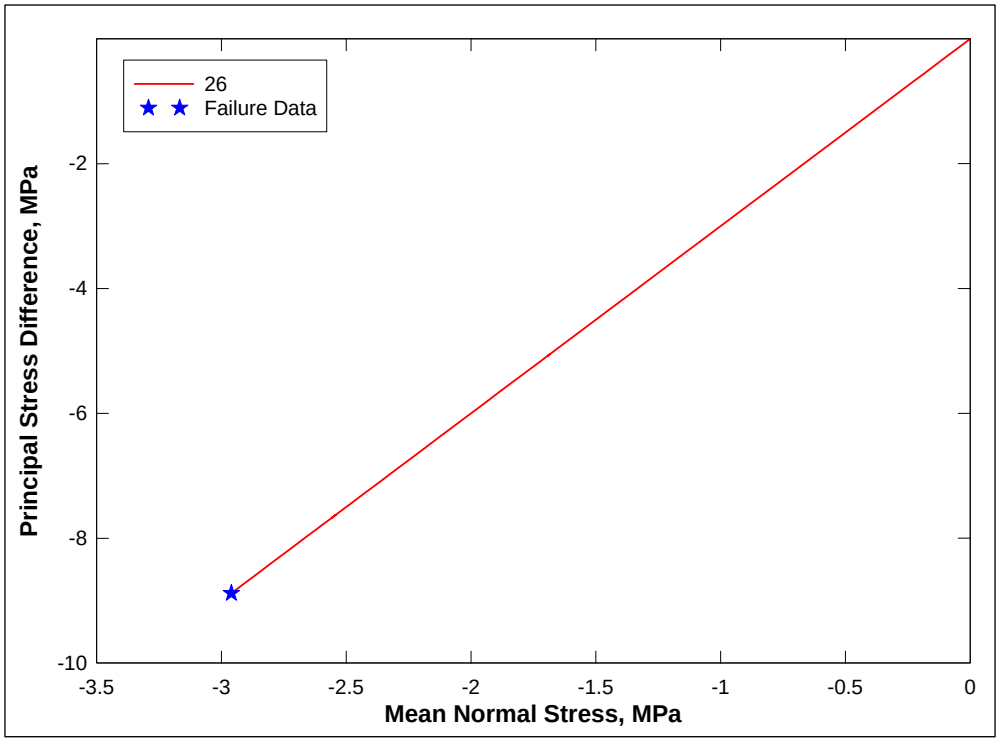

Figure 56. Stress paths and failure data from the DP test on Cor-Tuf2 concrete.

Failure from the DP test occurred at a mean normal stress of -2.96 MPa at a principal stress difference of -8.88 MPa. The absolute value of the tensile strength of Cor-Tuf2 concrete is 4.2% of the unconfined compressive strength (210 MPa). According to ACI 318-02 (2002), tensile strength of concrete is normally about 10 to 15% of the compressive strength. In this case, the DP test produced a much lower value than would generally be predicted.

Uniaxial strain tests

One-dimensional compressibility data were obtained from two undrained uniaxial strain (UX) tests with lateral stress measurements. Data from the tests are plotted in Figures 57 through 59. The stress-strain data from the UX tests are plotted in Figure 57, the pressure-volume data in Figure 58, and the stress paths with the TXC failure surface in Figure 59. During the UX loading, the membranes around test specimen 15 were punctured, and hydraulic fluid seeped into the specimen. The test data after the leak occurred were removed. The two complete UX responses indicate that neither test specimen reached a fully saturated state, i.e., the volumetric strains achieved during the tests were much less than the air voids contents of the specimens.

From the UX stress-strain loading data (Figure 57), an initial constrained modulus, M, of 43.1 GPa was calculated. An initial shear modulus of 15.3 GPa was calculated from the constrained modulus and the initial elastic bulk modulus, K, (22.7 GPa) that was determined from results of the HC and TXC tests. These two values may be used to calculate the other elastic constants, i.e., an initial Young's modulus of 37.5 GPa and Poisson's ratio of 0.22.

The stress paths from the UX tests are plotted with the failure surface in Figure 59. The UX stress paths trend below the TXC recommended failure surface even at very low stresses. As the principal stress difference increases, the paths soften slightly. The stress paths soften after the cement bonds start to crush, causing the data to plot below the failure surface. The two compete stress paths from the UX tests are similar, which is likely a result of the test specimens' having very similar intrinsic properties. For example, the dry densities for these specimens were 2.257 Mg/m^3 for test specimen 2 and 2.235 Mg/m^3 for test specimen 4. The pressure-volume responses from HC and UX tests are compared in Figure 60.

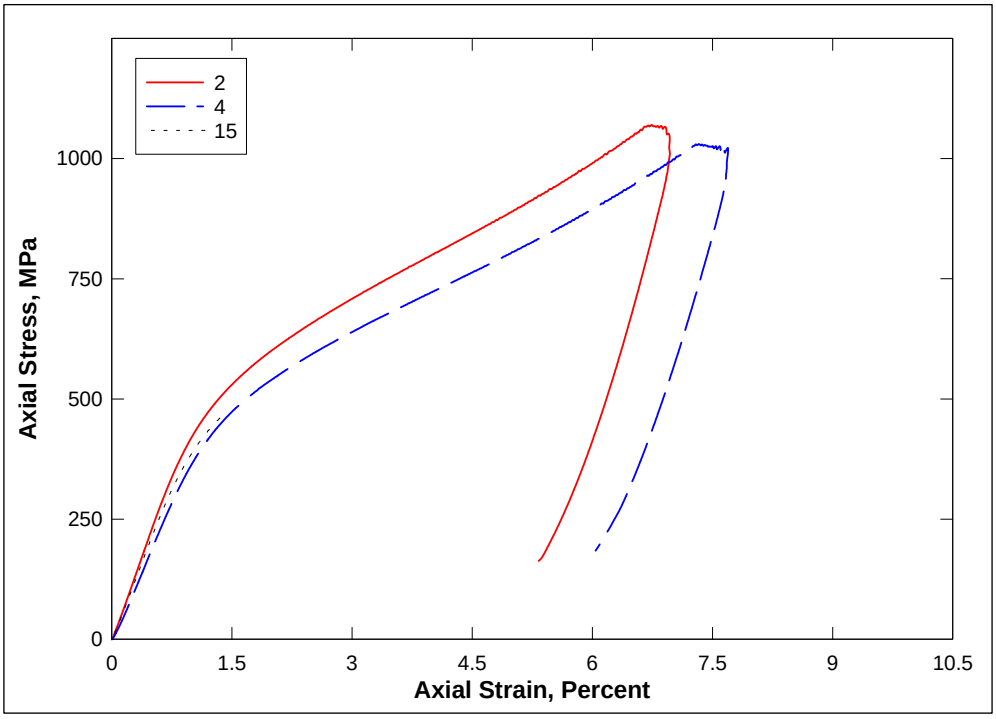

Figure 57. Stress-strain responses from UX tests on Cor-Tuf2 concrete.

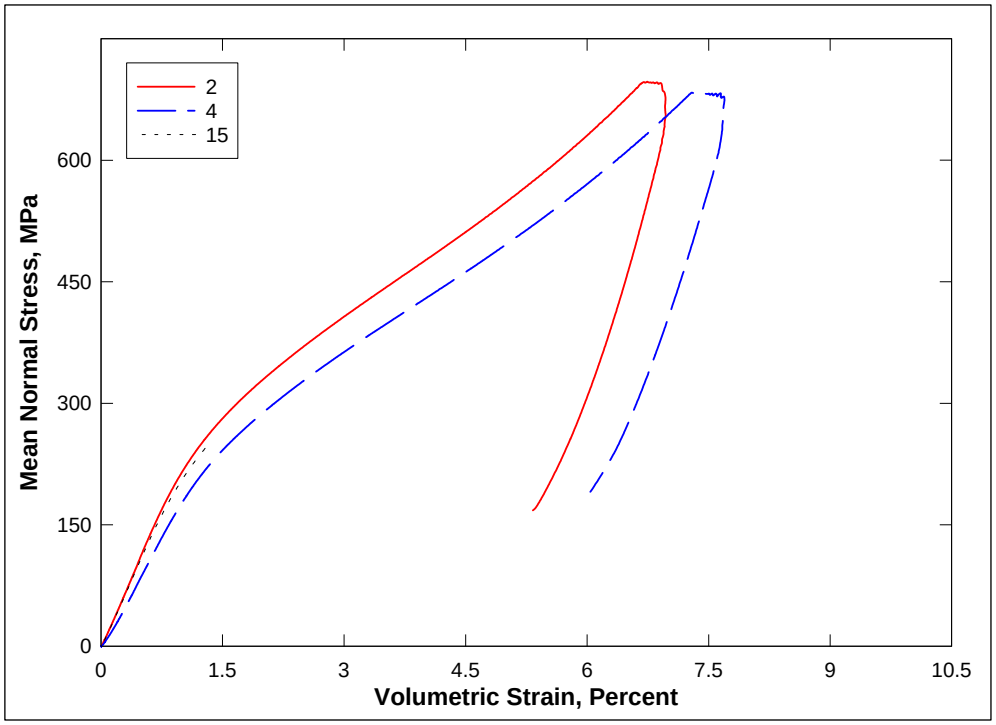

Figure 58. Pressure-volume responses from UX tests on Cor-Tuf2 concrete.

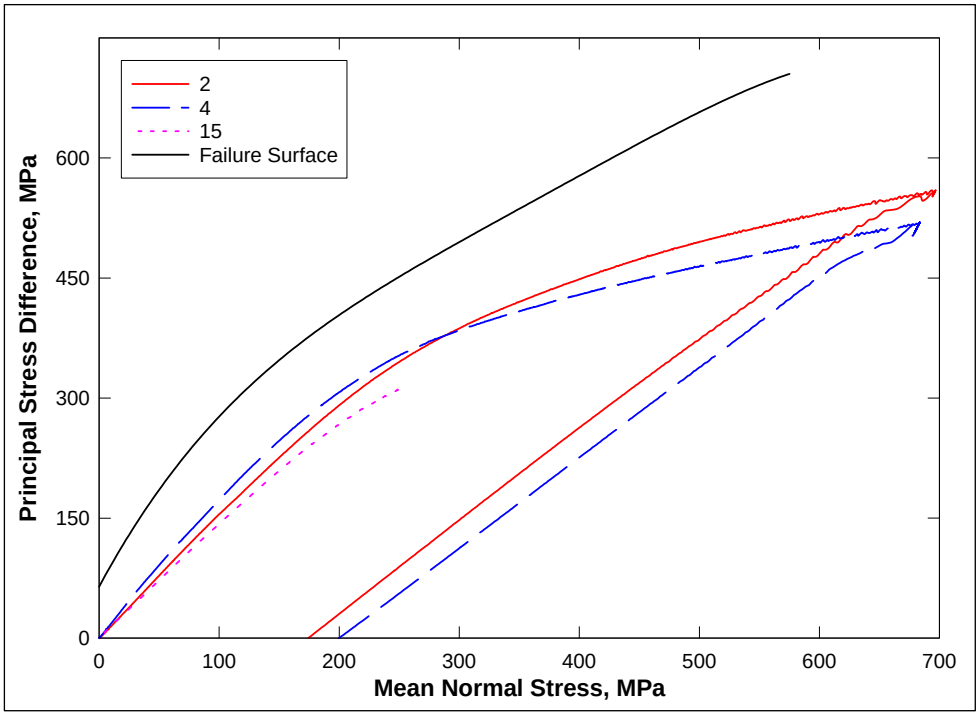

Figure 59. Stress paths from UX tests and failure surface from TXC tests on Cor-Tuf2 concrete.

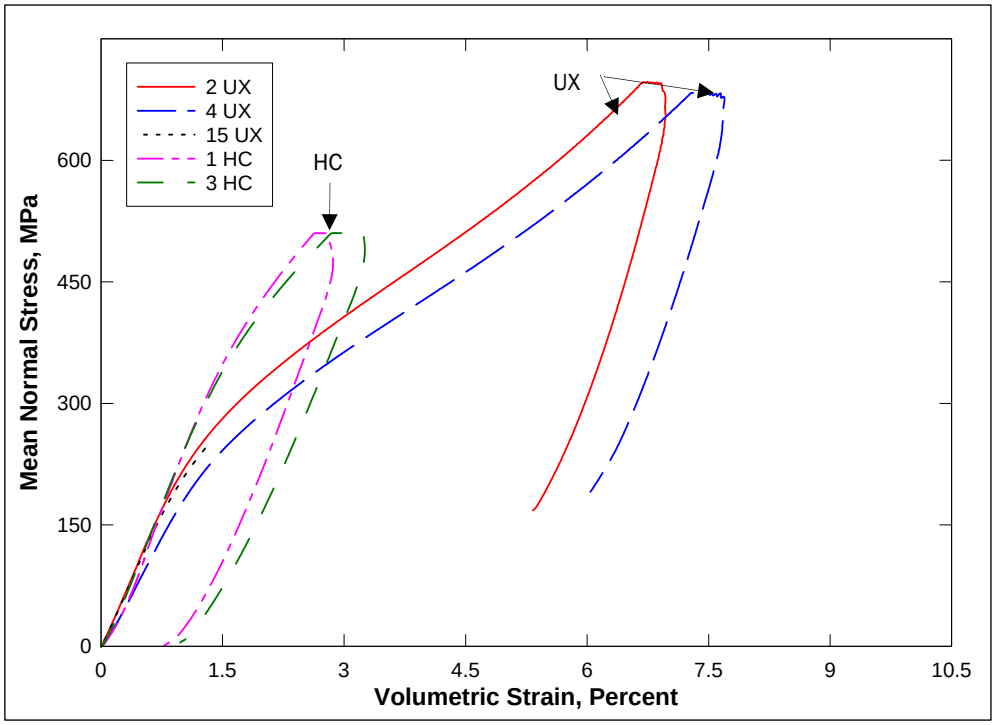

Figure 60. Comparison of pressure-volume responses from HC and UX tests on Cor-Tuf2 concrete.

The initial dry densities of test specimens 1, 2, 3, and 4 were 2.312, 2.257, 2.286, and 2.235 Mg/m^3, respectively. The dry density of test specimen 15 is unknown because of the membrane leak. The HC test specimens had higher initial dry densities than those for UX test specimens, which explain why the HC test specimens display a slightly steeper initial loading than the UX test specimens. The UX test specimens exhibited higher volumetric strains than the HC test specimens above a mean normal stress of about 250 MPa. This response comparison indicates additional shear-induced compaction due to UX loading that cannot occur during HC loading.

Strain path tests

Results from three UX/CV tests conducted at three different levels of peak axial stress during the initial UX phase are shown in Figures 61 through 64. The stress-strain data from the UX/CV tests are plotted in Figure 61, the pressure-volume data in Figure 62, the stress-paths with the TXC failure surface in Figure 63, and the strain paths in Figure 64. Mechanical problems occurred during the CV portion of each UX/CV test. The stress path data (Figure 63) from the UX/CV tests cannot be used to validate the failure surface developed from the TXC tests.

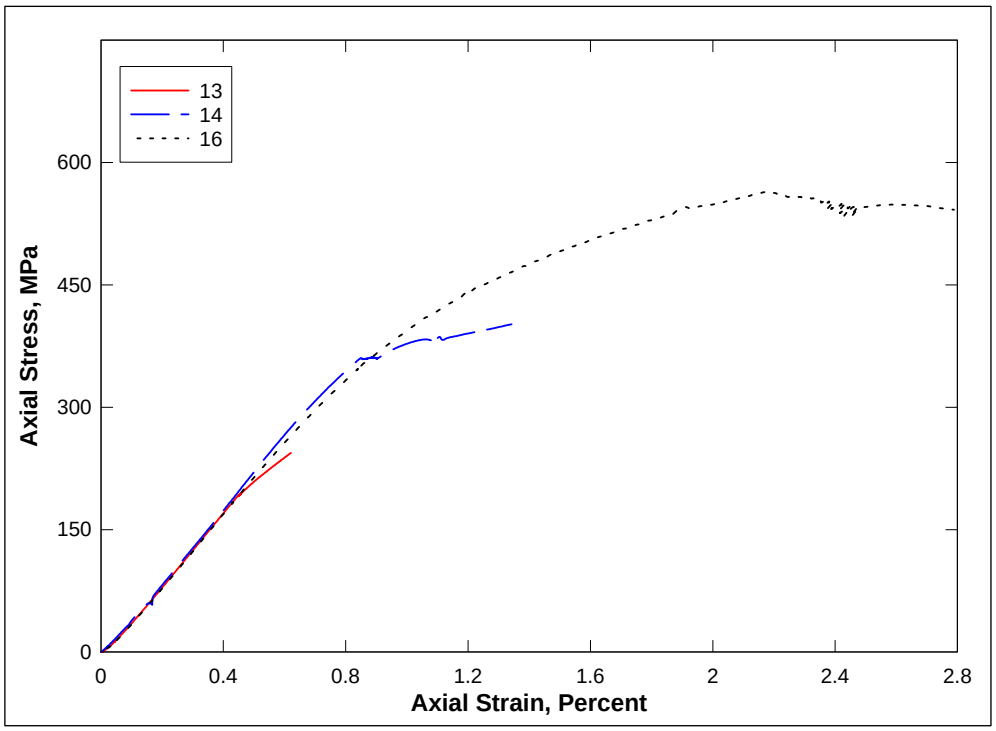

Figure 61. Stress-strain responses from UX/CV tests on Cor-Tuf2 concrete.

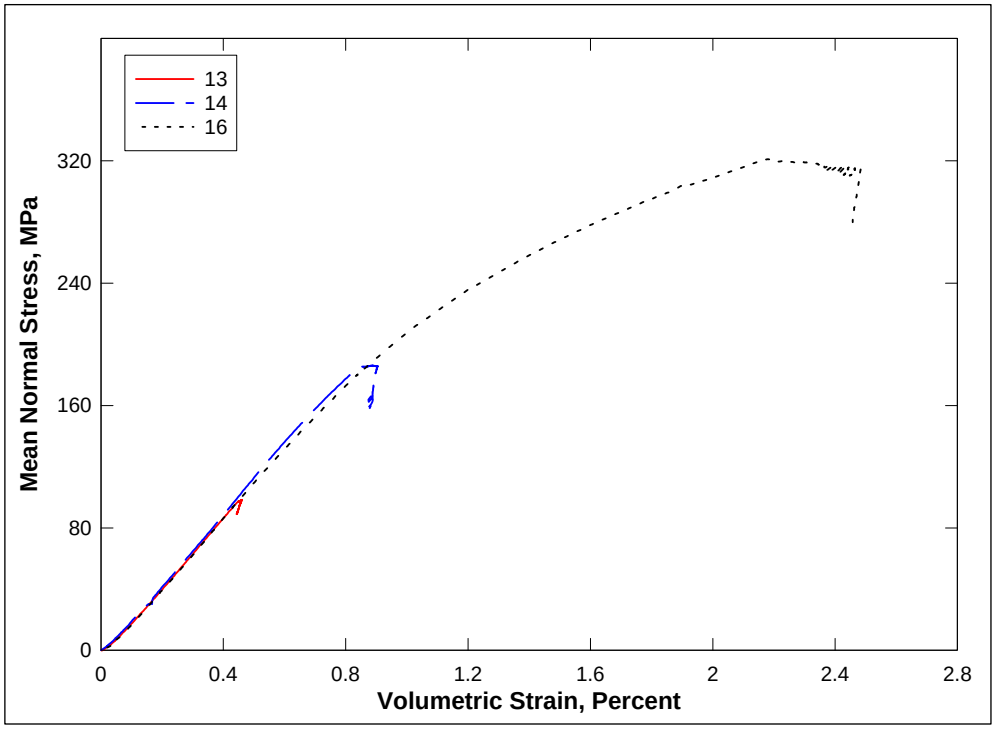

Figure 62. Pressure-volume responses from UX/CV tests on Cor-Tuf2 concrete.

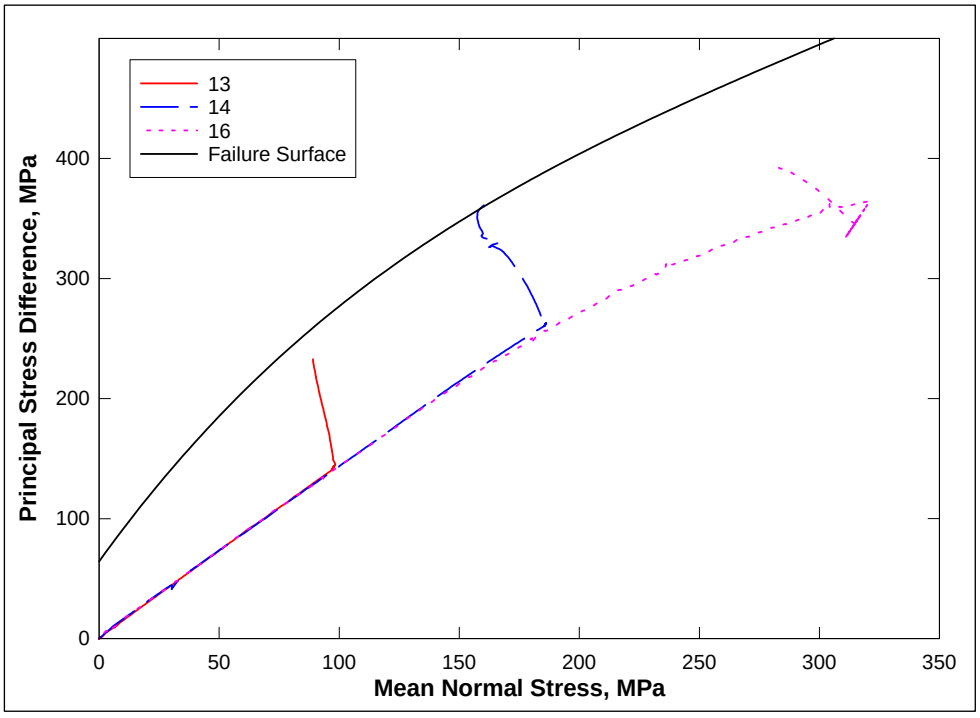

Figure 63. Stress paths from UX/CV tests and failure surface from TXC tests on Cor-Tuf2 concrete.

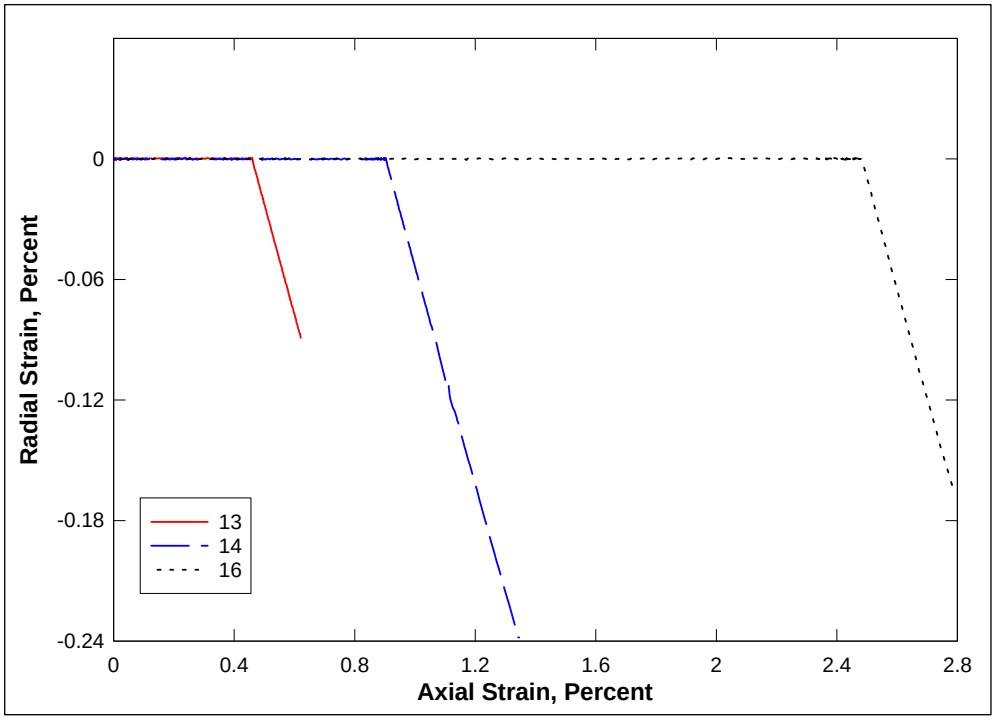

Figure 64. Strain paths from UX/CV tests on Cor-Tuf2 concrete.

5 Comparisons of Results from Tests on Cor-Tuf Concrete with and without Steel Fibers

Cor-Tuf1 and Cor-Tuf2 concrete are the same mixture with the exception that Cor-Tuf1 has steel fibers while Cor-Tuf2 is without steel fibers. The steel fibers likely caused the specific gravity of the Cor-Tuf1 concrete (2.93) to be slightly higher than that of the Cor-Tuf2 concrete (2.77). Because the concretes are the same mixture with the exception of steel fibers, the results of the mechanical property tests on the two concretes are compared in this chapter to determine if the mechanical responses vary significantly. In Figures 65 through 89 that follow, tests numbers for Cor-Tuf1 concrete are followed by the letter 1 while test numbers for the Cor-Tuf2 concrete are followed by a 2.

The pressure-volume data from the two HC tests conducted on each concrete are compared in Figure 65. The HC compressibility for Cor-Tuf1 and 2 are very similar with Cor-Tuf2 displaying a greater ability to compress. The greater densities of the Cor-Tuf1 test specimens slightly reduce the compressibility of Cor-Tuf1 concrete. Figure 66 presents the pressure time-histories for the HC tests. Both Cor-Tuf1 and Cor-Tuf2 concrete are susceptible to creep (Figures 65 and 66). Based on the data from HC tests, the initial elastic bulk modulus, K, is 25.2 GPa for the Cor-Tuf1 concrete and 22.7 GPa for the Cor-Tuf2 concrete.

Results from the UC tests conducted on the two concretes are plotted in Figures 67 and 68, and results from the TXC tests are plotted in Figures 69 through 80. In all the figures, the axial and volumetric strains at the beginning of the shear phase were set to zero, i.e., only the strains during shear are plotted.

Variations in the stress-strain and strength data in Figure 67 are caused primarily by variations in the specimens' initial dry densities. The mean unconfined compressive strengths of Cor-Tuf1 and Cor-Tuf2 concrete were determined to be 237 and 210 MPa, respectively.

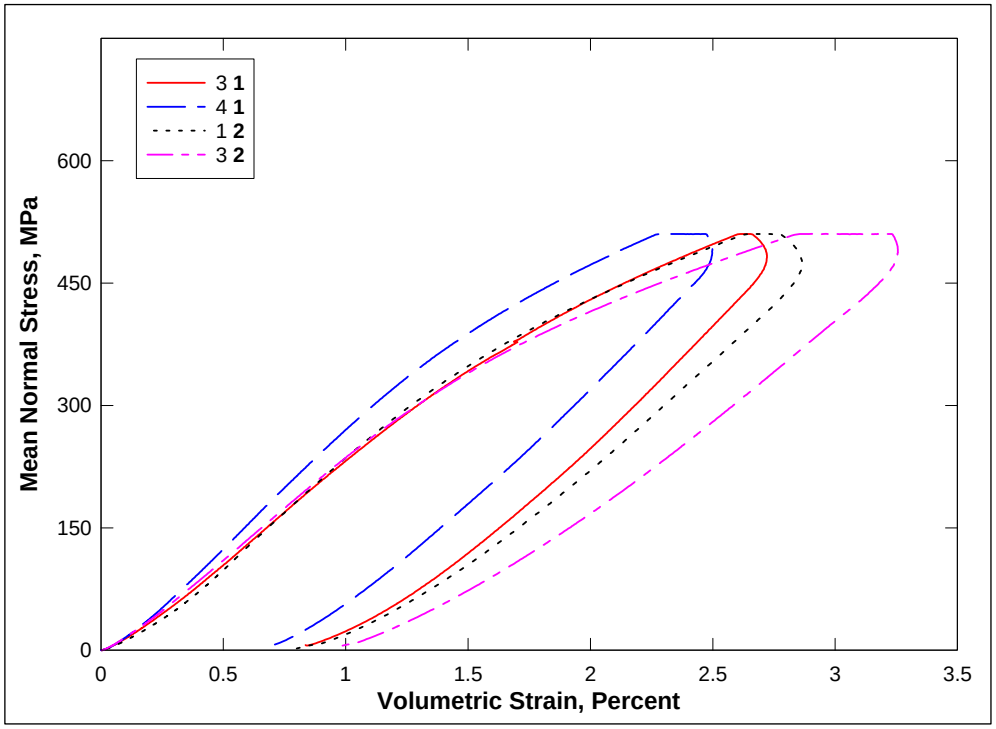

Figure 65. Pressure-volume responses from the HC tests.

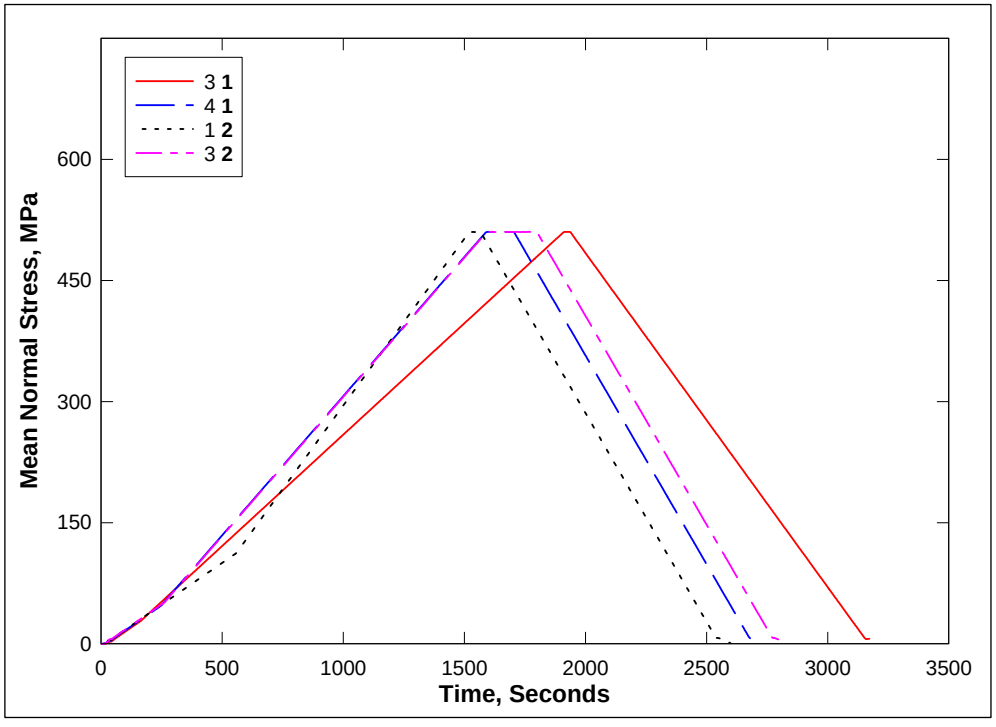

Figure 66. Pressure time-histories from the HC tests.

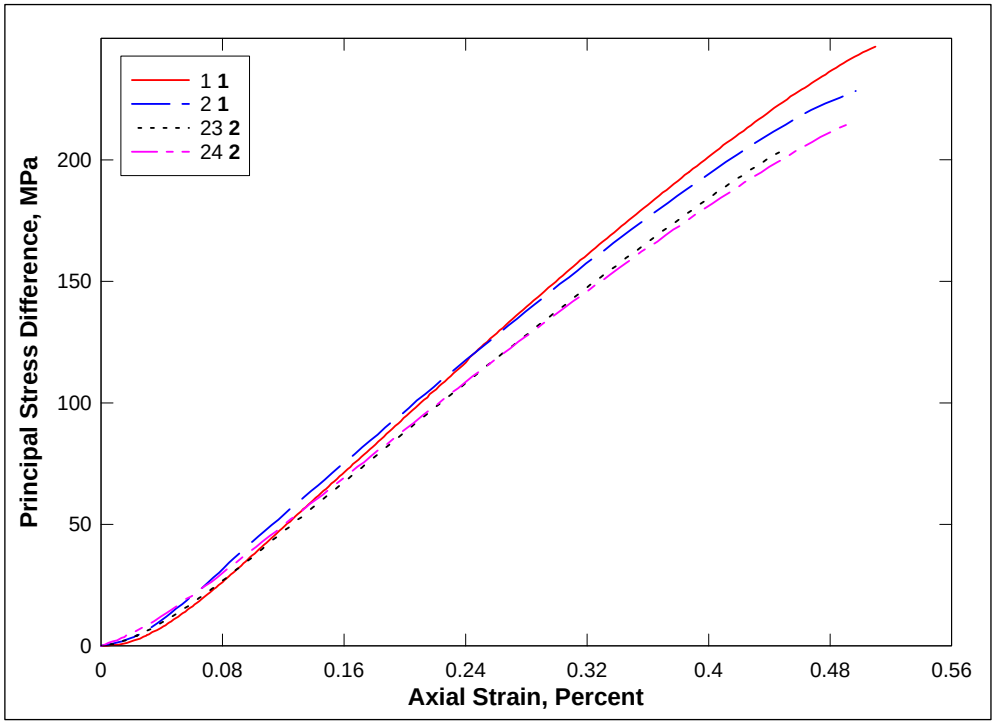

Figure 67. Stress-strain responses from UC tests.

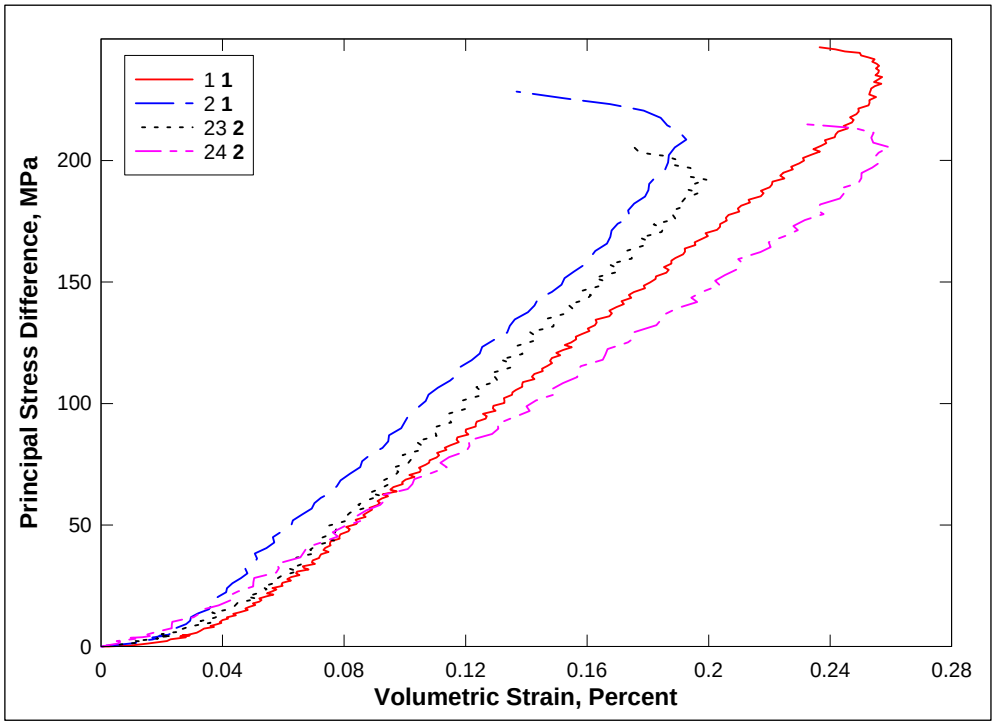

Figure 68. Stress difference-volumetric strain during shear from UC tests.

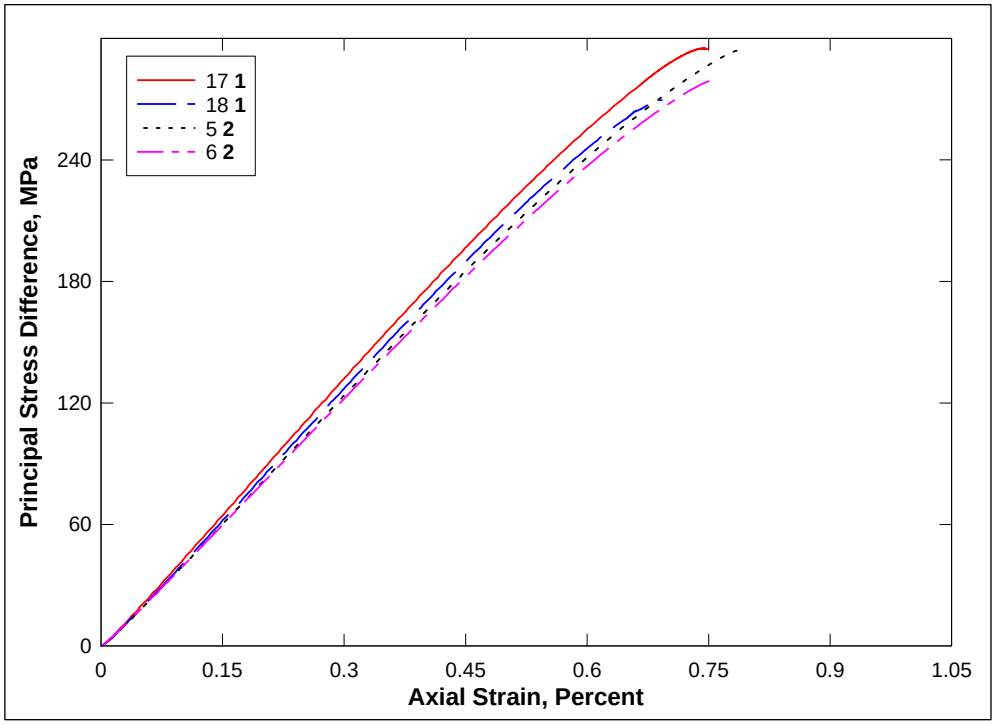

Figure 69. Stress-strain responses from TXC tests at a confining pressure of 10 MPa.

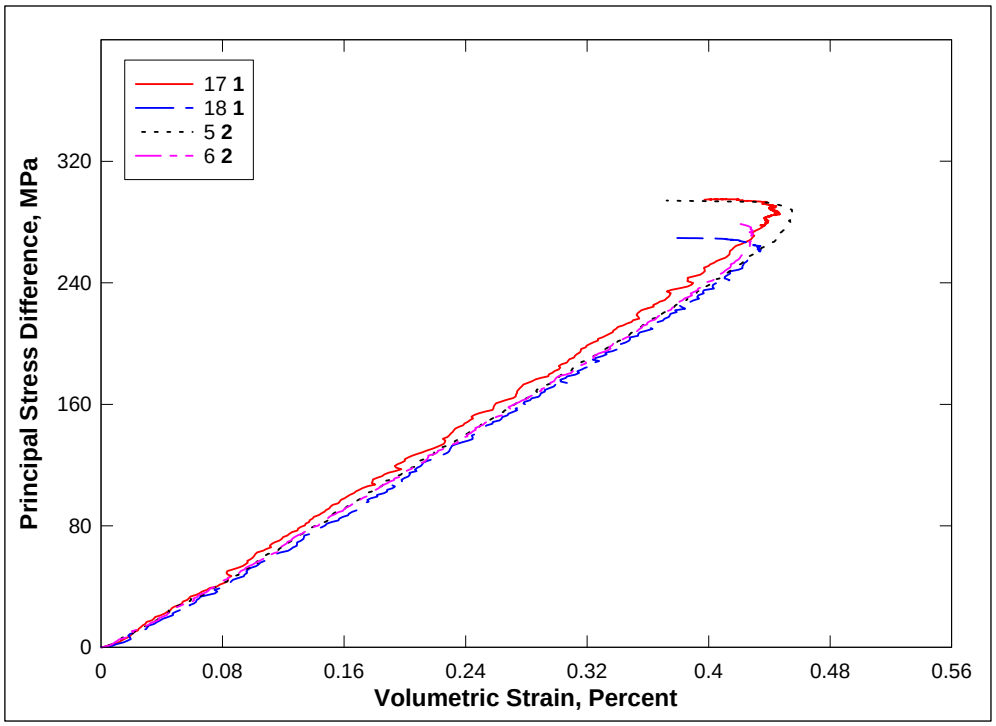

Figure 70. Stress difference-volumetric strain during shear from TXC tests at a confining pressure of 10 MPa.

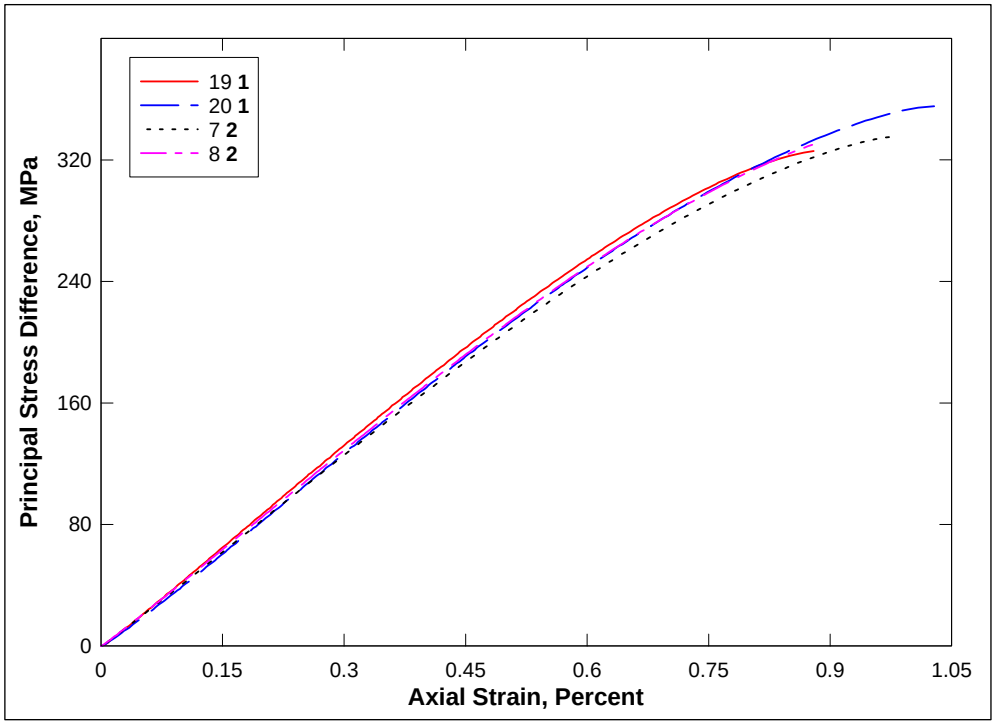

Figure 71. Stress-strain responses from TXC tests at a confining pressure of 20 MPa.

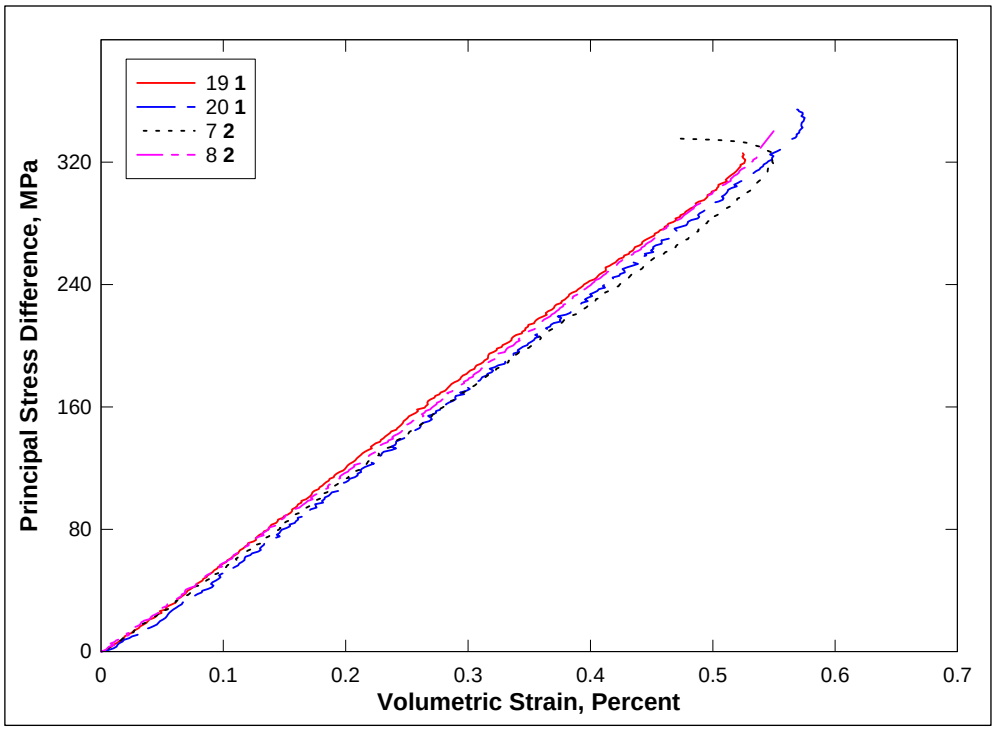

Figure 72. Stress difference-volumetric strain during shear from TXC tests at a confining pressure of 20 MPa.

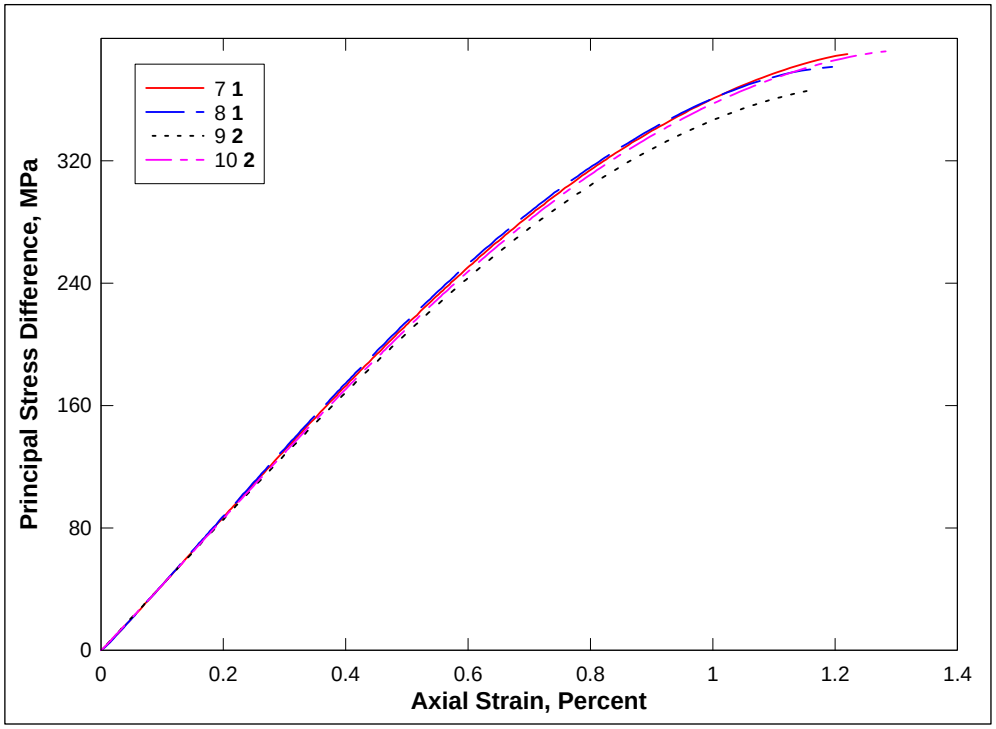

Figure 73. Stress-strain responses from TXC tests at a confining pressure of 50 MPa.

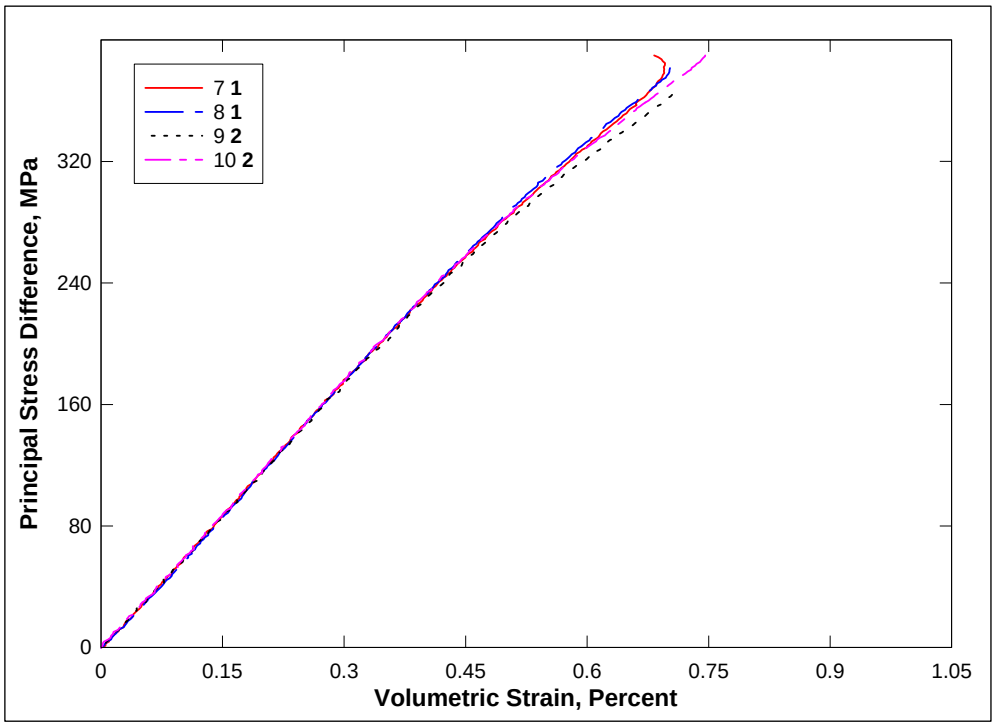

Figure 74. Stress difference-volumetric strain during shear from TXC tests at a confining pressure of 50 MPa.

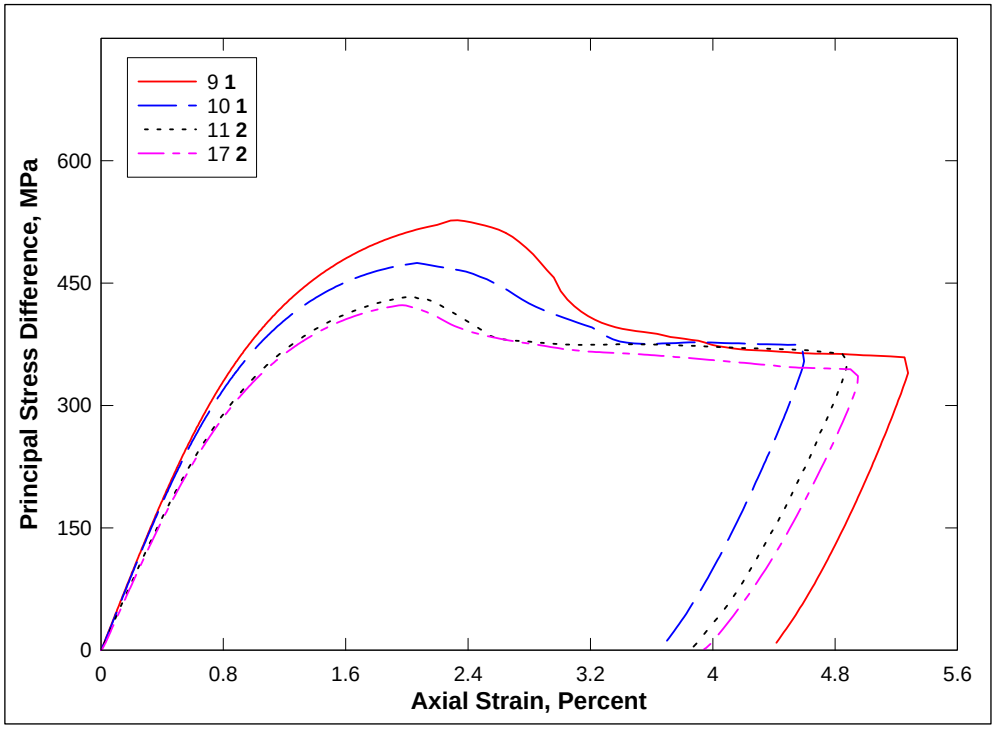

Figure 75. Stress-strain responses from TXC tests at a confining pressure of 100 MPa.

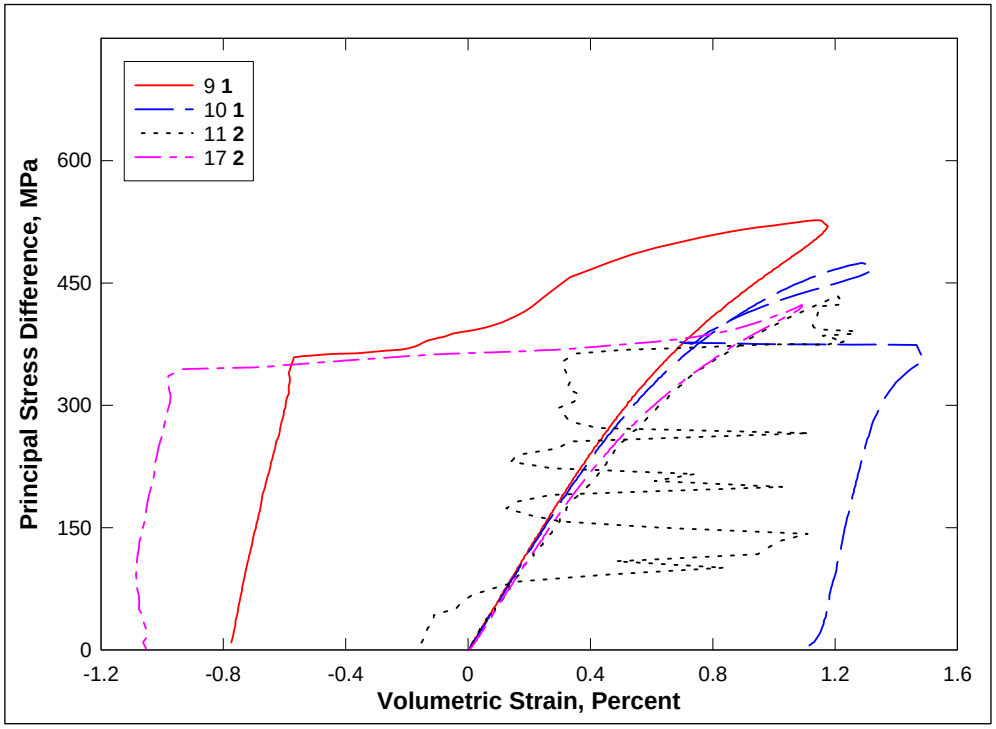

Figure 76. Stress difference-volumetric strain during shear from TXC tests at a confining pressure of 100 MPa.

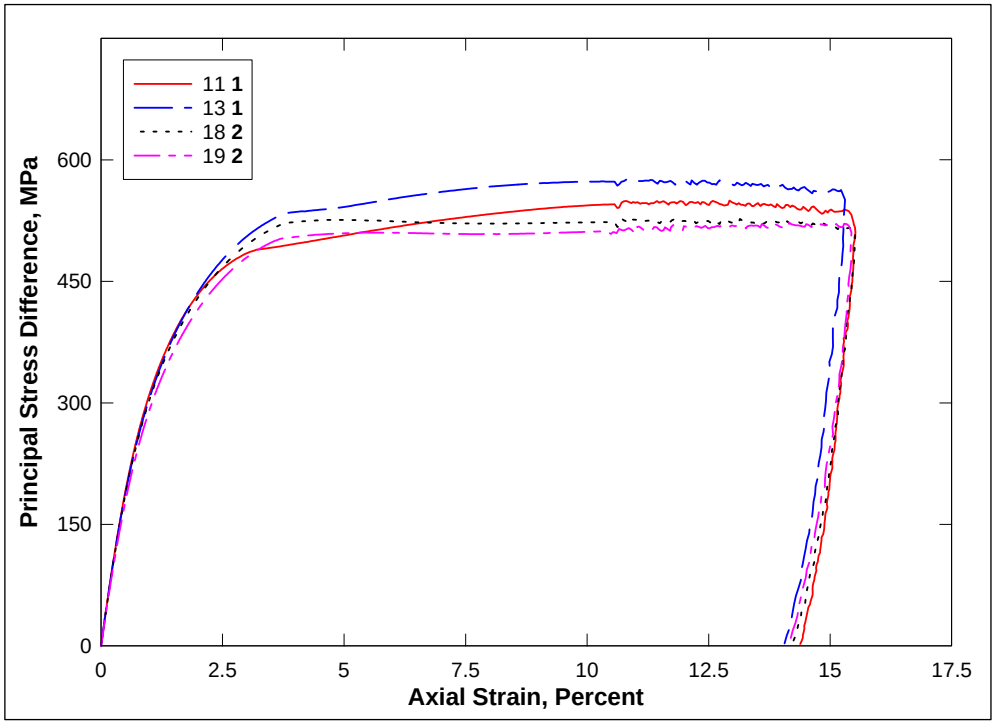

Figure 77. Stress-strain responses from TXC tests at a confining pressure of 200 MPa.

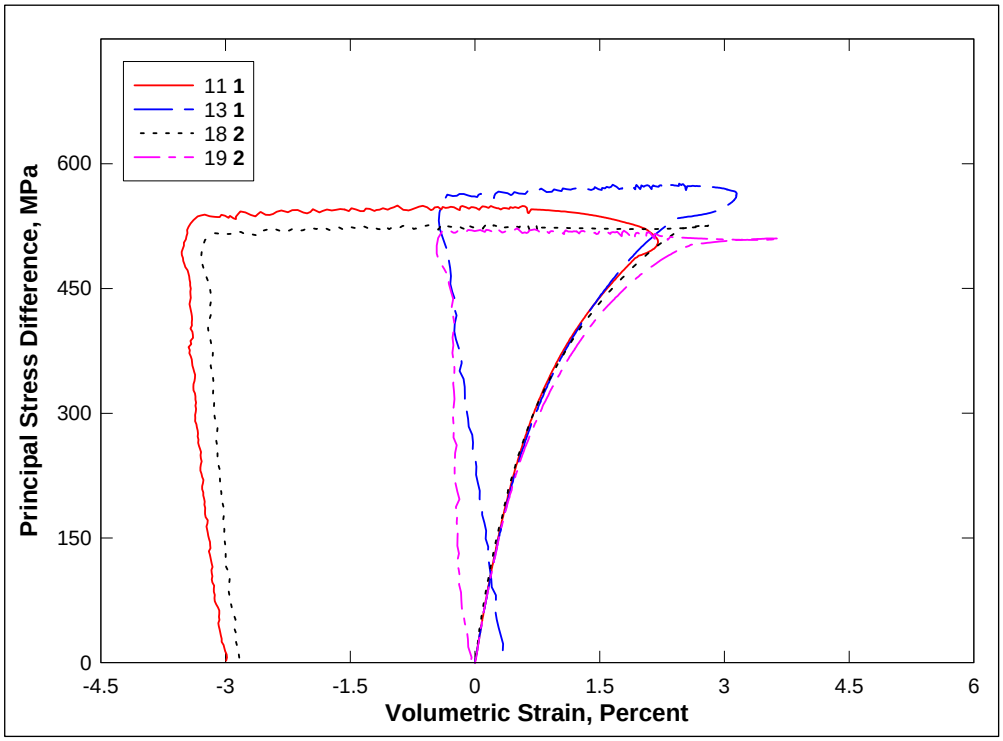

Figure 78. Stress difference-volumetric strain during shear from TXC tests at a confining pressure of 200 MPa.

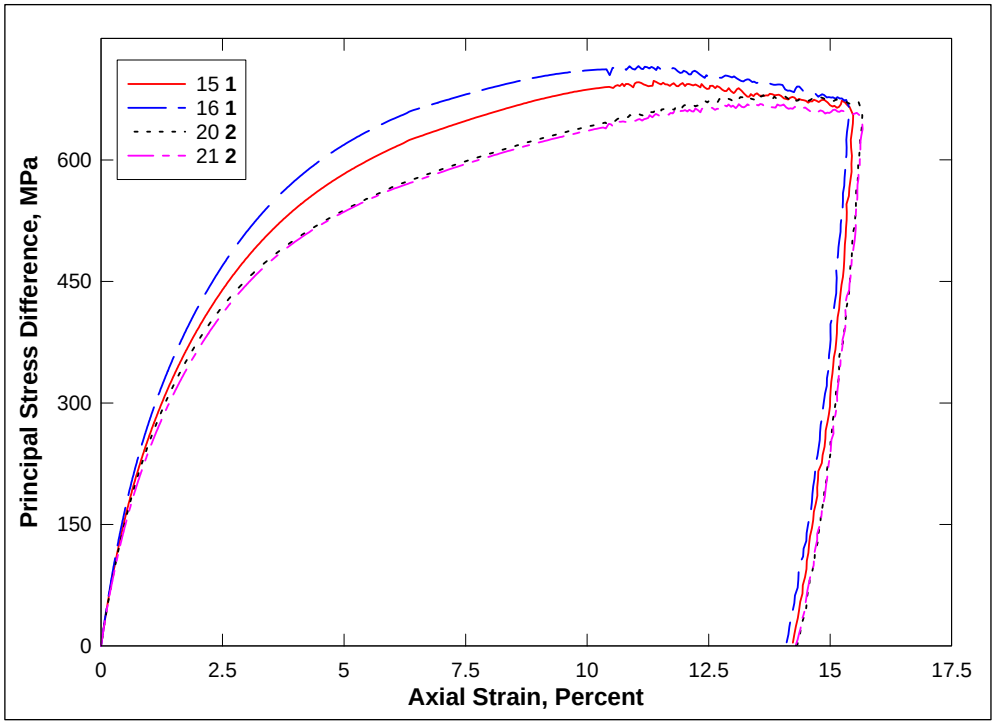

Figure 79. Stress-strain responses from TXC tests at a confining pressure of 300 MPa.

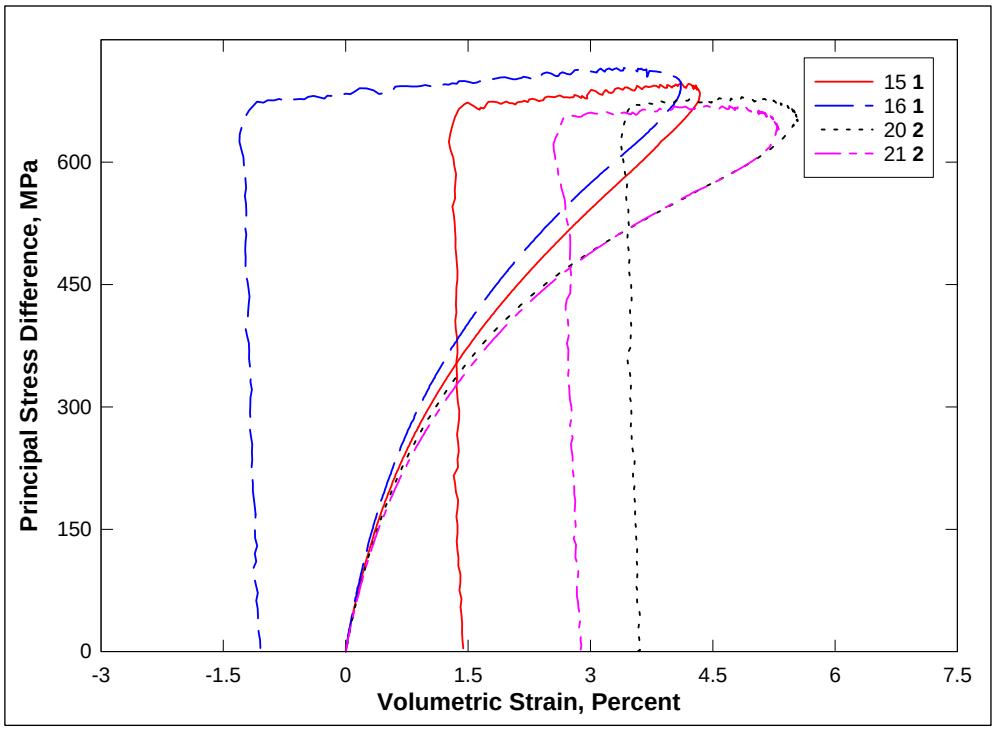

Figure 80. Stress difference-volumetric strain during shear from TXC tests at a confining pressure of 300 MPa.

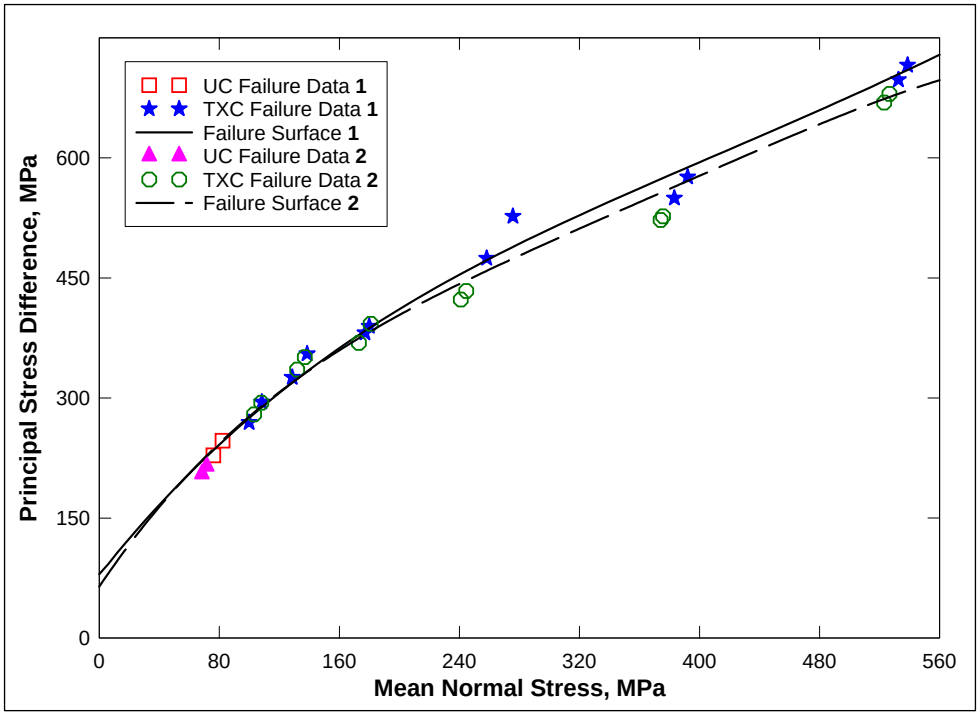

Figure 81. Failure data from UC and TXC tests and recommended failure surfaces.

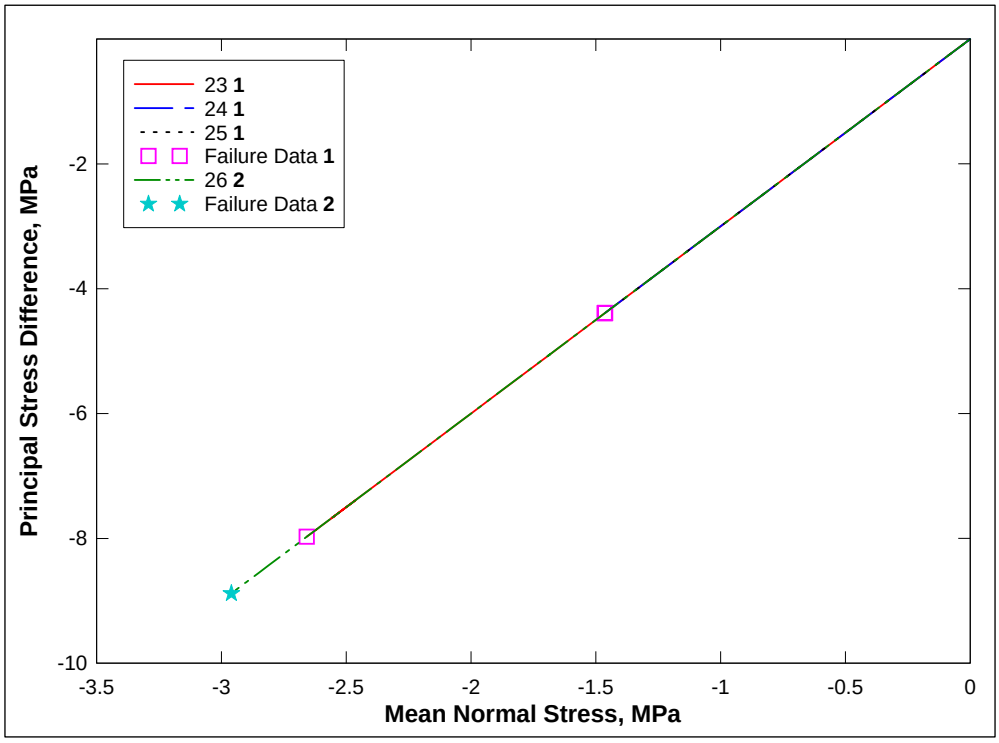

Figure 82. Stress paths and failure data from DP tests.

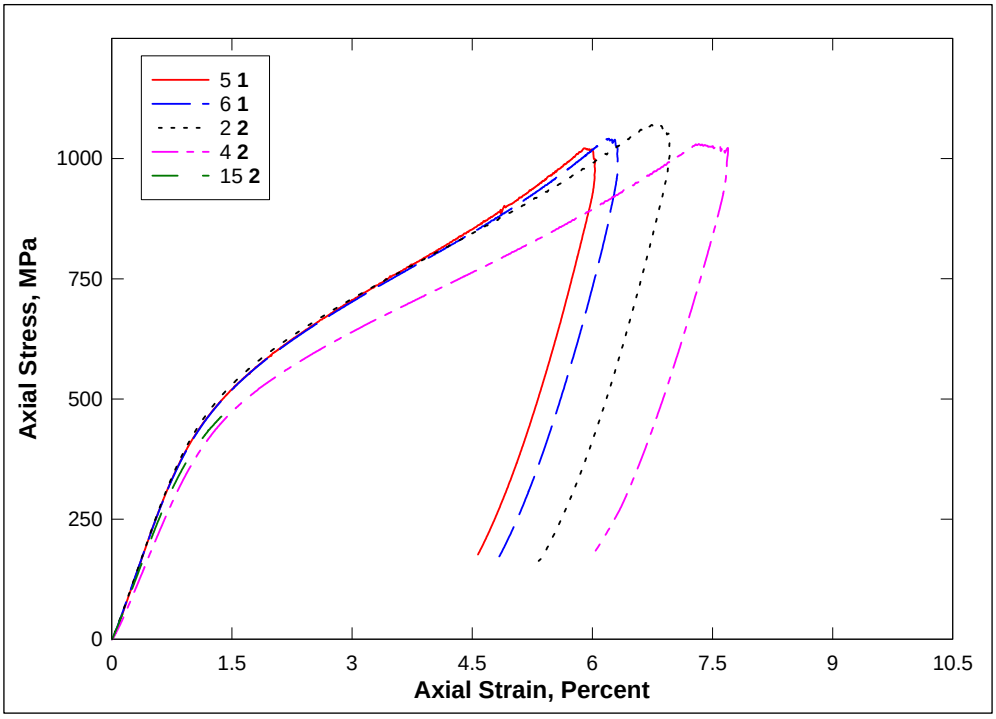

Figure 83. Stress-strain responses from UX tests.

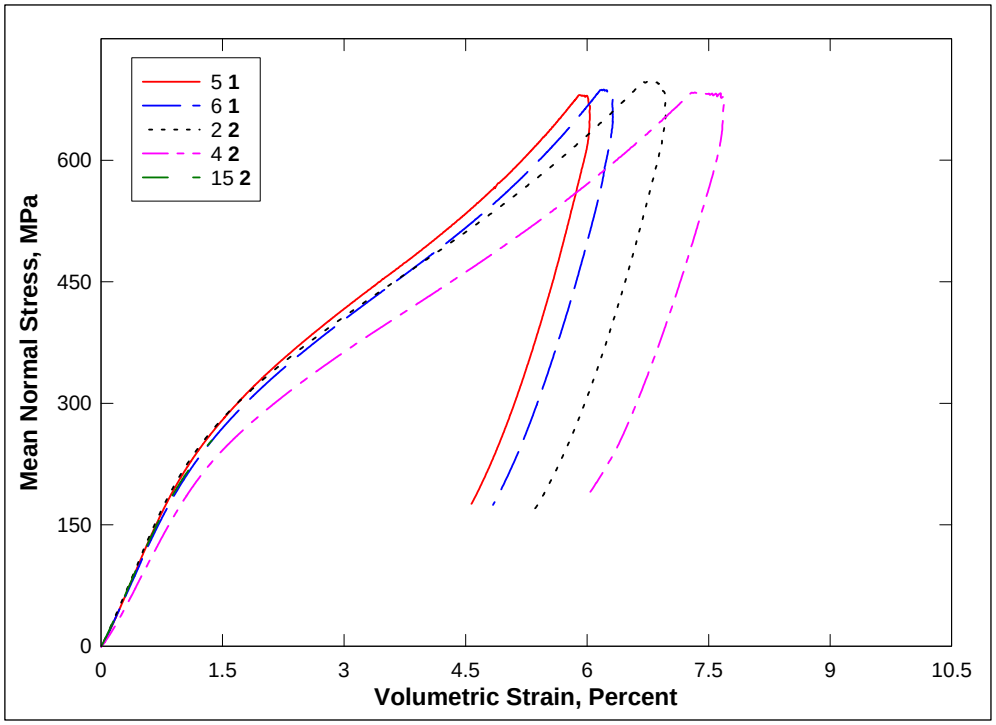

Figure 84. Pressure-volume responses from UX tests.

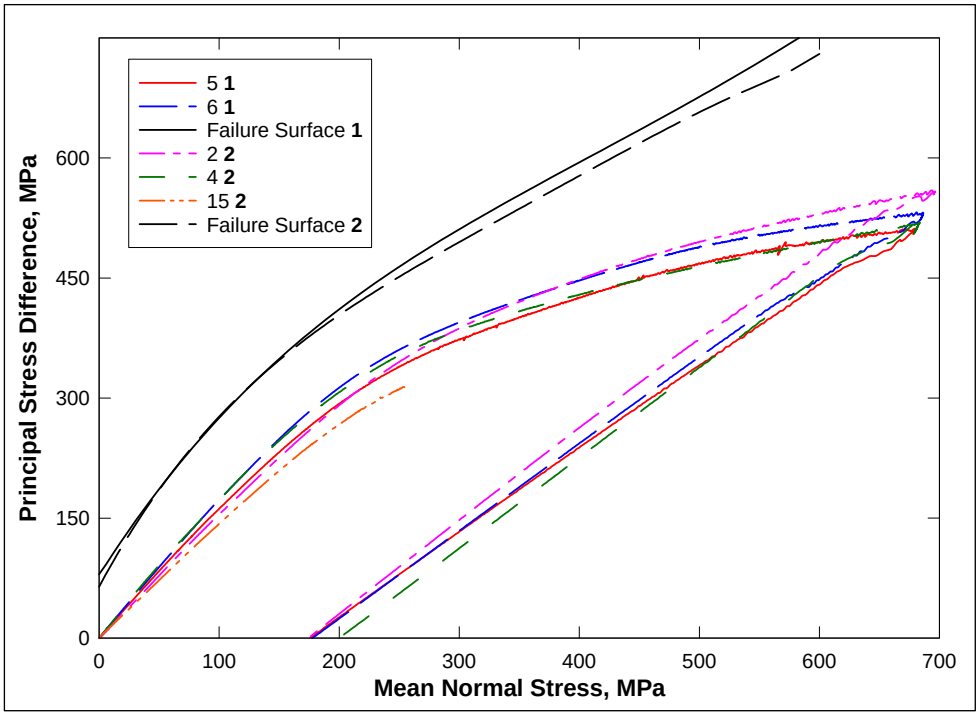

Figure 85. Stress paths from UX tests and failure surfaces from TXC tests.

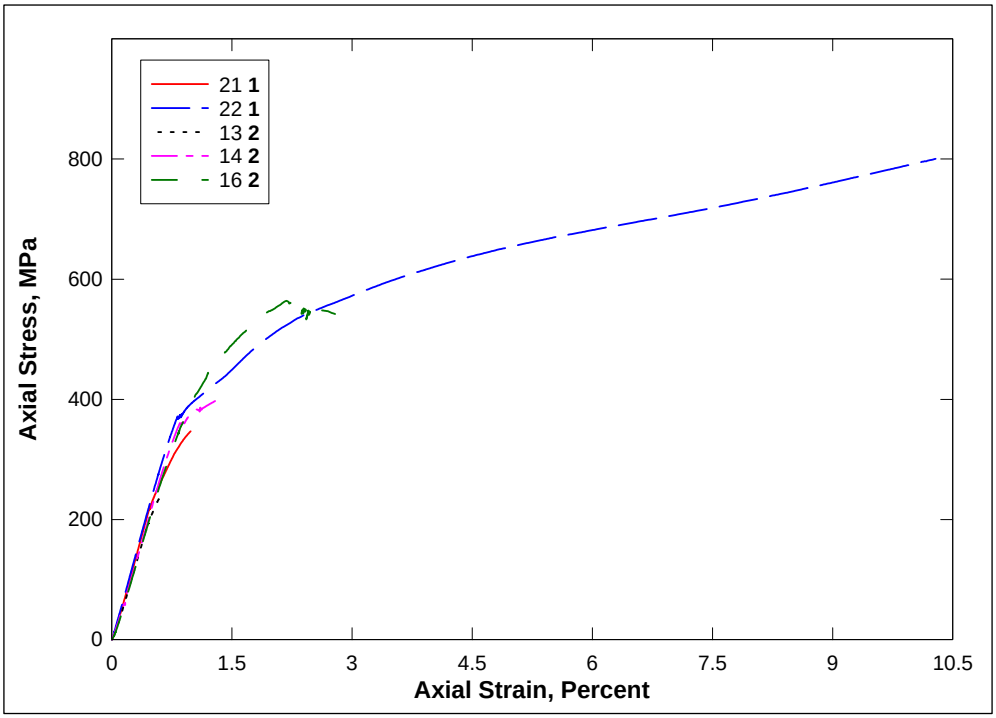

Figure 86. Stress-strain responses from UX/CV tests.

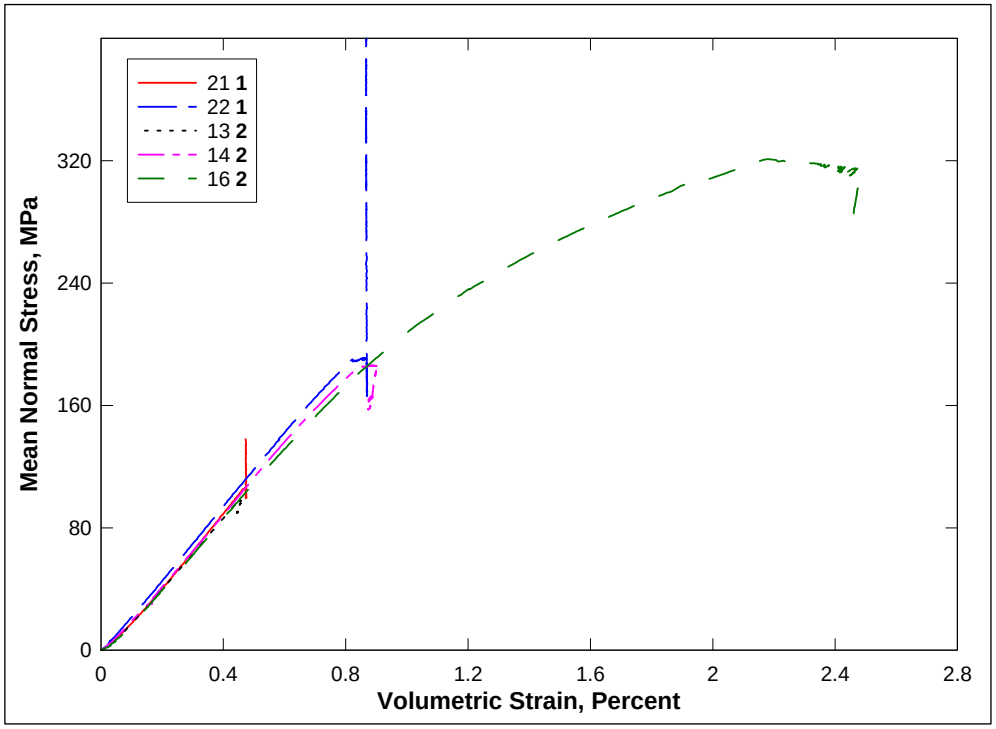

Figure 87. Pressure-volume responses from UX/CV tests.

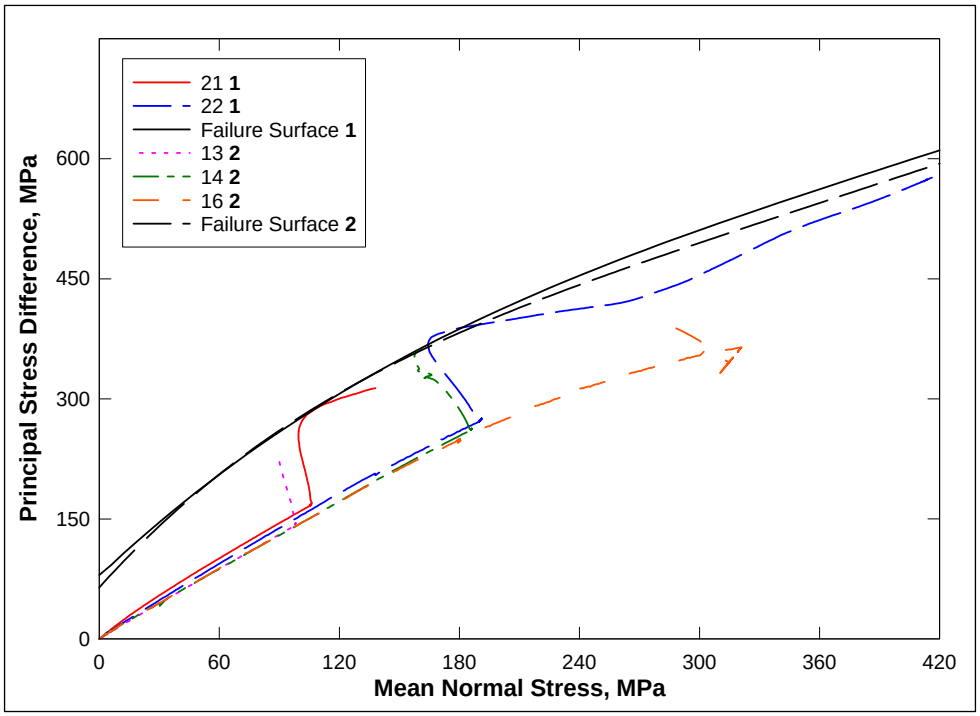

Figure 88. Stress paths from UX/CV tests and failure surfaces from TXC test.

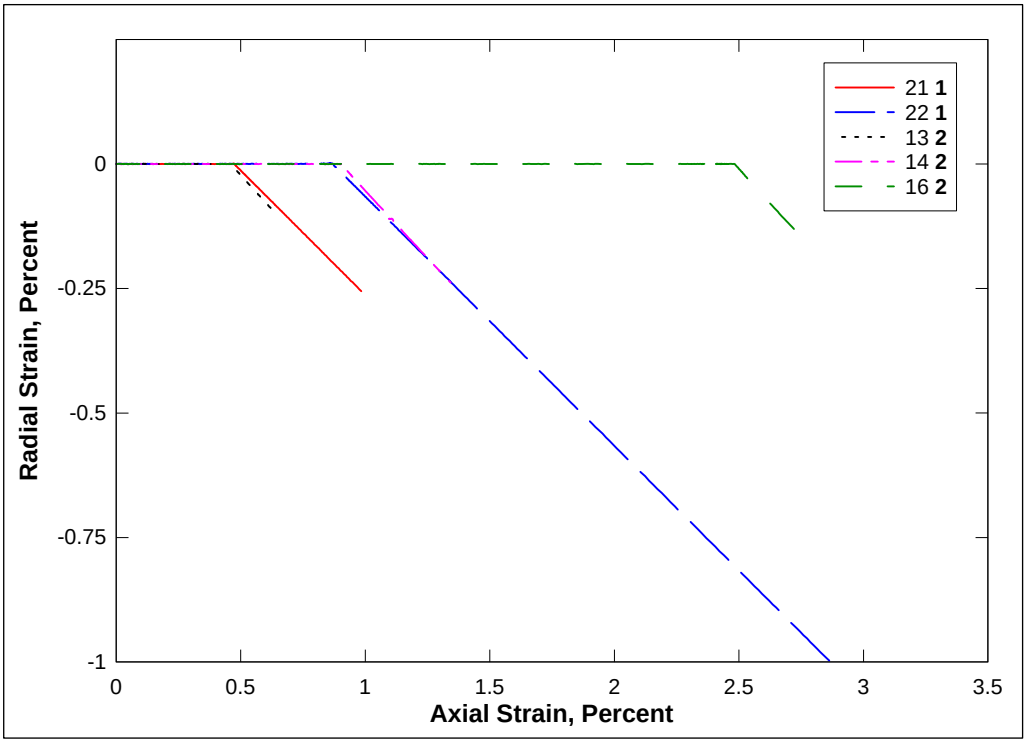

Figure 89. Strain paths from UX/CV tests.

Figures 69 through 80 compare the results from the TXC tests conducted on the two concretes at nominal confining pressures of 10, 20, 50, 100, 200, and 300 MPa. The peak strength of the test specimens for Cor-Tuf1 and 2 are very similar for confining pressures between 10 and 50 MPa. Cor-Tuf1 clearly displays increases in strength over Cor-Tuf2 with confining pressures of 100 MPa and greater. The increased strength of Cor-Tuf1 is likely a result of the greater density and lower water content of the Cor-Tuf1 test specimens than the Cor-Tuf2 test specimens. In Figure 81, the recommended failure surfaces for the Cor-Tuf1 and Cor-Tuf2 concrete are essentially the same initially. As the confining pressure increases, the failure surface for Cor-Tuf1 becomes slightly greater than the failure surface for Cor-Tuf2.

Results from the DP tests are plotted in Figure 82. All of the specimens fractured. The average tensile strength from the Cor-Tuf1 DP tests occurred at -5.58 MPa while the Cor-Tuf2 DP test specimen failed at -8.88 MPa. The tensile strength of Cor-Tuf1 concrete is 2.4% of its unconfined compressive strength while the tensile strength of the Cor-Tuf2 concrete is 4.2% of its unconfined compressive strength.

Comparisons of the UX test results for the two concretes are in Figures 83 through 85. The stress-strain data are plotted in Figure 83, the pressure-volume data in Figure 84, and the stress paths with the TXC failure surface in Figure 85. Cor-Tuf2 displays greater amounts of axial (Figure 83) and volumetric strains (Figure 84) than Cor-Tuf1; therefore, Cor-Tuf2 compresses more than Cor-Tuf1. The greater density of the Cor-Tuf1 test specimens reduces the compressibility.

The initial constrained modulus, M, for the Cor-Tuf1 concrete is 47.4 GPa, while the initial value for the Cor-Tuf2 concrete is 43.1 GPa. An initial shear modulus of 16.7 GPa was calculated for Cor-Tuf1 concrete and 15.3 GPa for Cor-Tuf2 concrete, based on each concretes' initial constrained modulus and bulk modulus determined from the HC tests.

The stress paths from the UX tests and the respective failure surfaces are plotted in Figure 85. The stress paths for both concretes are very similar; both concretes experience crushing of the cement bonds at approximately 300 MPa, and neither concrete displays full saturation.

Comparisons of the results of UX/CV strain-path tests conducted on the two concretes are shown in Figures 86 through 89. The stress-strain data from the UX/CV tests are plotted in Figure 86, the pressure-volume data in Figure 87, the stress-paths with the TXC failure surfaces in Figure 88, and the strain paths in Figure 89. Mechanical problems occurred during the CV portion of all the tests performed on Cor-Tuf2. In Figure 87, the pressure volume data for Cor-Tuf1 specimens were held at a constant volume. Test specimen 22 (Cor-Tuf1) and test specimen 14 (Cor-Tuf2) displayed similar results until the test on test specimen 14 was concluded because of a mechanical problem during the test.

6 Summary

Personnel of the ERDC Geotechnical and Structures Laboratory conducted a laboratory investigation to characterize the strength and constitutive property behavior of Cor-Tuf concrete with steel fibers (Cor-Tuf1) and without steel fibers (Cor-Tuf2). A total of 23 successful mechanical property tests were conducted for each material that included hydrostatic compression, unconfined compression, triaxial compression, direct pull, uniaxial strain, and uniaxial strain load/constant volume strain tests. In addition to the mechanical property tests, nondestructive pulse-velocity measurements were performed on each specimen.

The overall quality of the test data was very good. Cor-Tuf1 and Cor-Tuf2 concrete behaved similarly. Cor-Tuf1 exhibited greater strength with increased confining pressure, and Cor-Tuf2 displayed greater compressibility. For both materials, creep was observed during the HC tests. Results from the TXC tests exhibited a continuous increase in principal stress difference with increasing confining stress. A compression failure surface was developed from results of TXC tests conducted at six levels of confining pressure and from the results of the UC tests. The results for the DP tests were used to determine the tensile strength of the concretes. By comparing the unconfined compression and the unconfined tensile strengths, it is apparent that both concretes' tensile strengths are less than 10% of their unconfined compressive strengths. The CV loading for Cor-Tuf1 followed closely along the failure surface developed from the TXC tests, therefore validating the Cor-Tuf1 compression failure surface. The failure surface for Cor-Tuf2 was not validated from the CV loading of Cor-Tuf2 test specimens. Overall, the results from all of the compression tests for the Cor-Tuf concretes were very similar. More tensile dominant tests are required to demonstrate the effects of the steel fibers in Cor-Tuf.

References

ACI Committee 318. 2002. *Building code requirements for structural concrete (ACI 318-02) and commentary (ACI 318R-02)*. Detroit, MI: American Concrete Institute.

American Society for Testing and Materials. 2005. *Annual book of ASTM standards*. Philadelphia, PA.

a. Designation C 39-05. Standard test method for compressive strength of concrete specimens.
b. Designation C 42-04. Standard test method for obtaining and testing drilled cores and sawed beams of concrete.
c. Designation C 597-02. Standard test method for pulse velocity through concrete.
d. Designation D 2216-05. Standard test method for laboratory determination of water (moisture) content of soil and rock by mass.
e. Designation D 4543-04. Standard test method for preparing rock core specimens and determining dimensional and shape tolerances.

Bishop, A. W., and D. J. Henkel. 1962. *The measurement of soil properties in the triaxial test*. London: Edward Arnold, Ltd.

REPORT DOCUMENTATION PAGE

Form Approved
OMB No. 0704-0188

1. REPORT DATE *(DD-MM-YYYY)*	**2. REPORT TYPE**	**3. DATES COVERED** *(From - To)*
July 2009	Final report	

4. TITLE AND SUBTITLE

Laboratory Characterization of Cor-Tuf Concrete With and Without Steel Fibers

5a. CONTRACT NUMBER

5b. GRANT NUMBER

5c. PROGRAM ELEMENT NUMBER

6. AUTHOR(S)

Erin M. Williams, Steven S. Graham, Paul A. Reed, and Todd S. Rushing

5d. PROJECT NUMBER

5e. TASK NUMBER

5f. WORK UNIT NUMBER

7. PERFORMING ORGANIZATION NAME(S) AND ADDRESS(ES)

U.S. Army Engineer Research and Development Center
Geotechnical and Structures Laboratory
3909 Halls Ferry Road
Vicksburg, MS 39180-6199

8. PERFORMING ORGANIZATION REPORT NUMBER

ERDC/GSL TR-09-22

9. SPONSORING / MONITORING AGENCY NAME(S) AND ADDRESS(ES)

Headquarters, U.S. Army Corps of Engineers
Washington, DC 20314-1000

10. SPONSOR/MONITOR'S ACRONYM(S)

11. SPONSOR/MONITOR'S REPORT NUMBER(S)

12. DISTRIBUTION / AVAILABILITY STATEMENT

Approved for public release; distribution is unlimited.

13. SUPPLEMENTARY NOTES

14. ABSTRACT

Personnel of the Geotechnical and Structures Laboratory, U.S. Army Engineer Research and Development Center, conducted a series of laboratory experiments to investigate the strength and constitutive property behavior of baseline ultra-high-performance composite (Cor-Tuf) concrete with and without steel fibers. A total of 23 mechanical property tests were successfully completed for Cor-Tuf1 and Cor-Tuf2 concrete. The mechanical property tests included hydrostatic compression, unconfined compression (UC), triaxial compression (TXC), unconfined direct pull (DP), uniaxial strain, and uniaxial strain load/constant volume strain loading tests. In addition to the mechanical property tests, nondestructive pulse-velocity measurements and mass properties were obtained on each specimen. The TXC tests exhibited a continuous increase in maximum principal stress difference with increasing confining stress. A compression failure surface was developed from the TXC test results at six levels of confining pressure and from the results of the UC tests. The results for the DP tests were used to determine the unconfined tensile strength of the concretes, which were less than 10% of the unconfined compressive strength. The Cor-Tuf with the steel fibers exhibits slightly greater strength with increasing confining pressure than the Cor-Tuf without steel fibers. Overall, the results from all of the compression tests for both Cor-Tuf concretes were very similar.

15. SUBJECT TERMS

Fiber-reinforced concrete
Mechanical properties
Reactive powder concrete
Ultra-high-performance concrete

16. SECURITY CLASSIFICATION OF:			**17. LIMITATION OF ABSTRACT**	**18. NUMBER OF PAGES**	**19a. NAME OF RESPONSIBLE PERSON**
a. REPORT	**b. ABSTRACT**	**c. THIS PAGE**			**19b. TELEPHONE NUMBER** *(include area code)*
UNCLASSIFIED	UNCLASSIFIED	UNCLASSIFIED		82	